HAL
open science

Interferometry, Quantum Measurements and Cavity QED with Atoms

Andrea Bertoldi

To cite this version:

Andrea Bertoldi. Interferometry, Quantum Measurements and Cavity QED with Atoms. Atomic Physics [physics.atom-ph]. Université Bordeaux, 2019. tel-02986273

HAL Id: tel-02986273

https://hal.science/tel-02986273v1

Submitted on 2 Nov 2020

HAL is a multi-disciplinary open access archive for the deposit and dissemination of scientific research documents, whether they are published or not. The documents may come from teaching and research institutions in France or abroad, or from public or private research centers.

L'archive ouverte pluridisciplinaire **HAL**, est destinée au dépôt et à la diffusion de documents scientifiques de niveau recherche, publiés ou non, émanant des établissements d'enseignement et de recherche français ou étrangers, des laboratoires publics ou privés.

INTERFEROMETRY, QUANTUM MEASUREMENTS AND CAVITY QED WITH ATOMS

Laboratoire Numérique, Photonique et Nanosciences

University of Bordeaux

Mémoire d'Habilitation à Diriger des Recherches

December 19th, 2019

Andrea Bertoldi

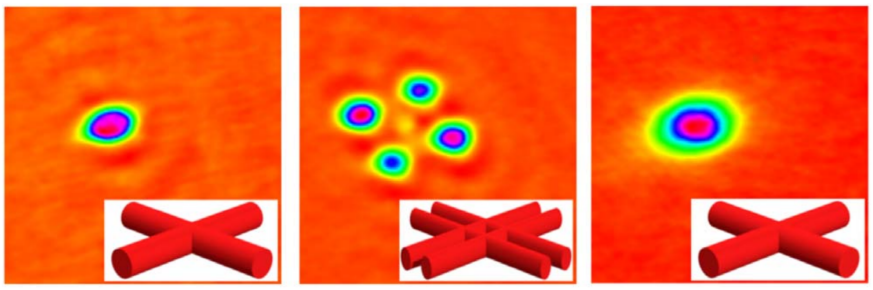

Jury:

Dr. B. Allen – AEI Hanover (Germany)	**Examiner**
Dr. A. Aspect – LCF Palaiseau (France)	**Examiner**
Dr. T. Freegarde – Univ. Southampton (UK)	**Rapporteur**
Dr. B. Lounis – LP2N Talence (France)	**Rapporteur**
Dr. A. Smerzi – INO Firenze (Italy)	**Rapporteur**
Dr. P. Bouyer – LP2N Bordeaux (France)	**Invited member**

Abstract

General Relativity (GR) and Quantum Mechanics (QM) are the two theories on which relies our present understanding of physical phenomena respectively at the macroscopic scale of astronomy and cosmology, and at the microscopic one of the atoms and subatomic particles. In their specific domains, the two theories have been so far successfully tested to an exquisite degree of accuracy in all their predictions; both are therefore considered as good candidates for a more general theory incorporating at once the effects of all the four fundamental forces. The problem arises because the two theories result mutually incompatible: cornerstone concepts of GR like causality, locality and continuity are replaced by non definite causal order, entanglement and quantized quantities. A great theoretical effort has been devoted in the so-called Quantum Gravity to develop a more general framework, capable of describing the whole reality; nevertheless the field is held back by the lack of experimental work which can provide guidance by selecting between some of the different ideas and approaches.

The last years saw a growing number of overlap regions between GR and QM, which increased the interest in Quantum Gravity given the possibility to achieve major progress in the near future. Quantum and Atom Optics can manipulate light and matter at an unprecedented level, and could soon produce systems affected by both GR and QM. Several experiments are testing cornerstone concepts of the two theories, as is the case of the equivalence principle for GR and non-locality for QM, at the boundaries between the two domains, with the aim of revealing violations and trigger progress. Increasing performances in matter wave interferometry open the possibility to verify effects produced by spacetime curvature and not described by QM. The recent observation of gravitational waves (GWs) opens the possibility to test configurations of extremely small scale and high mass, such as the case of black holes, neutron stars and potentially one day the early stages of the Universe.

Cold and ultra-cold atoms are the disruptive tool that in the 1980s revived atomic physics and increasingly lie at the heart of several fundamental and applied research fields, ranging from the simulation of complex systems and phenomena like superfluidity and disordered states, to the absolute measurement of inertial forces, frequency and time. The development of cooling and trapping techniques based on laser beams and magnetic fields brought in 1995 to the observation of degenerate quantum gases, which are nowadays routinely produced in several laboratories and even commercialized. The result has been a plethora of new research possibilities and applications, like quantum computing, analogue gravity and simulation of new states of matter when loaded in complex optical lattice geometries. Atom optics, based on the matter wave behavior of particles predicted by De Broglie, introduced an extremely sensitive way of probing inertial and fundamental forces, and especially with gravity is opening new avenues to test its basic principles, probe space and time with unprecedented precision and accuracy, promising to make feasible in the mid term the technological challenge called absolute navigation.

After my PhD obtained developing novel trapping configurations for neutral atoms, the central

subject of my research activity is represented by matter wave interferometry, investigated from different points of view: metrology, with the precise measurement of the Newtonian fundamental constant G; quantum measurements, in relation to enhancing the sensitivity exploiting the intrinsic properties of QM; inertial sensing, for the development of quantum sensors to measure inertial forces; fundamental physics, for the possibility of testing GR using atomic interference. For the latter, I am presently focused on the one hand on exploring QM in a degenerate cavity quantum–electrodynamics (QED) system, with the target of investigating so far inaccessible aspects of crystallization processes, on the other hand on adopting atom interferometry (AI) in the recently born field of Gravitational Wave Astronomy (GWA). AI promises to fill the sensitivity gap in the frequency spectrum between Earth- and space-based GW detectors based on optical interferometry, a very promising complimentary window in terms of potential signals going from the merging of intermediate mass binary black holes (BBHs) to the incoherent signal represented by the stochastic background. The synthesis of the two research lines is represented by the mid- and long-term goal of testing quantum mechanics and its validity in curved-spacetime with AI experiments in long baseline and cavity QED setups, with the aim of investigating the blurry boundary between GR and QM.

Contents

1 Atom Interferometry **11**
1.1 Matter wave interferometry . . . 12
1.2 MAGIA experiment . . . 21
1.3 AI for GWD . . . 22
1.4 MIGA experiment . . . 25
1.5 AI in space . . . 35

2 Quantum Measurements with Cold Atoms **41**
2.1 Quantum-enhanced measurements . . . 41
2.2 Quantum Feedback on an atomic state . . . 42
2.3 Atomic phase lock loop . . . 46

3 Atom Trapping and Cooling **49**
3.1 Light shift tomography of an optical cavity . . . 49
3.2 BEC array in a non-degenerate cavity . . . 50
3.3 Cavity based matter wave beamsplitter . . . 51
3.4 Dark state loading and cooling in a dipole trap . . . 52

4 Order emergence in a travelling wave cavity **59**
4.1 Self-organisation in a traveling wave cavity . . . 60

5 Technology for AMO physics **65**
5.1 Serrodyne based Pound-Drever-Hall . . . 65
5.2 Active control of magnetic field and its bias . . . 66
5.3 High efficiency magnetic field sources . . . 67
5.4 Control system for AMO physics experiments . . . 69
5.5 Optical clock signal at LP2N . . . 69

6 Curriculum Vitae **73**
6.1 Professional experience . . . 73
6.2 Education . . . 73
6.3 Honors, grants and appointments . . . 74
6.4 Research funding and participation . . . 75
6.5 Scientific production . . . 77
6.6 Teaching . . . 83
6.7 Science Review Activity and other Responsabilities . . . 84

Bibliography **87**

List of Acronyms

AI	Atom Interferometry
AMO	Atomic, Molecular and Optical physics
AOM	Acousto-Optic Modulator
AMU	Atomic Mass Unit
BEC	Bose-Einstein Condensate
BSM	Beyond Standard Model
BBH	Bynary Black Hole
BNS	Binary Neutron star
CAL	Cold Atom Lab
CNES	Centre national d'Etudes Spatiales
CSS	Coherent Spin State
EOM	Electro-Optic Modulator
FORT	Far Off-Resonance optical-dipole Trap
GGN	Gravity-Gradient Noise
GPS	Global Positioning System
GM	Gray Molasses
GR	General Relativity
GW	Gravitational Waves
GWA	Gravitational Wave Astronomy
GWD	Gravitational Wave Detection
EEP	Einstein's Equivalence Principle
ELGAR	European Laboratory for Gravitation and Atom-interferometric Research
HCF	Hollow Core Fiber
HDS	Hyperfine Dark State
HFT	High-Frequency Trading
ICE	Interférométrie Cohérente pour l'Espace
ISS	International Space Station
LIGO	Laser Interferometer Gravitational-Wave Observatory
LISA	Laser Interferometer Space Antenna
LMT	Large Momentum Transfer
LP2N	Laboratoire Photonique, Numérique et Nanosciences
LSBB	Laboratoire Souterrain á Bas Bruit
MIGA	Matter wave Interferometer–laser Gravitation Antenna
MOT	Magneto-Optical Trap
PLL	Phase-Lock Loop
PSD	Phase Space Density
QED	Quantum Electro-Dynamics
QND	Quantum Non-Demolition
QPN	Quantum Projection Noise

QM	Quantum Mechanics
RWA	Rotating Wave Approximation
SM	Standard Model
SNR	Signal Noise Ratio
SQL	Standard Quantum Limit
T/F	Time and Frequency
UHV	Ultra High Vacuum
WEP	Weak Equivalence Principle
WM	Weak Measurement
ZDS	Zeeman Dark State

Introduction

The feeling of awed wonder that science can give us is one of the highest experiences of which the human psyche is capable. It is a deep aesthetic passion to rank with the finest that music and poetry can deliver. It is truly one of the things that make life worth living and it does so, if anything, more effectively if it convinces us that the time we have for living is quite finite.

— Richard Dawkins, Unweaving the Rainbow: Science, Delusion and the Appetite for Wonder

This documents resumes my scientific activity between 2006 and 2019, first as a postdoctoral fellow and research associate in Florence (Italy), then as postdoctoral fellow in Palaiseau (France) and since 2013 as a research scientist in Talence (France). During this time, I worked on different topics in Atomic, Molecular, and Optical physics (AMO), with the subject of Atom Interferometry (AI) playing as a pivot. Atom trapping and cooling constitutes the required set of techniques to obtain atoms with an associated de Broglie wavelength [1] small enough to have them behave as waves in specifically engineered laboratory conditions. A dazzling development of the cooling techniques in the early 90's led in 1995 to the observation of the Bose-condensed state of the matter [2, 3, 4], in which the wavelets associated to each atom of an ensembles interfere constructively to form a macroscopic quantum state. AI deals with the evolution of matter waves when two (or more) possible paths are accessible, which makes possible the splitting of the wavefunction associated to a particle, and then the deflection of its components in order to observe interference phenomena. Nano- or micro-metric obstacles suitable to manipulate the atomic wave-function have been typically implemented with mechanical nano-gratings [5, 6] or optical gratings obtained with counter-propagating light beams [7, 8]. From the seminal experimental demonstrations in 1991 [9], AI has grown relentlessly, and nowadays it touches several fields in modern atomic physics, from metrology, to gravimetry and gradiometry, time-keeping, with connections to quantum measurements and diverse applications as is the case of Gravitational Wave Detection (GWD).

Ch. 1 is focused on AI, starting with a review of the techniques developed to manipulate the atomic wave-function, and the different mathematical formalisms introduced to obtain the measured interferometric phase. After a general presentation of the many applications where AI is nowadays employed, ranging from fundamental physics to applied sciences, I present the experimental work I carried out in Florence, in the group of Prof. G. M. Tino, to realize an atomic gravity-gradiometer to determine the Newtonian gravitational constant G. The activity culminated, first, with a measurement at the 1% level of G [10], and later with an improved value at 0.1% [11]. Since 2013 I am working as chief scientist at the Matter wave Interferometer–laser Gravitation Antenna (MIGA) experiment, lead

by Dr. Bouyer in the frame of an EquipEx project. After introducing the key concepts concerning the possibility and the potential advantages of detecting Gravitational Waves (GWs) with AI, I will describe the work being carried out at LP2N in Bordeaux to develop a giant interferometer at the underground laboratory of LSBB in Rustrel (France), with all the related activities. I will conclude the chapter describing the satellite activity represented by my implication in European studies to take advantage of AI in future space missions; the objectives of these missions range from improved tests of GR, e.g. of the weak equivalence principle (WEP) also in its quantum nuances, to applied physics purposes, e.g. the improved mapping of the Earth's gravitational field.

Ch. 2 describes how atomic sensors can exploit intrinsically quantum features to obtain an increased sensitivity with respect to protocols based on classical properties only. The sensitivity boost over classical statistic granted by quantum mechanics would be of immediate advantage in atom interferometry, as proven in proof-of-concept experiments [12, 13, 14, 15] surpassing the Standard Quantum Limit (SQL). After making the distinction between quantum-enhanced measurements exploiting entanglement [16] or alternative mechanisms [17], I will present related work I realized with a cavity QED experiment at the Institut d'Optique first in Palaiseau and then in Talence. We studied theoretically how to achieve spin squeezing in an atomic ensemble, and then built a weak, non-destructive probe that we exploited to implement pioneer experiments in quantum feedback and phase locking using an atomic quantum state as a reference.

Ch. 3 is focused on the results I obtained in the general context of atom trapping and cooling, often for the specific configuration of cavity QED. I will present an enhanced imaging technique exploiting light-shift engineering (Sec. 3.1), the direct production of an array of BECs in the high order transverse cavity modes of a resonator (Sec. 3.2), the progress towards a cavity based matter wave beamsplitter (Sec. 3.3) and the dark state loading and cooling in a dipole trap (Sec. 3.4, which has been key to realize an all-optical BEC in microgravity.

The subject of Ch. 4 is the present research activity on the cavity QED experiment, targeting the observation of self-organisation phenomena in the traveling wave configuration implemented by our bow-tie cavity. The principal aim is to investigate order emergence in a broader context with respect to what spectacularly demonstrated in the last years in standing wave resonators. The main ingredient characterizing our specific geometry is the absence of boundary conditions on the intracavity electric field at the mirrors; as a consequence, the phase of the optical and atomic lattice that should form in the cavity is a free parameter. The second-order phase transition to the ordered configuration is not only described in terms of a continuous phase parameter, but determines as well the entanglement between the atomic and the light component of the system. The scientific program foresees the realization of other exotic states of matter, like the entanglement between two components of a single BEC, or a network of entangled BECs. The latter is a potential breakthrough for quantum communication protocols.

Ch. 5 presents a selection of technological solutions I contributed to develop in the context of AMO physics, ranging from optics, servoing and electronics to generation and control of magnetic fields and exploitation of time and frequency (T/F) signals.

More information on the different topics treated in this synthesis can be found in the bibliographic references reported at the end of each chapters, and as well in the thesis manuscripts of the students I supervised in these years (see Par. 6.3.1).

Chapter 1

Atom Interferometry for Precision Measurements

Ed elli a me: "Tu imagini ancora
d'esser di là dal centro, ov'io mi presi
al pel del vermo reo che 'l mondo fóra.

Di là fosti cotanto quant'io scesi;
quand'io mi volsi, tu passasti 'l punto
al qual si traggon d'ogne parte i pesi."

[And he to me: "Thou still imaginest
Thou art beyond the centre, where I grasped
The hair of the fell worm, who mines the world.

That side thou wast, so long as I descended;
When round I turned me, thou didst pass the point
To which things heavy draw from every side."]

— Dante, Inferno XXXIV 106-111

Ch. 1 is focused on AI, starting with a review of the techniques developed to manipulate the atomic wave-function, and the different mathematical formalisms introduced to obtain the measured interferometric phase. After a general presentation of the many applications where AI is now employed, ranging from fundamental physics to applied sciences, I will present the experimental work I carried out in Florence, in the group of Prof. G. M. Tino, to realize an atomic gravity-gradiometer to determine the Newtonian gravitational constant G. The activity culminated first with a measurement at the 1% level of G [10], and later with an improved value at 0.1% [11]. Since 2013, I am working at the Matter wave Interferometer–laser Gravitation Antenna (MIGA) experiment, lead by Dr. Bouyer in the frame of an EquipEx project. After introducing the key concepts concerning the possibility and the potential advantages of detecting Gravitational Waves (GWs) with AI, I will describe the work being carried out at LP2N in Bordeaux to develop a long baseline interferometer at the Laboratoire Souterrain à Bas Bruit (LSBB; Low Noise Underground Laboratory) in Rustrel. I will draft the roadmap to bring the initial instrument from its commissioning phase to the measurement campaigns with an enhanced sensitivity; several actions to boost the instrument performances are already being pushed forward. I

will conclude the chapter describing the satellite activity represented by my implication in studies to take advantage of AI for fundamental or applied physics purposes in space missions.

1.1 Matter wave interferometry

Luois de Broglie introduced the concept of a wavelength associated to every piece of matter in his PhD thesis [1]. In his attempt to symmetrise the treatment of matter particles and photons, after the latter have been predicted [18, 19] and shown [20] to obey matter-wave duality, he assumed the same wavelength–momentum relation valid for photons to describe particles:

$$\lambda_{\mathrm{dB}} = h/p \tag{1.1}$$
$$= h/(mv) \tag{1.2}$$

where the proportionality factor h is the Planck's constant, m and v are the particle mass and velocity, respectively. Remarkably, the particle's wavelength varies with its velocity, unlike photons that move always at the speed of light. Only a few years later Schrödinger introduced the linear partial differential equation that describes the mechanics of quantum objects as an undulatory phenomenon [21], which was soon spectacularly corroborated by interference experiments with electrons [22, 23] and neutrons [24]. The weakness of the coupling constant confined interference experiments to light-weight particles for long time[1]. The leap forward to proving matter wave interference for more massive object, namely atoms and molecules, has been the development of cold and ultra-cold atomic, molecular and optical (AMO) physics. In the last decades, scientific advances in cooling and trapping of atoms and molecules allow the production of ensembles at increasingly low temperatures i.e. velocity [25, 26], and hence with increasingly big associated wavelengths. At the same time, technological developments in nano-lithography and in coherent optical sources brought to the capability of implementing "obstacles" commensurate with λ_{dB}. The first atom interferometry experiments in 1991 used alkali atoms at a few hundreds nK, which means with a wavelength of ~ 1 μm [9]; the atom optics elements could then be realized with material gratings and with periodic optical lattices using two counter-propagating laser beams.

Two main formulations have been developed to obtain the interferometric phase shift in the case of two–path configurations, with three or more light pulses: a path integral approach [27, 8, 28, 29, 30, 31], and a density matrix equation in the Wigner representation [32]. The improving experimental performances of atom interferometry require a refinement over time of the modeling for the phase shift calculation. Several effects have been investigated especially in the first formulation, such as the finite speed of light [33] or the wavefront aberration of the light beams [34]. The calculation has been also extended to the general relativistic case [35, 36].

In the next section, I derive the interferometric phase in a Mach-Zehnder interferometer. To this aim, I adopt a formalism based on the Heisenberg representation to describe the dynamics of a two–level atom in an external potential coherently manipulated with a pulsed laser beam [37]; following this approach we recently studied the effect of non-quadratic potentials and of the finite pulse duration [38]. This specific formulation provides the interferometric phase by adopting a series of unitary transformations to write the evolution operator in simple terms. Each of these unitary transformations

[1] A fascinating Sci-Fi book where Planck's quantum of action is imagined to be large enough to make weird quantum phenomena pervasive of human life is *Mr. Tompkins in Paperback*, Cambridge University Press, 1993 by George Gamow.

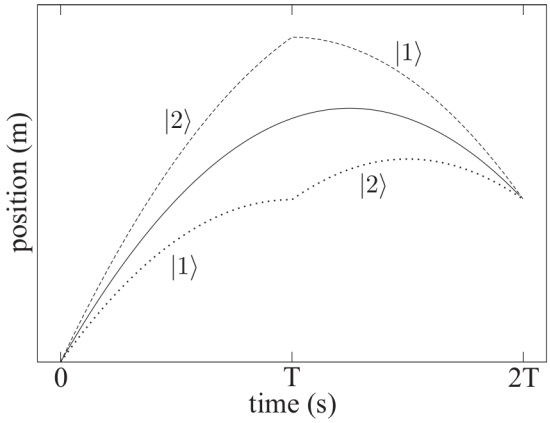

FIGURE 1.1 — [from [38]] Classical trajectories in a Kasevich-Chu [8] interferometer. The dashed and dotted lines represent the upper and lower interfering paths while the continuous line is the mean path, i.e., the trajectory of a particle with initial average momentum. At $t = T$ the π pulse exchanges the internal states and the momentum with respect to the mean path. For a linear potential $V(z)$ the three trajectories converge to the same point at $t = 2T$; this condition is in general not valid for a nonlinear potential.

consists of a sort of "change of reference frame", sometimes not intuitive to identify, but which can provide useful insight on the underlying physical meaning of the mathematical operation. The whole Sec. (1.1.1) is summarized in Eq. 1.16; Sec. (1.1.2) will then review the fields of applications of AI.

1.1.1 Atom interferometric phase

We consider a simplified two-level model in one dimension. Raman transitions between two stable levels $|1\rangle$ and $|2\rangle$ are characterized by a time-dependent Rabi frequency $\Omega(t)$, after adiabatic elimination of the excited level. The atoms are initially prepared in the internal state $|1\rangle$ and their initial wavefunction is assumed to be a Gaussian wavepacket in momentum. The atoms have been prepared with an initial velocity selection pulse of length τ_s, which fixes the momentum distribution width as $\sim m/(k\tau_s)$.

The Hamiltonian describing the effective two-level atom interacting with the Raman laser beams is [37]

$$H = \left[\frac{\hat{p}^2}{2m} + V(\hat{z})\right] I - \hbar\Omega(t)\cos\phi_L(\hat{z},t)\sigma_1 + \frac{\hbar\omega_{21}}{2}\sigma_3, \tag{1.3}$$

where $\hbar\omega_{21}$ is the energy difference between the two states, σ_i are the Pauli matrices ($i = 1, 2, 3$) and I is the identity matrix. We consider here an external potential at most quadratic in $\hat{z}$: $V(\hat{z}) = mg\hat{z} - m\gamma\hat{z}^2/2$. We assume that the laser fields are classical, so the non-commuting operators are only $\hat{z}$ and $\hat{p}$. From now on we drop the hat from $\hat{z}$ and $\hat{p}$ and their functions, to alleviate the notation.

Mean path

We consider a Kasevich-Chu type interferometer [8], where a sequence of three pulses $\pi/2 - \pi - \pi/2$ of temporal lengths $\tau, 2\tau$ and τ, respectively, are separated by two free evolution intervals of length $T - 2\tau$ so that the total duration of the interferometric sequence is $2T$ (see Fig. 1.1). Different sequences of pulses can also be considered [32, 31]. In present day interferometers the orders of magnitude of τ and T are 10^{-5} s and 1 s, respectively. We also assume $\tau_s \sim 10^{-4}$ s.

To keep the optical field in resonance with the atoms during their free fall, a phase-continuous, linear frequency chirp on the laser fields partially compensates the Doppler effect. Thus, the phase ϕ_L can be written as a function of position and time as

$$\phi_L(z,t) = \omega_0 t + \frac{\alpha t^2}{2} - kz. \tag{1.4}$$

Here ω_0 is the frequency difference between the two Raman beams, k is the sum of the Raman beams wavenumbers and α is the chirp rate. We make the simplifying assumption that k is constant in time, and we neglect any effect due to the finite speed of light.

The unitary transformation[2] generated by $U_3(t) = \exp[i\sigma_3\phi_L(z,t)/2]$ eliminates the time-dependent phase $\phi_L(z,t)$. After adopting the rotating–wave–approximation (RWA) [42] to cancel the terms oscillating as $\exp[i2\phi_L(z,t)]$, the Hamiltonian reads

$$H^{\mathrm{I}}(t) = -\frac{\hbar\Omega(t)}{2}\sigma_1 - \frac{\hbar}{2}\delta(t)\sigma_3 + \left(\frac{p^2}{2m} + \frac{\hbar^2 k^2}{8m} + V(z)\right) I, \tag{1.5}$$

where $\delta(t)$ is defined as the Doppler-shifted detuning

$$\delta(t) = \Delta(t) + \frac{pk}{m}, \tag{1.6}$$

with $\Delta(t) \equiv \omega(t) - \omega_{21}$ and $\omega(t) \equiv \omega_0 + \alpha t$. The transformed momentum is $U_3(t) p I U_3^\dagger(t) = pI - \hbar k \sigma_3/2$: the momentum of state $|1\rangle$ is increased by $\hbar k/2$, that of state $|2\rangle$ diminished by the same amount. The classical upper and lower trajectories are thus translated on the mean path, i.e., the trajectory with average momentum after the first beam–splitter pulse, as shown in Fig. 1.1.

An additional unitary transformation will eliminate the term proportional to I in $H^{\mathrm{I}}(t)$, which is equivalent to moving to a reference frame in free fall. This operation is straightforward if $V(z)$ is at most quadratic in z. For the earth's gravitational field we use the second–order potential $V(z) = mgz - m\gamma z^2/2$, define $H_\gamma = (p^2/2m + mgz - m\gamma z^2/2)I$, and apply the unitary transformation $U_0(t) = \exp(iH_\gamma t/\hbar)$ to H^{I}. The result is

$$H^{\mathrm{II}}(t) = -\frac{\hbar}{2}\left[\Omega(t)\sigma_1 + \delta(t)\sigma_3\right], \tag{1.7}$$

where the momentum p in $\delta(t)$ is now replaced by $p(t)$, i.e. the momentum time-evolved according to the Heisenberg representation with Hamiltonian H_γ:

$$p(t) = p\cosh\sqrt{\gamma}t + mz\sqrt{\gamma}\sinh\sqrt{\gamma}t - \frac{mg\sinh\sqrt{\gamma}t}{\sqrt{\gamma}}. \tag{1.8}$$

Similarly, the time-evolved operator $z(t)$ is:

$$z(t) = z\cosh\sqrt{\gamma}t + p\frac{\sinh\sqrt{\gamma}t}{m\sqrt{\gamma}} + \frac{g(1-\cosh\sqrt{\gamma}t)}{\gamma}. \tag{1.9}$$

[2] Under a generic unitary transformation $|\psi'\rangle = U(t)|\psi\rangle$, the Hamiltonian transforms as $H'(t) = U(t)HU^\dagger(t) + i\hbar(\partial_t U)U^\dagger(t)$. The time-evolution operator over the generic time interval $[t_1, t_2]$ obeys the differential equation $i\hbar\partial_{t_2}\mathcal{U}(t_2,t_1) = H(t_2)\mathcal{U}(t_2,t_1)$ with the boundary condition $\mathcal{U}(t_1,t_1) = I$, whose general solution is the well-known time-ordered exponential [39]: $\mathcal{U}(t_2,t_1) = \mathcal{T}\exp\left(-\frac{i}{\hbar}\int_{t_1}^{t_2} H(t')\,dt'\right)$. Under the generic time-dependent unitary transformation the evolution operator is also transformed: $\mathcal{U}'(t_2,t_1) = U(t_2)\mathcal{U}(t_2,t_1)U^\dagger(t_1)$. While $\mathcal{U}(t_2,t_1)$ is usually calculated through the Dyson series [39], we use the alternative Magnus expansion [40, 41], for which $\mathcal{U}(t_2,t_1)$ is written as the exponential of a series: $\mathcal{U}(t_2,t_1) = \exp\left(\sum_{n=1}^{+\infty} M_n(t_2,t_1)\right)$. Differently from the Dyson series, the Magnus expansion preserves the unitarity of $\mathcal{U}(t_2,t_1)$ at any order but, as a drawback, it requires an operator exponentiation. Further details on the mathematical support of our formulation can be found in the Appendixes of [38].

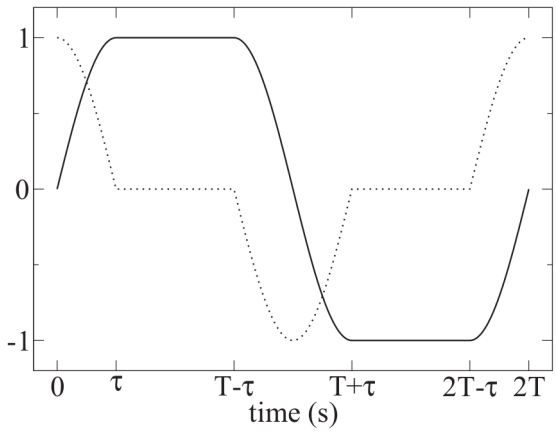

FIGURE 1.2 — [from [38]] Plot of the functions $\sin\phi_1(t)$ (continuous line) and $\cos\phi_1(t)$ (dotted line) for ideal rectangular pulses in a Mach-Zehnder interferometer. The two functions are formed either by sinusoidal functions or horizontal lines. In this figure $\eta = \tau/T$ is 0.25 for clarity; typical experimental values for η are in the $10^{-4} \sim 10^{-5}$ range.

In the Hamiltonian of Eq. (1.7) the effects of the free evolution and of the interferometer pulses are not separated: while the term proportional to $\Omega(t)$ vanishes during the free evolution, its temporal integral, i.e., the corresponding accumulated phase, cannot be neglected since the pulses have an area of $\sim \pi$. Therefore, we define a third unitary transformation:

$$U_1(t) \equiv \exp[-i\phi_1(t)\sigma_1/2], \tag{1.10}$$

$$\phi_1(t) \equiv \int_0^t \Omega(t')\,dt'. \tag{1.11}$$

The resulting Hamiltonian

$$H^{\rm III}(t) = \frac{\hbar}{2}\delta(t)\left[\sin\phi_1(t)\sigma_2 - \cos\phi_1(t)\sigma_3\right] \equiv H_L^{\rm III}(t) + H_S^{\rm III}(t) \tag{1.12}$$

has the required form, being the sum of a dominant term, $H_L^{\rm III}(t)$, proportional to $\sin\phi_1(t)\sigma_2$, plus a small term, $H_S^{\rm III}(t)$, proportional to $\cos\phi_1(t)\sigma_3$, which vanishes during the free evolution for pulses with ideal area (see Fig. 1.2). We neglect $H_S^{\rm III}(t)$, whose effect is fully taken into account in [38]. To evaluate the probability amplitude we need the off-diagonal matrix element of the evolution operator from $t = 0$ to $t = 2T$, for which we revert to the Magnus expansion. Since in the present approximation $[H(t), H(t')]$ is a c–number, the Magnus series terminates at M_2. Defining

$$\begin{aligned} \phi_2(t) &\equiv \int_0^t \delta(t')\sin\phi_1(t')\,dt', \\ \psi_2(t) &\equiv \frac{1}{8}\int_0^t dt' \int_0^{t'} c_{\delta,\delta}(t',t'')\sin\phi_1(t')\sin\phi_1(t'')\,dt'', \end{aligned} \tag{1.13}$$

we have $M_1 = -i\phi_2\sigma_2/2$, $M_2 = -i\psi_2 I$, and

$$\mathcal{U}^{\rm III}(2T,0) = \exp(-i\psi_2)\exp\left(-i\frac{\phi_2}{2}\sigma_2\right). \tag{1.14}$$

The evolution operator in the mean path frame then reads $\mathcal{U}^{\mathrm{II}}(2T,0) = U_1^\dagger(2T)\mathcal{U}^{\mathrm{III}}(2T,0)$. Since $U_1^\dagger(2T) = \exp[i\phi_1\sigma_1/2]$, the transition probability P_{21} from $|1\rangle$ to $|2\rangle$ at the output of the interferometric sequence can be evaluated directly:

$$\begin{aligned} P_{21} &= |\langle 2|\exp(i\phi_1\sigma_1/2)\exp(-i\psi_2)\exp(-i\phi_2\sigma_2/2)|1\rangle|^2 \\ &= \frac{1}{2}\left(1-\cos\phi_1\cos\phi_2\right), \end{aligned} \tag{1.15}$$

where the internal states $|n\rangle$, with $n = 1$ or 2, are evaluated in the reference frame II, i.e., $|n(t)\rangle = U_0(t)U_3(t)|n\rangle$.

Ideally, the total pulse area ϕ_1 in Eq. (1.15) is equal to 2π and the contrast $\cos\phi_1$ is equal to 1; slightly imperfect pulses reduce the contrast of the interference fringes. Assuming ideal, rectangular pulses, it is simple to obtain a closed form expression for ϕ_2 from Eqs. (1.6), (1.8) and 1.9). Here we report only an approximate expression keeping only terms up to the first order in the small parameter $\eta = \tau/T$. This expression depends only on the area, not on the actual shape, of the pulses:

$$\phi_2 = T^2(gk-\alpha-k\gamma z_0)\left(1-\frac{2\pi-4}{\pi}\eta\right) - k\gamma T^3\left[v_m\left(1-\frac{2\pi-4}{\pi}\eta\right) - gT\left(\frac{7}{12}-\frac{4\pi-8}{3\pi}\eta\right)\right], \tag{1.16}$$

where we have used $p_0/m = v_0 + v_r/2 = v_m$ for the motion on the mean path, and $v_r \equiv \hbar k/m$ is the recoil velocity.

The formula for P_{21} (Eq. 1.15)can be easily understood by noting that $H_L^{\mathrm{III}}(t)$ is diagonalized by the time independent eigenvectors

$$|\pm\rangle = \frac{|1\rangle \pm i\,|2\rangle}{\sqrt{2}} \Rightarrow |1\rangle = \frac{|+\rangle + |-\rangle}{\sqrt{2}}, |2\rangle = \frac{|+\rangle - |-\rangle}{i\sqrt{2}} \tag{1.17}$$

with the time dependent eigenvalues

$$E^{\pm}(t) = \pm\frac{\hbar\delta(t)\sin\phi_1(t)}{2}. \tag{1.18}$$

Due to the interference between $|+\rangle$ and $|-\rangle$, one must have

$$P_{21} = \frac{1}{4}\left|1-\exp\left(\frac{i}{\hbar}\int_0^{2T} E^+(t)-E^-(t)\,dt\right)\right|^2, \tag{1.19}$$

which is equivalent to Eq. (1.15) for ideal pulses. This is analogous to observing the Rabi oscillations in the dressed atom picture [43].

Loss of contrast

In general, in a nonlinear potential, the end points of the upper and lower paths do not coincide. The loss of contrast induced by this effect and the strategies to mitigate it are discussed in Refs. [44, 45] and experimentally implemented in Refs. [46, 47]. Here we derive in our formalism the conditions to achieve high contrast in the case of a constant gradient, and in [38] we extended them to an arbitrary weak perturbing potential.

We start by evaluating the operators $z(t)$ and $p(t)$ after the unitary transformation generated by $H_L^{\rm III}$ at time $t = 2T$ obtaining[3]

$$\begin{aligned} z(2T) &= z_m(2T)I + \frac{i\sigma_2}{2}[\phi_2(2T), z_m(2T)] \\ &= z_m(2T)I + \frac{\sigma_2 v_r}{2}\int_0^{2T} \sin\phi_1(t)\,\cosh\sqrt{\gamma}(2T-t)\,dt \\ &\simeq z_m(2T)I + \frac{\sigma_2 v_r \gamma T^3}{2}, \end{aligned} \tag{1.20}$$

and, similarly,

$$p(2T) \simeq p_m(2T)I + \frac{\sigma_2 m v_r \gamma T^2}{2}. \tag{1.21}$$

The eigenvectors of both operators are again $|\pm\rangle$. The separation in position and momentum is given by the difference between the eigenvalues, i.e. $\Delta z(2T) = v_r\gamma T^3$ and $\Delta p(2T) = m v_r \gamma T^2$.

In Ref. [44] it is shown that the conditions $\Delta z(2T) = 0$ and $\Delta p(2T) = 0$ at the end of an interferometric sequence ensure high contrast independently from the detection time. More generally, high contrast is obtained when $\Delta z(2T) - \Delta t_d \Delta p(2T)/m = 0$, where Δt_d is the time interval between the last pulse and detection. By slightly changing the duration of the second free–evolution period it is possible to fulfill only the latter condition.

A better strategy, suggested in Ref. [45] and demonstrated in Refs. [46, 47], is to change the momentum of the Raman beams by an amount δk at the π pulse. In this way v_r is changed by an amount $\delta v_r = \hbar\delta k/m$ during the second free evolution: by choosing $\delta v_r/v_r = -\gamma T^2/2$, $\Delta z(2T)$ vanishes while the effect of $\Delta p(2T)$ is negligible. Now, however, in Eq. (1.4) we have $k = k(t)$ and an extra term appears in the Hamiltonian due to the time derivative when the unitary transformation is applied; such term provides a momentum kick at the π pulse that exactly compensates $\Delta p(2T)$. The key to the possibility of compensating simultaneously $\Delta z(2T)$ and $\Delta p(2T)$ lies in the relation $m\Delta z(2T)/\Delta p(2T) = T$. This condition does not hold in general if $V(z)$ is more than quadratic.

Comparison with previous results

Here we show that Eq. (1.16) is consistent with previous literature.

Except for a sign, $\sin\phi_1(t)$ coincides with the sensitivity function introduced in Ref. [48] for rectangular pulses and it is immediately applicable to more general cases, i.e., Gaussian or imperfect pulses. If we use the expression for $\delta(t)$ given in Eq. (1.6) and, moving to the expectation values, apply the Ehrenfest's theorem replacing p/m with $\dot{z}$, we can integrate by parts the first expression in Eq. (1.13) in the case of ideal rectangular pulses of negligible duration:

$$\begin{aligned} \phi_2 &= -\int_0^{2T} [\phi_L(t) + k z_m(t)]\Omega(t)\cos\phi_1(t)\,dt \\ &\simeq -D_2[\phi_L] - k D_2[z_m], \end{aligned} \tag{1.22}$$

where $\phi_L(t)$ is the primitive of $\Delta(t)$ and, to simplify the notation, we have defined $D_2[f] \equiv f(2T) - 2f(T) + f(0)$. The boundary term of the integration by parts vanishes, for ideal pulses, as $\sin\phi_1(2T) = \sin\phi_1(0) = 0$. In $D_2[\phi_L]$ the terms constant and linear in t disappear so $-D_2[\phi_L] = \alpha T^2$ while, since $z(t)$ and $p(t)$ are linear in z and p in Eqs. (1.8, 1.9), then $2z_m(t) = z_u(t) + z_l(t)$, so

$$D_2[z_m] = \frac{z_u(2T) + z_l(2T)}{2} - (z_u(T) + z_l(T)) + z_m(0), \tag{1.23}$$

[3] For this passage one uses the results described in the previous note.

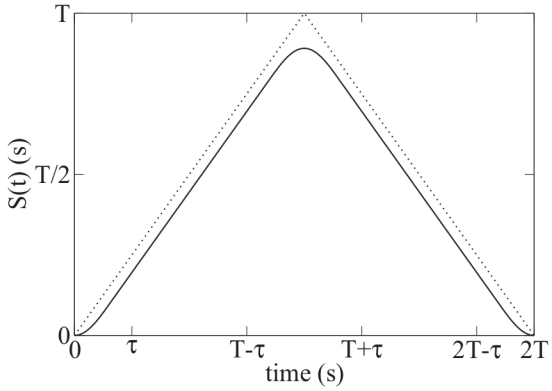

FIGURE 1.3 — [from [38]] Plot of the function $S(t) = \int_0^t \sin\phi_1(t')\,dt'$ for $\eta = 0.25$ (continuous line) and $\eta = 0$ (dotted line) for square pulses.

which is the result given in Ref. [49].

Next, we compare Eq. (1.22) with the path integral prescription, as described, for example, in Ref. [30], where the phase shift is evaluated as the sum of three terms, $\delta\phi_L + \delta\phi_p + \delta\phi_s$. The "laser" term $\delta\phi_L$ is given by

$$\begin{aligned}\delta\phi_L = \phi_L(0) + kz_m(0) - 2\phi_L(T) - k[z_u(T) + z_l(T)] \\ + \phi_L(2T) + kz_l(2T),\end{aligned} \tag{1.24}$$

where $\phi_L(t) \equiv \phi_L(0,t)$ and $\phi_L(z,t)$ is given by Eq. (1.4).

The "propagation" term $\delta\phi_p$ is given by

$$\delta\phi_p = \frac{1}{\hbar}\left(\int_u \mathcal{L}dt - \int_d \mathcal{L}dt\right) \equiv \frac{1}{\hbar}\oint_{cp} \mathcal{L}dt, \tag{1.25}$$

where the two integrals are along the upper and lower classical paths and $\mathcal{L}$ is the Lagrangian. To simplify the notation the difference of the two integrals is denoted as a circulation integral along the classical path, cp, even if this is open.

In the case of a quadratic potential it is easy to see that the kinetic and the potential energies give equal contributions to the integral so $\delta\phi_p = 0$.

Finally the "separation" term is defined, as

$$\delta\phi_s = \frac{k(z_u(2T) - z_l(2T))}{2}, \tag{1.26}$$

where we have taken into account that the average momentum of the two states in an output channel must be measured on the mean path. Clearly the path integral prescription gives the same result as Eq. (1.22).

Another possibility to evaluate ϕ_2 involves integrating by parts the term $kp(t)/m$ in $\delta(t)$ in the other order, replacing $\dot{p}$ with $-\partial_z V$ and obtaining, in the same hypothesis as above, the contribution to ϕ_2 due to V, ϕ_2^V as

$$\phi_2^V \simeq \frac{v_r}{\hbar}\int_0^{2T} S(t)\partial_z V(t)\,dt, \tag{1.27}$$

where $S(t)$ is the primitive of $\sin\phi_1(t)$ [see Fig. 1.3]. Noting that for a quadratic potential $V(z+\Delta z)-V(z-\Delta z)=2\Delta z\partial_z V(z)$ we can write

$$\phi_2^V = \frac{1}{\hbar}\oint_c V(t)\,dt, \tag{1.28}$$

where the closed path c is delimited by $z_m(t)\pm v_r S(t)/2$. We can also express ϕ_2^V as the difference of two integrals on the upper and lower classical paths by taking $z_u(t)-z_l(t)\equiv S(t)v_r+\delta z(t)$ as a definition of $\delta z(t)$ to obtain

$$\begin{aligned}\phi_2^V =&\frac{1}{\hbar}\oint_{cp} V(t)\,dt - \frac{1}{\hbar}\int_0^{2T}\delta z(t)\partial_z V\,dt\\ =&\frac{1}{\hbar}\oint_{cp} V(t)\,dt + \frac{p(2T)[z_u(2T)-z_l(2T)]}{\hbar}\\ &-\frac{1}{\hbar}\int_0^{2T} p(t)\delta v(t)\,dt,\end{aligned} \tag{1.29}$$

where $\delta v=\delta\dot{z}$ and $\delta v=0$ during the free evolution. Here the phase shift can be interpreted as a propagation term depending only on the potential, a separation term, and finally a term that contains the correction for the finite duration of the pulses.

Other configurations

The representation free method we adopted to calculate the interferometric phase gives results in agreement with what obtained with more traditional approaches. In [38] we adopted it to treat the effect of the small term $H_S^{\mathrm{III}}(t)$ in Eq. 1.12, and that of a gravitational potential more than quadratic in $\hat{z}$, i.e. $V(\hat{z})=mg\hat{z}+\mathcal{V}(\hat{z})$, where $\mathcal{V}(\hat{z})$ is sufficiently weak to be treated as a small perturbation. More in general, this method can be extended to calculate the high–order corrections imposed by multi-pulse sequences adopted to increase the momentum separation of the interfering trajectories [50, 51] or to enhance the instrument sensitivity at a specific frequency [52]. Other sensor geometries optimized to be sensitive to other inertial effects, like rotation or gravity gradients, can also be described in this way.

1.1.2 Atom Interferometry: applications

The first experimental demonstrations of matter wave interferometry with atoms [9] opened a wealth of new possibilities, ranging from tests of the foundations of quantum mechanics and general relativity, measurements of fundamental constants, to applications in metrology, as is the case for the measurement of time and frequency and inertial forces. The main results are here summarized, together with several bibliographic references to delve into the subject.

Fundamental physics

Atoms are nearly ideal probes of space and time: they can be set in a coherent superposition of their internal or external degrees of freedom [53]. In the first case they are turned into exquisite primary standards for time and frequency measurements [54], nowadays allowing for clock synchronization surpassing the 18th decimal [55]. Among other research contexts, their extreme performances in terms of accuracy and precision are at the basis of their adoption to investigate possible variations of

fundamental constants [56], put bounds on dark matter theories [57], and search for beyond-standard-model (BSD) physics [58].

When the atomic matter-wave is split on an external degree of freedom – typically momentum – the system follows at once separate trajectories and is made later to interfere; it becomes thus a sensor of spatially dependent effects, as is the case of gravity [59, 60], inertial effects [61, 62], and even the tidal force induced by the spacetime curvature [63]. Specific configurations of external source masses have been devised to measure the Newtonian gravitational constant G [64, 10], study the gravitational version of the Aharonov-Bohm experiment [65] and the attractive force determined on atoms by the blackbody radiation [66], and set limit on the dark energy forces [67, 68, 69]. Precisely tailored electro-magnetic fields could instead be used to test atom neutrality [70].

Matter wave interferometry is increasingly investigated as a "Swiss army knife" with a variety of applications to study fundamental physics: (i) it allows the measurement of constants of nature, like the aforementioned gravitational one and the fine structure constant [71]; (ii) is a formidable tool to test several aspects of general relativity [72], ranging from the verification of the different postulates of the Einstein's equivalence principle (EEP) [73, 74, 75, 47] even in its quantum formulations [76, 77, 78], to the possible detection of GWs in the mid-band frequency range (see [79], references therein and Sec. 1.3); (iii) given the macroscopic separation of the trajectories followed by the different components of the wavefunction (in [80] a 54 cm separation was demonstrated), AI could effectively offer the key to investigate decoherence models developed to explain the transition of the quantum realm to classicality [81, 82, 83]; (iv) it is investigated in very diverse contexts, like tests of the standard model [84], and antimatter interferometry [85].

Applied physics

The outstanding performances of interferometric quantum sensors make them ideal not only to test the foundations of physics, but also as exceptional instruments in applied contexts; unlike their classical counterparts, the measurement is ultimately operated in terms of the frequency of an atomic transition, and results hence absolute. Such feature is of key importance in long term measurement campaigns, for example to determine the gravitational acceleration [59, 86, 87], the gravitational gradient of acceleration [60, 88], and the rotation rate [89, 90, 62]. Inertial stations capable of measuring the full inertial base – i.e. rotations and accelerations along three orthogonal axes – have been demonstrated as laboratory setup [61]. The same instrument can even measure at the same time the gravitational acceleration and its gradient [88, 91]. An increasing effort of miniaturization [92, 93, 94] and augmented data rate [95, 96] is opening towards the deployment of atom interferometers in diverse field as geodesy [97], geophysics [98, 99, 100], and inertial navigation [101]. For the latter application, a recent study proposed the implementation of multi-dimensional atom optics to create coherent superposition of atomic wave packets along three spatial directions, and achieve thus simultaneous sensitivity to all the three components of acceleration and rotations [102].

A whole branch of atom interferometry adopts experimental setups in freely-falling environments, as is the case of the capsules dropped in the Bremen tower [103], and parabolic flights operated on Einstein elevators [104], aircrafts [105], and rockets [106]. The final target of these activities is represented by the possibility in the near future to operate atom interferometers in space, on the ISS [107] or a satellite [74, 97]. The perpetual free-fall of space eliminates the issue represented by the atomic motion with respect to the vacuum apparatus, which on Earth typically requires tall atomic fountains [108] or suspension methods for the atoms [109, 110, 25, 111]. The result will be compact devices with long interrogation times and hence high sensitivities, adapt to perform tests of general relativity as described in the previous paragraph, and to operate space geodesy [97].

In the next sections I present my research activities related to AI since I obtained my PhD. In details, Sec. (1.2) focuses on the determination of the Newtonian constant G; Sec. (1.3) describes how AI will contribute to GW astronomy; Sec. (1.4) is dedicated to the ongoing experiment MIGA, which consists of an underground demonstrator for GW detection with AI; Sec. (1.5) summarizes my implication in different experiments and study missions for portable and spatial AI.

1.2 MAGIA experiment: measuring G by AI

In the period 2005-08 I worked first as a postdoctoral fellow and then as a Research Assistant in the group Prof. G. M. Tino in Florence (Italy), at a metrological experiment aiming to accurately determine the Newtonian gravitational constant G by atom interferometry. The experiment adopted an original doubly-differential scheme to precisely detect the gravitational effect of heavy source masses by atom interferometry [112]. Two atomic clouds launched in free fall in a fountain configuration and vertically separated are used to simultaneously measure the vertical acceleration; in this way one differentially cancels the the main gravitational contribution of planet Earth, i.e. its bias acceleration $g_0 \sim 9.81$ m/s and is down to its gradient contribution $\nabla_z g \sim 3000$ E (1 E=10^{-9} s^{-2}) [60]. Such gradiometric measurement is repeated twice for different configurations of heavy source masses (see Fig. 1.4, left), in order to differentially remove the linear contribution of the Earth's gravity so as to remain with the source masses' contribution only. A careful geometrical and density characterization of these masses leaves the Newtonian constant G as the unique unknown constant, obtained from the atom interferometric measurement.

We obtained the first proof-of-concept measurement of G after completing the experimental apparatus and, using a first set of source masses realised in lead [10]. Key to this first result has been the implementation of a juggled launch sequence, to have two atomic ensembles with a high atom number flying on simultaneous parabolic trajectories vertically separated by ∼30 cm. The measurement precision was at a 1% level, not enough to be considered for the weighted mean of G reported in the CODATA 2006 [113]. Nevertheless, our measurement is there mentioned together with that realized in the group of Kasevich at Stanford [64] as a new potentially valuable method: *Although neither of these results is significant for the current analysis of G, future results could be of considerable interest* (from [113]).

A significant overhaul of the setup led in 2008 to a new improved value with a total uncertainty at the 1.7×10^{-3} level, mainly limited by the statistical component [11]. Key improvements have been the replacement of the lead masses with a higher density tungsten set [114], and the adoption of an optimal reciprocal positioning of the masses and the atomic probes in order to get rid of main systematic effects (Fig. 1.4). Despite a further improvement by a factor 10 achieved in 2014 by my previous colleagues [115], once more in the CODATA 2014 [116] measuring G by atom interferometry has not been taken into account to evaluate the recommended value, but is referenced because *Although not competitive, the conceptually different approach could help identify errors that have proved elusive in other experiments* (from [116]). Its main merit could be to help finding hidden systematics thanks to the radically new approach of determining G, given that since the beginning and for more than 200 years [117, 118] is has been measured essentially in the same way, i.e. by evaluating the torque on macroscopic masses suspended to fibers[4]. Atom interferometry adopts instead quantum probes in

[4]The unique exception is a measurement obtained by closing the second arm of a Michelson interferometer with a freely falling corner cube [119]

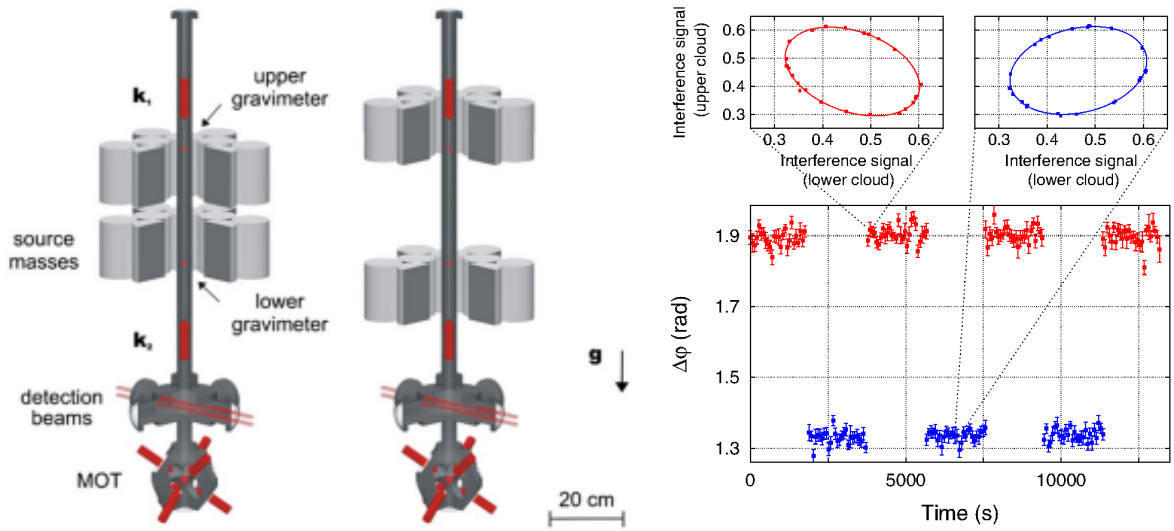

FIGURE 1.4 — [from [11]] (Left) Schematic of the gravity gradiometer setup with the Raman beams propagating along the vertical direction. During the G measurement, the position of the source masses is alternated between the close and far configuration. (Right) Modulation of the differential phase shift measured by the atomic gravity gradiometer when the distribution of the source masses is alternated between the two configurations. Each phase measurement is obtained by fitting a 24–point scan of the two phase–linked interference fringes to an ellipse.

free fall, and measures the gravity gradient and not the gravity acceleration.

On-going efforts in the research groups in Florence [120] and Stanford [121] target a reduction of one order of magnitude on the overall uncertainty for the measurement of G, so as to become really competitive with the traditional methods. In this regard, [121] already proved a compatible sensitivity and stability of the measurement, but the challenge is to control systematic effects at the required level. It is worth mentioning that two different approaches have been recently proposed to improve the performance of atom interferometers in measuring G: the first promises to increase the SNR of the measurement by confining the atoms in hollow-core-fibers (HCF) to drastically reduce the distance between the atomic ensemble and the source masses [122]; the second exploits weak measurements to amplify the atomic motion and then the measured signal [123].

1.3 Atom Interferometry for GW detection

GWs are predicted by GR, and their indirect observation relied on the accelerated pulsar rate in binary systems as first measured by J. H. Taylor and J. M. Weisberg [124]. The first direct detection of GWs in 2015 arrived after 50 years of technological development thanks to LIGO-Virgo, when the coalescing phase of a binary black hole system was detected by the two giant Michelson interferometers operated in US [125]. Virgo soon joined the race, and in only three years several landmark discoveries have been achieved; to mention a few, the detection so far of 11 BBH mergers [126], the standard-siren measurement of the Hubble constant [127], the observed merger of binary neutron stars [128], which resulted in a multi-messenger detection thanks to several electro-magnetic coincident observations and gave a first measurement of the gravity propagation speed, equal to c within 1 part in 10^{15}.

Despite being so successful, only a tiny frequency window (40 Hz – 1 kHz) of the gravitational spectrum is open to observe the Universe, and the development in the field is mainly driven by two objectives: (i) broaden the worldwide network of active instruments (LIGO-India and KAGRA should

join the measurement runs in the early 2020s), to increase the confidence margin in each detection event and to improve the parameter estimation - especially as concerning directionality - thanks to the increased amount of data; (ii) enlarge the observation window with improved instruments (e.g. Einstein-Telescope project) or add new ones with novel detection methods (LISA and DECIGO space-based optical interferometers in the mHz to deci-Hz band; several Pulsar Timing Array projects in the nano-Hz range; EinsteinHome project [129] to find continuous GWs from pulsars in the tens of Hz range), to increase our knowledge of cosmology and astrophysics by detecting new kinds of GW sources and approaching the temporal observation horizon to the Early Universe.

Earth-based instruments have the advantage of requiring only a fraction of the funding of space-based devices, and allow a far simpler maintenance. Nevertheless, two critical issues must be faced: (i) the masses probing spacetime must achieve a high quality free fall in the measurement bandwidth, task of increasing difficulty when approaching frequencies around 1 Hz or below and analyzed in [130], where several solutions are proposed (notably, one adopts atoms in free fall along geodesics, and AI to track their motion); (ii) the GW signal must be discriminated form the huge background caused by Gravity-Gradient Noise (GGN) [131], i.e. the gravity signal due to all what is moving nearby the instrument whether due to seismic, atmospheric, human or any other sources of activity. The standard approach to cancel – or at least mitigate – the impact on GGN on the GW measurement relies on optimized arrays of seismometers surrounding the optical interferometer to monitor seismic and atmospheric perturbations [132]. As we proposed in [133], the AI approach to GWD can adopt more than two ensembles of atoms on the optical link used to track spacetime evolution, which allow to separate pure gradients from signals with a more complex spatial signature, hence to mitigate the limitation represented by GGN.

A common problem for all the different approaches is how to optimize the data analysis in order to get the best output from the data streams. Different methods have been already adopted, like massive parallel computing adopted in LIGO-Virgo and with EinsteinHome, and combine data from different sources as is the case of multi-messenger astronomy and the detection of coalescing binary neutron stars that can count on both gravitational and electromagnetic data. A recently proposed technique uses data collected at different times and in different frequency bands with a potential high payout: by coupling LISA and advanced LIGO [134] it would be possible to have precise pre-alerts, improved sky localization and parameter estimation, and in general a more complete view of the detection events.

In this context AI is a novice technique, with the first feasible proposal being only 10 years old [79] (previous attempts were more speculative [135, 136, 137]). The basic scheme consists in monitoring the evolution of an optical link at its two far end not with suspended mirrors set in free fall in a well defined frequency window, but with atomic matter waves in free fall. The AI approach presents similarities to the optical interferometry one – tracking the motion of the gravity probes along geodesics with an optical link; being subject to laser technical noise in the initial configuration, which demands two orthogonal baselines – but also pivotal differences – quantum instead of classical probe masses, and possibility to put them in free fall also on Earth and not only in space; feasibility of a single baseline detector configuration using atoms normally adopted for timekeeping [138]; tweaking of the sensitivity function by simply changing the pulse sequence, useful to peak it at specific frequency intervals [52]; possibility to mitigate GGN using arrays of probes along the optical link [133]. Interestingly, a recent proposal to adopt atomic clocks for GWD [139] has been proved to be fully equivalent to the standard AI approach [140].

After an initial phase when several Earth- and space-based configurations specifically oriented towards GWD were considered, we are now in a second phase that sees demonstrator instruments being developed: the horizontal, 150 m long MIGA [141] will soon be installed at LSBB, and its underground

infrastructure is being realized; the 100 m long MAGIS-100 [142] will make use of an existing vertical shaft at FERMILab; a horizontal, 3×1 km device is in construction in Wuhan (China) [143]. Other activities are being proposed at the national (UK with AION [144], Italy) and international level (European ELGAR project [145], and AEDGE proposal [146]) to build other facilities targeting the mid-band frequency band (10 mHz – 10 Hz) on Earth or in space. At the same time, initial studies are addressing the potential payoff of having gravitational observatories in this band, in terms of possible sources [147] or an improved knowledge of the events eventually detected at higher frequency by optical interferometers [148].

This first generation of instruments will have a peak sensitivity of 10^{-13}–10^{-14} $\mathrm{Hz}^{-1/2}$ in terms of strain PSD, which means 5 orders of magnitude short in relation to the strongest expected signals in the target window. Several technological and fundamental issues must be tackled to achieve the required performance, starting with improved manipulation techniques required to boost the sensitivity, as is the case of large momentum splitting [50, 149, 150] and spin squeezing [151, 152], and combining them on the same experimental setup; data analysis protocols for AI based GWD have to be devised; known background noises, as GGN, as well as unknown potential systematic effects must be carefully addressed to evaluate and mitigate their impact [153].

1.3.1 Role of AI in Gravitational Wave Astronomy

The prospect of achieving strain sensitivities compatible with a detection in the infrasound band with AI responds to the need of widening the observation window opened by LIGO-Virgo in the gravitational spectrum. A future AI based GWD will be complimentary to the Earth based (LIGO-Virgo) and the planned space (LISA) optical interferometers, filling the sensitivity gap between them in the frequency spectrum. An open issue concerns the identification of potential GW sources in the specific bandwidth: astro-physical sources of GWs at ≈ 0.1 Hz have been studied in [147, 154, 155], and other more exotic sources have been taken into account like environmental effects from scalar fields and Dark Matter (DM) particles around merging compact objects [156, 157, 158], cosmological phase transitions [159], and the formation of primordial black holes [160]. Unlike for LISA where millions of BHBs and NS-NS inspirals will clog the observation band, astro-physical events will rather separately sweep the AI target band in the infrasound, opening towards the detection of stochastic GW background from the early evolution of the Universe [161, 153, 162].

More in general the role of AI in GW astronomy has to be defined. A first work [148] has shown what would have meant having a working AI based GWD – on Earth or even better in space – for the GW150914 event, i.e. the first detection operated by LIGO-Virgo: the chirping GW frequency signal would have spent almost 10 months in the detection band, giving time and data for a much improved sky localization and a precise alert signal to the optical interferometers for the optimal detection of the merging. But other fascinating possibilities have to be investigated in relation to the so-called *Multiband GW Astronomy*, studied in [134] for the coupling of eLISA and Adv-LIGO: combining the two instruments will make possible precise gravity and cosmology tests by tracking compact binary inspirals till their merging, and as well the mutual validation and calibration of the two instruments. Combining an AI based GWD with optical interferometry instruments (see Fig. 1.5-right) will give multiple outcomes: (i) the coupling to the very low frequency eLISA will make the AI-GWD the high frequency side instrument, targeting the merging of massive binary systems (10^3 to 10^4 $M_\odot$) which will never reach the LIGO-Virgo detection window; (ii) the coupling to LIGO-Virgo will instead give to the AI-GWD the task of tracking the inspiral phases of events later to be detected by the optical interferometer. Another possibility is to use an AI-GWD to mitigate the effect of GGN on Earth based optical GWD [133]: adopting the two approaches on the same optical link would improve the

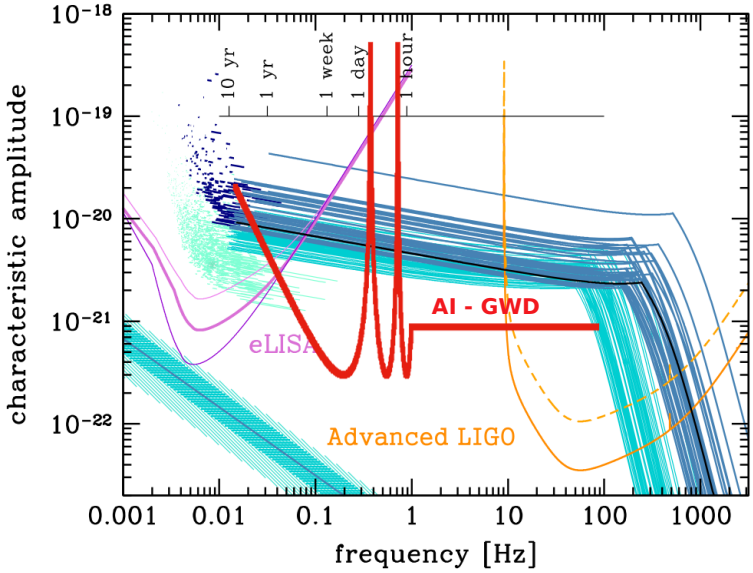

FIGURE 1.5 — [adapted from [134]] Multiband GW astronomy: the sensitivity curve of a future AI based GWD (red) is compared to the sensitivity curves of Adv-LIGO (yellow) and eLISA (violet). The blue curves represent characteristic amplitude tracks of BHB sources; the track completed by GW150914 is shown in black. AI will fill the sensitivity gap between space and Earth based optical GWDs, opening the possibility to follow the inspiral phase of merging events that will be detected by the advanced-LIGO, or to see the merging of events at lower frequency.

sensitivity curve at low frequency for the optical instrument, specially if the AI array geometry is adopted to map the GGN. It will be interesting to evaluate the impact of different generations of AI GWD for this specific purpose, starting with the MIGA demonstrator.

1.4 MIGA experiment: demonstrator for GW detection and geophysics

Since 2013 I moved to LP2N–Bordeaux, and I am working at the Matter wave-laser based Interferometer Gravitation Antenna (MIGA) experiment as chief scientist. The project has been financed as an Équipement d'Excellence (ÉquipEx program), and its PI is Dr. P. Bouyer. MIGA will realize a 150 m long, horizontal atom gradiometer to study gravity at large scale. The experiment will be realized at the underground facility of the LSBB in Rustrel–France, a site located away from major anthropogenic disturbances and showing very low background noise. Three atom interferometers will be simultaneously interrogated by the resonant mode of an optical cavity. The instrument will be a demonstrator for GW detection in the mid-frequency band (10 mHz–10 Hz). In the initial instrument configuration, standard atom interferometry techniques will be adopted, which will bring to a peak strain sensitivity of $2{\cdot}10^{-13}/\mathrm{Hz}^{-1/2}$ at 2 Hz. This demonstrator will enable to: (i) study the techniques to push further the sensitivity for the future development of gravitational wave detectors based on large scale atom interferometers; (ii) devise specific measurement protocols for GW astronomy; (iii) test noise rejection protocols to mitigate the issue represented by GGN. Moreover, MIGA will bring the study of both fundamental and applied aspects of gravitation to a new level, thanks to its tenfold size increase with respect to existing experiments. The result will be an equally tenfold increase in the gravity-gradient sensitivity, with important implications for geophysical studies at the underground laboratory – we are studying how to couple the AI based instrument to other instrumentation moni-

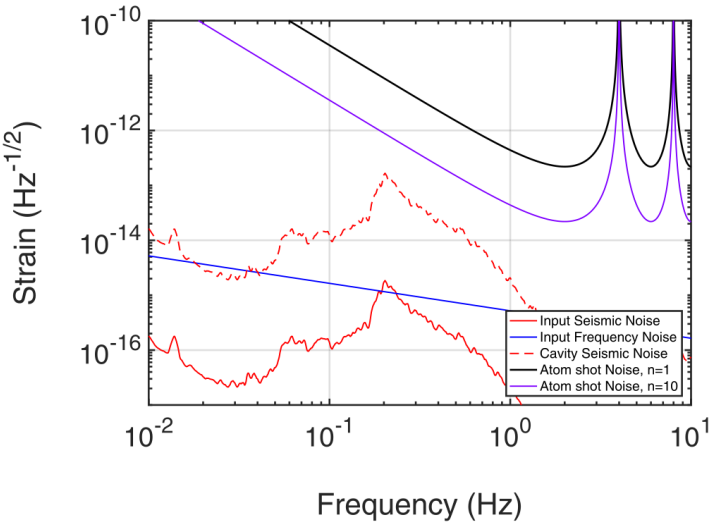

FIGURE 1.6 — [from [141]] Projection of the different noise sources on strain sensitivity, for the specific case of the MIGA instrument and typical seismic conditions at the underground site of LSBB.

toring the underground environment, like seismometers, tiltmeters and radar spectrometers, in order to extend the concept of hybrid classical-quantum sensor introduced in [163].

1.4.1 Atomic gradiometer as GW sensor

The use of an atomic gravity-gradiometer as a GW detector has been first considered in [36], where two configurations are considered, one terrestrial and another satellite based. This solution builds on the sensitivity of each atomic sensor to the local phase of an optical link, and exploits them as "quantum replacements" of the optical components in a Michelson-Morley interferometer. Several studies followed, with improved multi-pulses configurations to shape the sensitivity curve [52] or remove certain kinds of backgrounds [164, 165], specific space configurations [164, 166, 167, 139], or clever solutions to address certain noise sources, e.g. the laser technical noise [138] and GGN [133].

The ultimate limit for these detectors is represented by the phase sensitivity of the instrument, which is typically given by the quantum projection noise (QPN) [168] improved by two techniques: (i) the statistic noise reduction obtained by the exploitation of non classical atomic states [151, 152]; (ii) the repeated imprinting of the optical link phase on the atomic wavefunction by means of large momentum transfer (LMT) atom optics [50, 149, 150]. However, several factors will effectively limit the detector sensitivity before reaching the quantum limit, and each one with specific spectral signatures. A detailed review of these factors has been presented in [36], where however the focus is on the stochastic component of each background source. Noise contributions with long coherence time, that cannot be efficiently mitigated by averaging, are assumed to be cancelled by correlating the signals of far located detectors [161].

In [141] we studied the instrument sensitivity curve for the MIGA instrument, without taking into account any data analysis techniques. In details, we studied the impact of the technical noise of the interrogation laser, the vibrations of the instrument elements, the fluctuations of the atomic initial conditions, and of GGN. As shown in Fig. 1.6, all these backgrounds will not impact the initial sensitivity of MIGA, but will soon become dominating when the instrument performances will be improved. Increasingly stringent requirements will be set on the phase and frequency noise of the interferometric laser, on the timing of the interferometer sequence, and on the residual motion of the

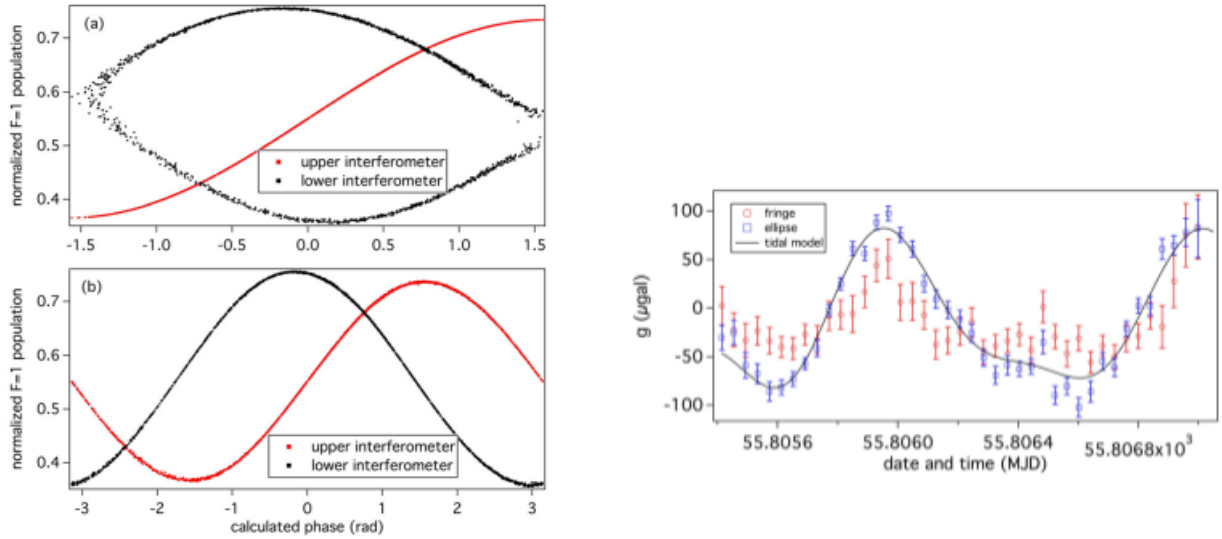

FIGURE 1.7 — [from [88]] (Left) Fringes for T=160 ms reconstructed by computing the phase ϕ in (a) from the upper interferometer, in (b) from the two simultaneous Raman atom interferometers, subject to the same seismic noise and with a fix phase offset given by the Earth gravity gradient and their vertical separation. (Right) Earth's gravity as a function of time, measured with a single interferometer (red), and with the dual one (blue); in black is shown the predicted Earth's tide according to the Earth Gravitational Models (EGMs) [169].

retro-reflecting mirror. The latter effect will need high quality isolation and suspension systems, which adopt and push forward key concepts devised for GW detection at low frequency based on optical interferometry. Nevertheless, the main limitation in a large section of the sensitivity window will be represented by GGN: to mitigate its impact we introduced a configuration based on an array of sensors (see ref. [133]), as described in the next section.

1.4.2 Signal from an array of AIs

The possibility to utilize two or more atomic sensors on the same optical link can be exploited to gain spatial information on the gravity field. In Florence, we already demonstrated that two interferometers allow the simultaneous measurement of gravity and its gradient [88], and my previous colleagues further worked on the topic by measuring gravity curvature using three atomic sensors in [170]. These finding could have important applications in geophysics: our scheme reduces the effect of seismic noise on the gravity measurement, and we demonstrated a 3 times higher sensitivity on the acceleration (Fig. 1.7). The experiment reports the first implementation of sensitivity enhancement in gravity probing using correlated measurements, method similar to phased array detection in radio-astronomy.

With these basis, we devised a scheme to tackle GGN, which is a fundamental problem affecting gravity-gradient sensors using two probe masses as is the case of LIGO-Virgo. We proposed to bypass this limitation with an array of gravity-gradiometers run simultaneously and coherently manipulated with the same optical link (see Fig. 1.8-left) [133]. By appropriately choosing the gradiometer baseline, and the spacing between successive gradiometers it is possible to efficiently average the effect of seismic or/and atmospheric perturbations (Fig. 1.8-right). Adopting at least 3 sensors instead of the common 2 has become the baseline configuration in the recent proposals for AI based GWD on Earth, as is the case of MAGIS-100 being realized in US [142].

We are now evaluating optimized configurations to increase the rejection factor in specific frequency bands, and considering real atmospheric and seismic noise data collected at LSBB [171, 172]. In 2018

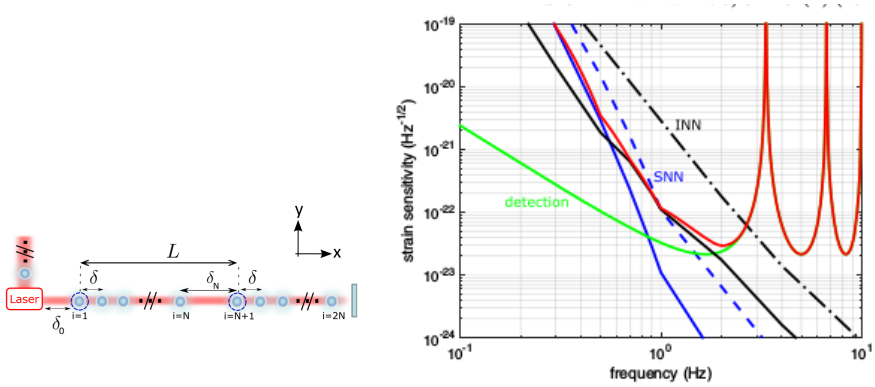

FIGURE 1.8 — [from [133]] (left) Array of gravity-gradiometers to sample the spatial variations of GNN and average its effect, so as to increase the signal-to-noise ratio for a GW detection. (right) Strain sensitivity curve for an array of interferometers (red curve), after mitigating the effect of atmospheric (black dashed-dotted curve) and seismic (blue dashed curve) so as to obtain the continuous curves. The detection noise is shown in green.

we realized a measurement campaign at the site where the MIGA antenna will be installed, and we compared noise spectra recorded in the galleries and outside. Projecting the real noise curves into strain PSD for the foreseen antenna geometry confirmed that GGN will not limit the sensitivity of the demonstrator in its initial phase. Nevertheless, the instrument will allow the study of GGN signals by integrating the signal over a few tens of seconds; this possibility relies on the intrinsic accuracy of the AI based measurement. In this way it will be possible to validate and refine GGN noise models by comparing the Allan variance of the averaged atomic phase with its expected value from the projection of external seismic and pressure measurements.

1.4.3 MIGA instrument

The realization of the very-large baseline atom interferometer (VLBAI) represented by MIGA represents a new paradigm in AI: till now the common experiments in the field could fit on standard optical bench-tops, and only in a handful of cases they reached the 10 m size [108, 173, 174] or required bigger infrastructures [103, 105, 106]. The underground experiment we are building required a new approach for its realization, with the formation of a consortium where each partner is dedicated to a specific sub-system (a scheme of the experimental setup is shown in Fig. 1.9). Namely, SYRTE Observatoire de Paris realizes the atomic sensors, the company μQuans the laser system, CELIA the high power laser for the coherent manipulation, and LSBB the underground infrastructure. At LP2N we realize the cavity enhanced interrogation of the atoms, and we coordinate the activities of the other partners. In this regard, my specific activity has been multifaceted: I contributed to the design of the laser architecture developed by the μQuans company for the preparation of the Rb atomic clouds [175]; devised the cavity locking scheme (see Fig. 1.10), on the basis of the know-how acquired on the cavity QED experiment described in the following chapters, and that allows to implement a cavity enhanced pulsed sequence by tracking the cavity length fluctuations with a telecom laser; I am in charge of realizing a strontium atomic fountain, a key development for MIGA, in the frame of the ANR project "ALCALINF" (see Sec. 1.4.5); I developed the complex real-time control system required to synchronize several distant atomic sensors, in collaboration with Dr. Prevedelli (Bologna Univ. – Italy) [176]; I contributed to the definition of the requirements for the tunnel boring and for the 150 m long UHV system.

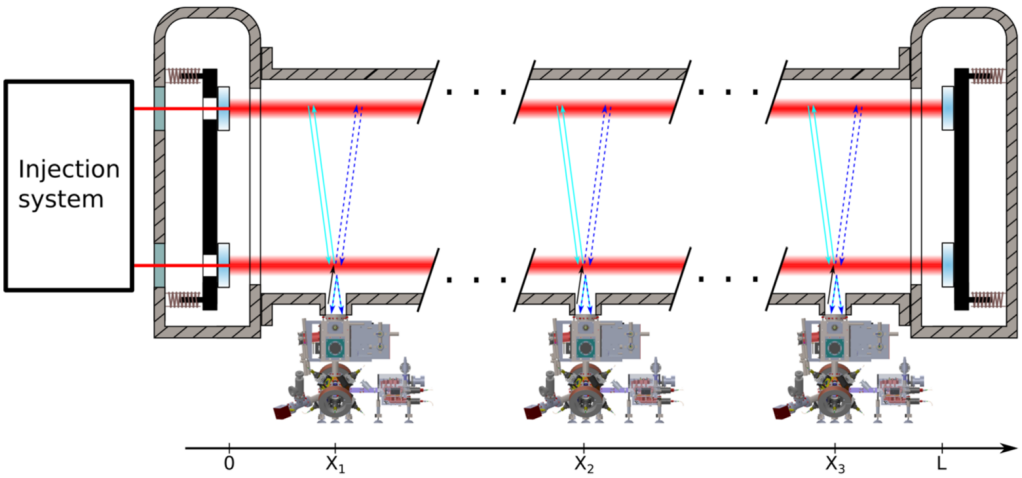

FIGURE 1.9 — [from [141]] Overview of the MIGA instrument with the main sub-systems, not in scale. Three atomic heads at positions $X_{1,2,3}$ launch atomic clouds in an almost vertical parabolic flight (dotted lines); the atoms are manipulated in the upper part of the parabola with a Bragg interferometric sequence with light pulses at 780 nm (red horizontal lines) resonant with two horizontal cavities. The ultra-high-vacuum system encompassing the optical cavities, the mirrors payloads and their stabilization system is represented in gray; the atomic heads are connected to its lower side. The control system of the experimental setup, the laser systems dedicated to each atomic head, and the μ-metal shield enclosing each interferometric region and the related atomic head are not represented in the figure.

1.4.4 Cavity enhanced AI

A specific topic we are studying in relation to MIGA and LP2N's main contribution to the project is cavity-enhanced AI; this subject shares a consistent overlap with the techniques I developed on the cavity QED experiment. Generating the light pulses for the coherent manipulation of matter waves with a resonator bring three advantages: (i) power enhancement; (ii) spatial filtering; (iii) interferometric control of the light wavefront [177]. The related drawback is given by the obvious need to maintain the light frequency locked to the resonator, task that becomes more demanding when the experimental sequence requires a pulsed beam. The adopted solution relies on the stability transfer obtained via frequency doubling of a telecom laser at 1560 nm continuously locked to the interrogation resonator (see Fig. 1.10). The cavity optics need a double reflecting coating at 1560 nm, used for the continuous tracking of the cavity, and 780 nm, required for the coherent manipulation of Rb atoms via pulses generated with an AOM.

To test the cavity aided interferometry on freely-falling atoms we realized a prototype experiment, where cold Rb atoms launched in a fountain configuration are probed along the horizontal direction using the e.m. field of a compact optical cavity. Since the experiment uses atoms at the μK temperature, the ballistic expansion of the atomic cloud results a limiting factor for the fringe contrast. Having a wide manipulation beam is thus key for maintaining a good SNR, not an easy target with a short cavity configuration. To solve such problem we revisited optical solutions devised in the '70s to reduce the transit broadening in high resolution spectroscopy using parabolic mirrors [178]: using a lens inside the cavity we could obtain a configuration that combines a big waist and a short length [179] (Fig. 1.11). This solution and its implication in AI and more in general in AMO physics are the subject of a patent [180]. It must be remarked, however, that the specific problem of having a wide cavity waist will not affect longer configurations, as is the case of the MIGA demonstrator.

Another subtle limitation that affects cavity-enhanced AI has been pointed out by the group of A.

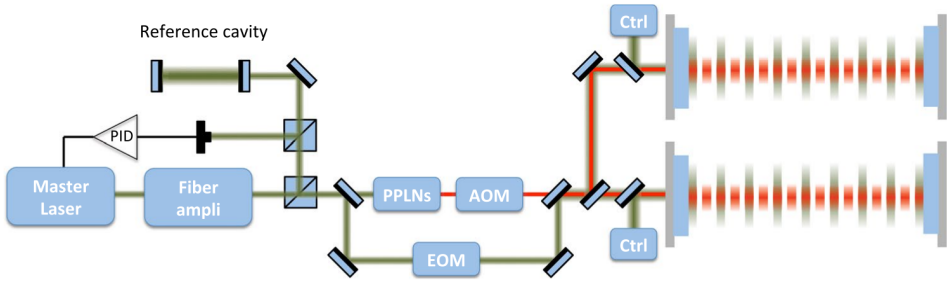

FIGURE 1.10 — [from [141]] Scheme of the laser interrogation system. A master laser at 1560 nm (in green) is amplified and locked to a reference cavity, before being frequency doubled to obtain the interrogation radiation at 780 nm (in red). The master laser is frequency locked to one of the two interrogation cavities, whereas the component at 780 nm is pulsed via an AOM.

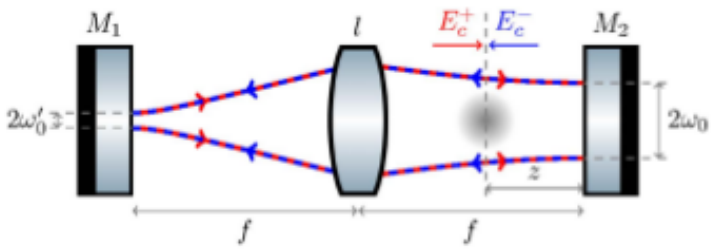

FIGURE 1.11 — [from [179]] Parallel-plane resonator with a lens at its center to obtain a wide waist on the right side of the configuration, and make possible the manipulation there of a thermal cloud.

Freise in Birmingham. The coherent manipulation of matter waves requires multiple, short and intense light pulses [177, 179, 181], which implies high cavity finesse $\mathcal{F}$. Increasing the strain sensitivity in gradiometric configurations considered for GW detection requires a long cavity length L [36, 79, 133, 141]. Increasing $\mathcal{F}$ and L of the cavity has the effect of reducing its linewidth:

$$\Delta\nu = c/\left(2nL\mathcal{F}\right), \tag{1.30}$$

where c is the speed of light in vacuum, and n the index of refraction inside the cavity. Despite seeming promising to reduce the cavity linewidth to increase the sensor performances, a limitation exists for $\Delta\nu$, beyond which the pulses used to manipulate the matter waves undergo important deformation, and the effective optical power enhancement worsens. In short, the inherent frequency response of the cavity sets a physical limit to the product $L\mathcal{F}$, and forbids long baseline detectors based on high optical gain resonators for manipulating matter waves.

This issue directly seems to hamper the very basic scheme of MIGA based on long, high finesse cavities for AI. To circumvent it, we proposed a novel scheme to coherently manipulate the atomic wavefunction in a narrow linewidth cavity, "designing" the interaction pulses not changing the intensity of the intra-cavity laser, but acting on an auxiliary process, whose function is to enable or inhibit the coherent process that relies upon the cavity enhanced laser. The latter is always injected in the optical resonator, hence its intensity is constant in time. The main approach we analyzed exploits light-shift engineering of the atomic levels, a technique adopted in several contexts concerning cold atoms, e.g. to cancel the trapping light perturbation in optical lattice clocks [182], laser cool atoms to BEC [183], precisely characterize the geometry of an optical cavity [184], and compensate gravity [111]. We are also considering an alternative protocol based on magnetic field induced spectroscopy [185] to control

the coherent process.

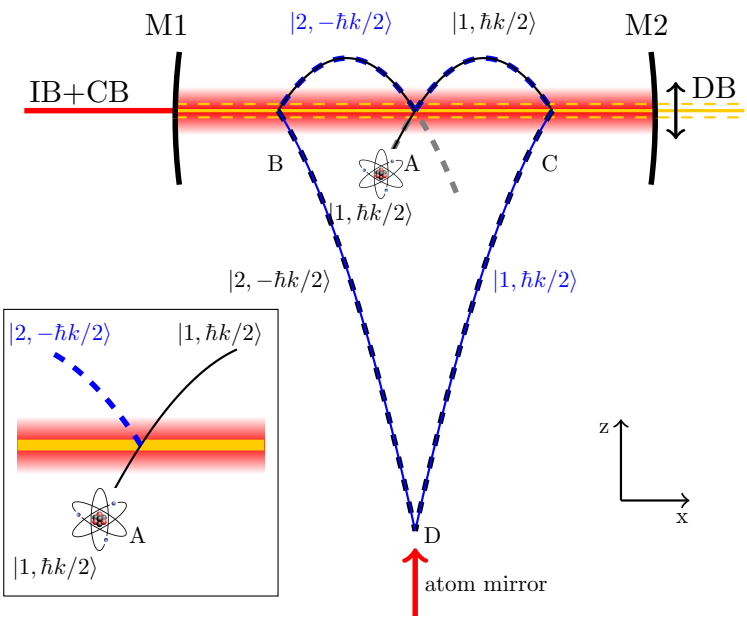

FIGURE 1.12 — [from [186]] Schematic of the proposed experimental setup not to scale: the atomic ensemble, initially in the state $|1\rangle$, crosses the cavity-enhanced IB with a positive horizontal velocity equal to half the recoil velocity $v_r/2$, and is split in the region A (see inset). The two parts of the wavefunction are horizontally reflected with a π pulse in the regions B and C; in D their vertical velocity is reflected, and after a second horizontal velocity reflection in C and B, respectively, they are recombined in A with a last $\pi/2$ pulse. The two trajectories at the output of the interferometer are shown in gray. The horizontal DB (yellow) is not resonant with the cavity, is shone on the atoms and vertically follows their motion to have an optimal overlap. CB is the beam required to compensate the differential light shift induced on the clock transition by IB. M_i: cavity mirrors.

We studied the scheme for strontium atoms, manipulated on the narrow clock transition at 698 nm by an interferometric beam (IB), as shown in Fig. 1.13-left. The 2 m long, $\mathcal{F}$=10^5 cavity considered in Fig. 1.12 has a linewidth of 750 Hz, which means a photon lifetime $\tau_\gamma \sim 220$ μs. The action of IB, always injected in the cavity, is controlled through a dressing beam (DB) that shifts the levels $|1\rangle$ and $|2\rangle$ so as to break the resonance condition for IB. The DB must satisfy several conditions, namely induce an associated negligible scattering of photons while generating a large light shift on the clock transition: in the visible spectrum only a narrow frequency band fulfills the requirements to implement AI, as shown in colors in Fig. 1.13-right. Interferometric pulses with a duration comparable or even smaller than τ_γ can thus be implemented, without modulating the IB driving the two photon transition. The result is that cavities with a very narrow linewidth – hence long baseline required for GWD and high Finesse needed to clean the spatial mode – can be used in AI.

1.4.5 MIGA road-map

The two orthogonal, dedicated galleries for the MIGA antenna have been bored in the first half of 2019, and they will be finalized as concerning the electrical and connectivity installations by the end of the year. The company SAES-RIAL already started to realize the 25 sections of vacuum pipe, each 6 m long, that will constitute the vacuum enclosure of the optical link, as can be seen in Fig. 1.14. At the same time the colleagues at SYRTE are completing the 3 atomic sensors to be installed along the antenna arm, and the related laser systems are already functioning. Our – most probably

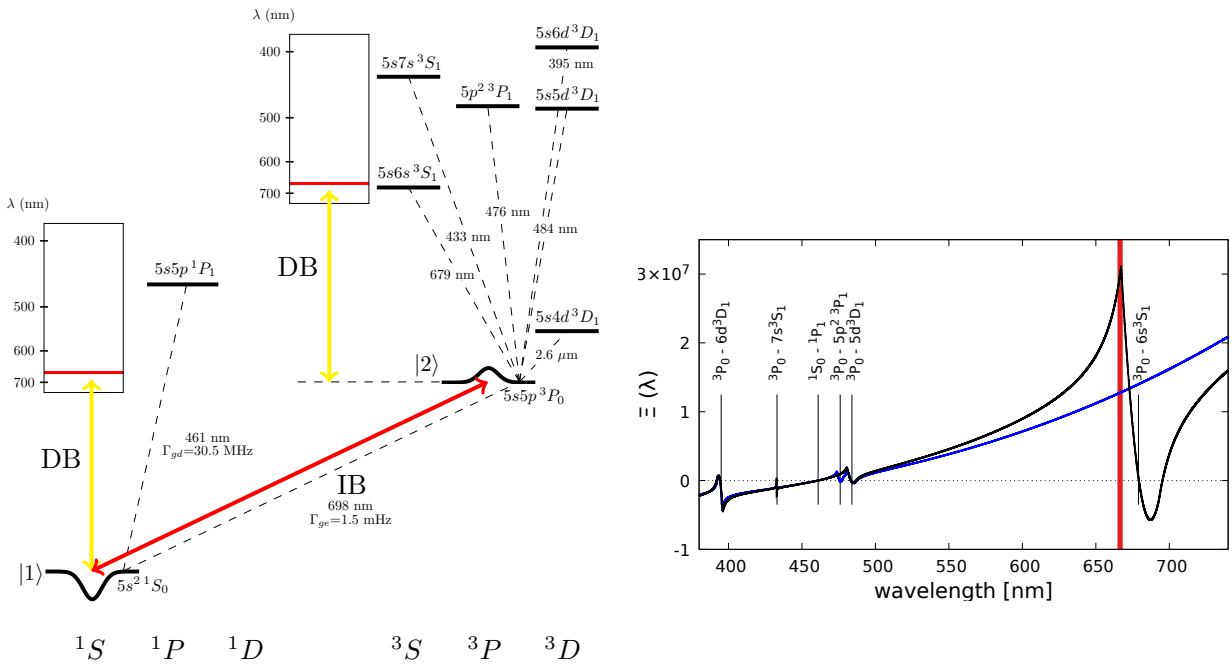

FIGURE 1.13 — [from [186]] (left) Diagram with the relevant levels for ^{87}Sr atoms. The red arrow shows the IB resonant to the $|1\rangle \rightarrow |2\rangle$ transition at 698 nm adopted for the coherent manipulation of matter waves; the yellow arrows the DB used to shift the two levels $|1\rangle$ and $|2\rangle$. The action of the DB is considered when varying its wavelength over the range [380–700] nm, indicated by the vertical bars referenced to the two levels $|1\rangle$ and $|2\rangle$. The narrow red band indicates the spectral interval where the DB constitutes an effective switch for the coherent action of IB, by light shifting in a differential fashion the clock levels $|1\rangle$,$|2\rangle$. The level structure has been taken from [187, 188]. (right) Ratio $\Xi(\lambda)$ between the light shift induced on the $|1\rangle - |2\rangle$ transition and the overall scattering rate by a laser at a wavelength λ, with 380 nm$< \lambda <$700 nm. In black (blue) the curve when the polarization of the DB is parallel (perpendicular) to the magnetic field. The region where $\Xi(\lambda) > 2.8 \times 10^7$ is indicated with a vertical red band. The relevant transitions contributing to the atomic polarizability in the visible spectrum are indicated with vertical lines.

too optimistic – plan reserves the first half of 2020 to the installation of the instrument, whereas the second half of the year will be dedicated to its commissioning.

Following such schedule, in 2021 the MIGA instrument will be fully operative. Running the experiment will be on its own an important achievement given its unprecedented baseline size. The main task will be then to finely tune the machine to achieve the expected PSD strain peak sensitivity of $2 \cdot 10^{-13}$ Hz$^{-1/2}$; this task will require the optimization of all the instrument sub-units, and of the measurement protocol. The three initial atomic sensors separated by ∼70 m will need a precise synchronization to optimize the overall SNR. Last, a metrological and physical approach to the measurements will be essential: large amount of data will need precise time-stamp to track time dependent signals; systematic effects must be identified and evaluated; complex experimental sequences, based e.g. on interleaved measurements [189, 62], must be devised and implemented.

Once attained the expected performance, it will be time to overhaul the experiment to push the sensitivity to better levels. As said, the MIGA gravitation antenna will be a demonstrator for AI based GWD: its strain sensitivity will be too low by at least 5 orders of magnitude to observe the GW signals expected in the band of interest. Filling this gap demands a major effort at several levels: upgrade of the experimental setup, definition of data analysis and measurement protocols, addressing systematic effects, test new geometries and experimental procedures. Several of these actions are already being addressed with specific research activities at LP2N, that range from the development of

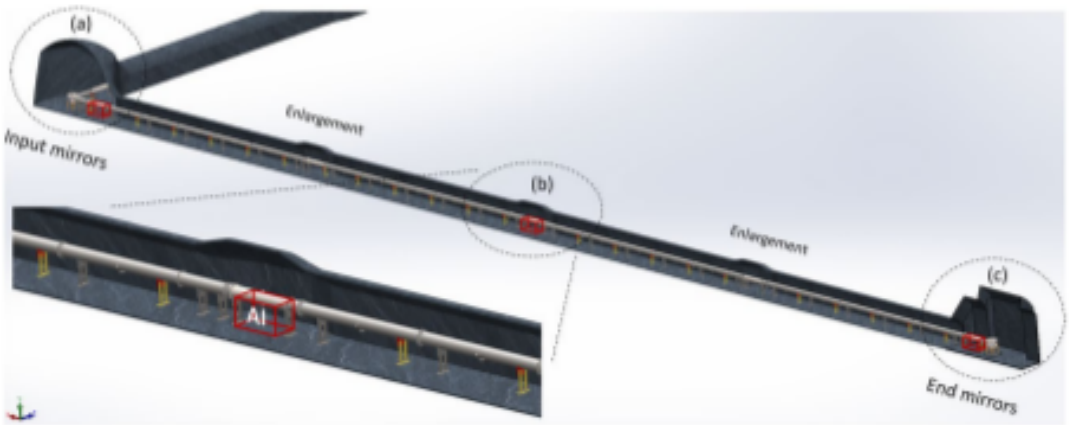

FIGURE 1.14 — [from [141]] Design of the galleries dedicated to the MIGA experiment at LSBB. The three atom interferometers of the antenna are located at (a), (b) and (c). The optical setups for cavity injection will be hosted in room (a).

new experimental techniques, and data analysis protocols as summarised in the following. On these topics we are leading the ELGAR (European Laboratory for Gravitation and Atom-interferometric Research) consortium at the European level; its target is to enable GW detection in the mid-frequency band, building on the first generation demonstrators like MIGA [145].

Sensitivity enhancement An AI-based GWD with a PSD strain sensitivity at 10^{-18} Hz$^{-1/2}$ or below in the target frequency band will require the simultaneous implementation of several state-of-the-art techniques, so far only separately demonstrated on dedicated experiments. That is the case of: (i) LMT techniques [50, 149, 150] to linearly increase the phase sensitivity with the number of photons coherently exchanged; (ii) improvement of the phase resolution capability, by implementing non-classical input states to beat QPN [152, 151], and adopting a higher atomic flux to make use of standard statistical enhancement; (iii) increase the baseline of the antenna to linearly improve the strain sensitivity. Different relevant approaches are being investigated in several French and European laboratories, and it will be crucial to define common requirements, geometries and experimental procedures for a next generation instrument that will contribute to the measurement runs in GWD. More in details, within the MIGA consortium LMT techniques are being investigated at LP2N and SYRTE-Observatoire de Paris, and I extensively studied the possibility to exploit quantum enhanced measurements in atom interferometry [190, 191]. The cavity approach pursued by MIGA has been recently put in question [192], in relation to the impossibility of using a narrow linewidth cavity – required to have a long baseline L (i.e. strain sensitivity) and a high Finesse $\mathcal{F}$ (i.e. good quality of the cavity mode) – to produce the short light pulses needed to implement the interferometric sequence. As explained above (Sec. 1.4.4), we studied an innovative solution to bypass such issue, based on light-shift engineering techniques [186]. Adopting the cavity configurations considered for advanced optical interferometers like ET (i.e. L=10 km and $\mathcal{F}$=10^2) seems feasible.

Systematic effects and data analysis At least as important as reaching the required sensitivity will be an in-depth analysis and estimation of a broad spectrum of systematic effects, ranging from uncertainties in the preparation of the internal/external degrees of freedom of the atomic samples, to black-body radiation, atomic interactions, and coupling with the environment to mention a few. In addition, low frequency GWD has to face the main issue represented by GGN, caused by the movements of all nearby masses, either of seismic, atmospheric or different origin. We recently proposed an innovative method exploiting arrays of atom interferometers simultaneously operated on the same

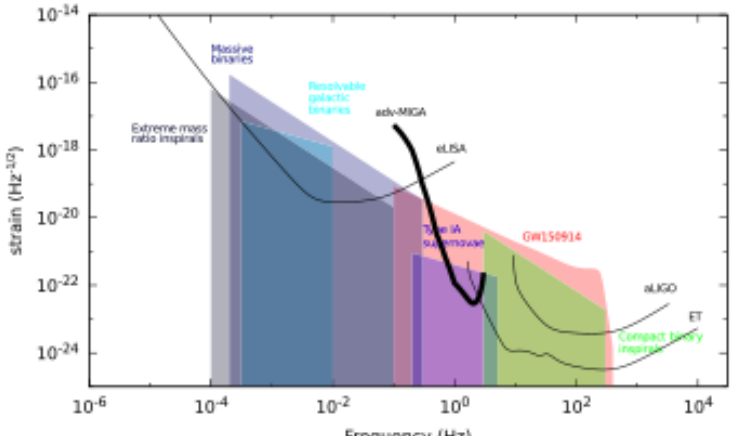

FIGURE 1.15 — [from [141]] GW strain sensitivity curves of the AI array proposed in [133] and those of eLISA, aLIGO and ET, compared to different low frequency GW sources taken from http://gwplotter.com/

optical link to discriminate between a potential GW and GGN [133]; the solution would mitigate the problem of differential gravity noise that limits LIGO-Virgo at the lower end of its sensitivity curve, and will ultimately allow the detection of GWs in the mid-frequency band with AI (see Fig. 1.15). We are now extending this work, studying configurations of atomic sensors optimized for the suppression of GGN in specific frequency bands, and using the LSBB as test-site to measure real noise spectra on which to evaluate the noise rejection algorithms [172].

Analysis of data from optical GWDs involves challenging problems in mathematics, statistics and signal processing: extremely weak signals must be isolated in a much louder instrumental noise, background rates must be estimated in the presence of non-Gaussian data, and signals described by multi-dimensional parameter spaces have to be detected and estimated. AI based GWD will have to develop similar analysis tools to process the data streams available in the future instruments; we envisage a dedicated research line to start addressing this subject, in collaboration with experts on LIGO-Virgo data analysis.

Atom interferometry using single-photon transitions As in LIGO-Virgo, laser frequency noise imposes the adoption of a two orthogonal arm configuration in AI-based GW detectors relying on two-photon transitions. A new detection protocol based on the advances of optical lattice clocks [193, 194, 55] can operate a single baseline GW detector immune to frequency laser noise [138]. Several laboratories started dedicated experiments to develop such scheme [195, 196], and begin to study the possibilities it opens, such is the case of improved sky localization in GW detection by exploiting the motion of the Earth around the Sun or of a satellite setup around the Earth [52]. In this context, I am coordinating at LP2N the realization of a strontium atom gradiometer in the frame of the ANR "ALCALINF"; its target is to realize a 8 m tall fountain to implement AI free of the technical limitation imposed by the laser phase/frequency noise, an use it to develop GW measurement schemes for vertically separated atomic sensors. The experiment already produced its first cold atoms: a compact atomic source similar to [197] and developed in collaboration with Majulab in Singapore routinely produces a 2D magneto-optical trap (MOT) and then an atomic beam that has been already detected in the science chamber. The laser system for the second stage red MOT (narrow cooling laser at 689 nm plus repumpers at 679 nm and 707 nm), as well as the narrow, cavity stabilized clock laser at 698 nm are implemented. The activity is presently slowed down by the difficulty of obtaining the required optical power for the first stage blue MOT at 461 nm, for which we developed a fibered based

amplifier [198] that we are actually testing for the second harmonic generation in a linear cavity.

This experimental activity originated the novel cavity interrogation scheme described in Sec. 1.4.4 to produce effective pulses shorter than the photon lifetime in the resonator [186]; we plan to push forward this idea by considering a rapid succession of vertical atomic launches in a lattice, by means of an auxiliary process acting as a switch.

1.5 AI for experiments operated in space

Reseach activity mainly carried out within the frame of three projects financed by ESA: "QWEP" and "STE-QUEST" to study a WEP tests in space; "CAI-GG" for space geodesy. Following this activity, I have been recently admitted to the Fundamental Physics Advisory Group of CNES.

Space is the ideal environment to operate an atom interferometer, given the perpetual free fall condition that removes the limitation set by the gravitational acceleration, namely the relative motion of the freely-falling atomic ensemble with respect to the experimental apparatus. This unique issue has several technical consequences that make the realization of long interrogation times T on Earth challenging: first of all the UHV setup must grow quadratically in size with T, to avoid the atom colliding with the internal surfaces of the vacuum setup; controlling the systematic effects over a large region becomes increasingly demanding; the gravitational acceleration determines a linearly varying Doppler shift that must be compensated to probe the atoms. In addition, often limiting issues of Earth-based experiments, like seismic noise and GGN, are substantially reduced in space.

Surrogate solutions to reproduce space representative conditions are: (i) atomic levitation [199, 200, 109, 201, 202, 111]; (ii) atomic bouncing [110, 203, 25] – an effective levitation with the action against the gravity pull "concentrated" in periodic pulses instead of being constant in time; (iii) temporary free-fall in microgravity conditions [103, 105, 106, 104]. All these techniques are of key importance to develop and test the technology in view of spatial missions, but they are affected by limitations. Levitating schemes suffer of vibration noise coupled in by the trapping potential, and in the case of magnetic trapping gravity limits the minimum achievable confinement strength, hence temperature [204]. Microgravity environments obtained on parabolic flights, rockets, or Einstein elevators offer only short time intervals of free fall.

On the other hand, space can allow very long interferometric sequences, hence intrinsic sensitivity, by optimally exploiting the extremely low expansion energy of pico- or femto-kelvin ensembles obtained by releasing a BEC and later collimating it with the "delta kick" technique [205, 103, 80]. Space is therefore the ideal environment to combine the extreme precision and accuracy achievable with atomic inertial sensors. As a consequence, a big effort has been focused in the last 10 years on preparing missions for space-based atom interferometry, and thanks to this heritage there is now a first cold atom experiment running on the ISS, which is planned to produce interferometric fringes soon: the Cold Atom Lab (LAB) developed by NASA [107]. CAL is a multi-purpose platform with several targeted research applications, ranging from the observation of new ultra-low temperature regimes and long probe times to pilot atom interferometry experiments. The field of space AI is however in turmoil, as proven by the recent surge in the number of AI proposals for fundamental and applied science in space [164, 138, 167, 139, 206, 52, 97], also in response to the ESA call "Voyage 2050" [146, 207].

During the last 8 years, I dedicated a consistent share of my activity to the sub-field of air- and space-borne AI, spanning different guidelines:

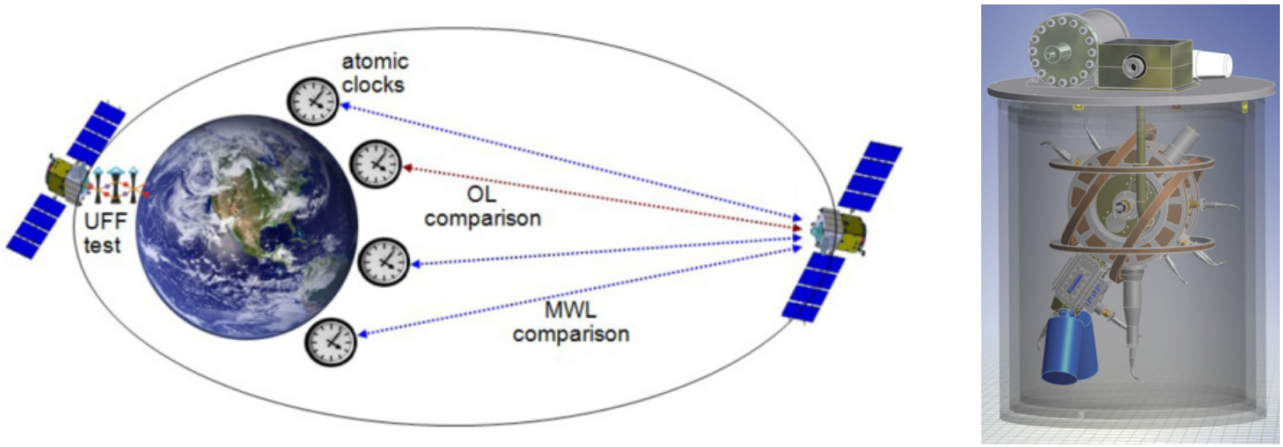

FIGURE 1.16 — [from [208]] (left) General concept of the STE-QUEST mission. The clock on the satellite is compared with one or more ground clocks as the satellite orbits earth on a highly elliptic orbit. During the perigee the local acceleration of two rubidium isotopes is measured and compared. (right) CAD drawing of the STE-QUEST physics package.

- specific contributions to the ICE (Interférométrie Cohérente pour l'Espace) experiment lead by P. Bouyer and B. Battelier, and operated on the 0-g plane of Novespace. In details, I helped improving the data extraction technique from the two species correlated interferometers operated simultaneously to test the WEP [209]; contributed to solve a thorny mechanical issue during a parabolic flight campaign, which allowed the realization of the first double interferometer operated in weightlessness [105]; collaborated to the recent realization of a Rb BEC in microgravity [104], by adapting the dark state cooling technique developed on the cavity experiment [210];

- participation to international collaborations to study possible space missions employing AI to test the Weak Equivalence Principle on the ISS (ESA study "Q-WEP", targeted accuracy on WEP: 10^{-14}) and on a satellite (proposal "STE-QUEST" for a Cosmic Vision Mission, targeted accuracy on WEP: 10^{-15}) [208, 74, 211, 212, 207] (see Fig. 1.16). My contribution concerned the telecom technology at 1.5 μm and successive doubling to obtain radiation at 780 nm to address rubidium atoms; the study of the optical dipole trap for the two atomic species (isotopes ^{85}Rb and ^{87}Rb); the definition of the instrument specifications and requirements;

- participation to the ESA study "CAI-GG" to perform high resolution space geodesy with a satellite-based gravity-gradiometer [97]. My specific role concerned the study of the high resolution atomic detection system to recover diverse components of the inertia tensor;

- study the potential future contribution of AI to the field of GW detection, as described in detail in Sec. 1.3.1. Even if the present effort is directed toward the realization of an Earth-based demonstrator, there is no doubt that space will be the ideal setting to take advantage of the intrinsic performances of AI in relation to GWD. In this direction heads the White Paper proposing "AEDGE" [146], a cold atom experiment in space to search for ultra-light dark matter, and to detect GWs in the frequency range between the most sensitive ranges of LISA and LIGO-Virgo (see Fig. 1.17).

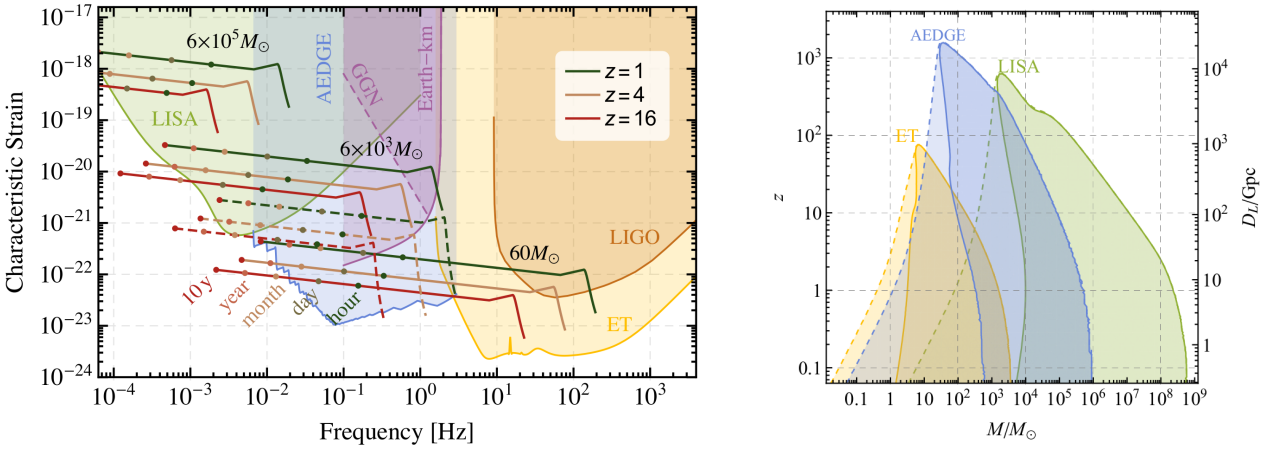

FIGURE 1.17 — [from [146]] (left) Comparison of the strain measurements possible with AEDGE and other experiments, showing their sensitivities to BH mergers of differing total masses at various redshifts z, indicating also the time remaining before the merger. The solid lines correspond to equal mass binaries and the dashed ones to binaries with very different masses, namely $3000M_\odot$ and $30M_\odot$. Also shown is the possible GGN level for a km-scale terrestrial detector, which would need to be mitigated for its potential to be realized. This figure illustrates the potential for synergies between AEDGE and detectors observing other stages of BH infall and merger histories. (right) Comparison of the sensitivities of AEDGE, ET and LISA with threshold SNR=8. In the lighter regions between the dashed and solid lines the corresponding detector observes only the inspiral phase.

List of my articles related to MAGIA and gradiometry:

1. A. Bertoldi et al. **Atom interferometry gravity-gradiometer for the determination of the Newtonian gravitational constant G**. in: *Eur. Phys. J. D* **40**.2 (2006), pp. 271–279. DOI: 10.1140/epjd/e2006-00212-2

2. G. Lamporesi et al. **Source mass and positioning system for an accurate measurement of G**. in: *Rev. Sci. Instrum.* **78**.7 (2007), p. 075109. DOI: 10.1063/1.2751090

3. G. Lamporesi et al. **Determination of the Newtonian Gravitational Constant Using Atom Interferometry**. In: *Phys. Rev. Lett.* **100**.5 (2008). DOI: 10.1103/physrevlett.100.050801

4. M. de Angelis et al. **Precision gravimetry with atomic sensors**. In: *Meas. Sci. Technol.* **20**.2 (2008), p. 022001. DOI: 10.1088/0957-0233/20/2/022001

5. F. Sorrentino et al. **Precision measurements of gravity using cold atom sensors**. In: *J. of the Europ. Opt. Soc. – Rapid Comm.* **4** (2009). DOI: 10.2971/jeos.2009.09025

6. A. Bertoldi. **Flattening Earth acceleration in atomic fountains**. In: *Phys. Rev. A* **82**.1 (2010). DOI: 10.1103/physreva.82.013622

7. F. Sorrentino et al. **Simultaneous measurement of gravity acceleration and gravity gradient with an atom interferometer**. In: *Appl. Phys. Lett.* **101**.11 (2012), p. 114106. DOI: 10.1063/1.4751112

8. B. Barrett et al. **Correlative methods for dual-species quantum tests of the weak equivalence principle**. In: *New J. Phys.* **17**.8 (2015), p. 085010. DOI: 10.1088/1367-2630/17/8/085010

List of my articles related to MIGA:

1. W. Chaibi et al. **Low frequency gravitational wave detection with ground-based atom interferometer arrays**. In: *Phys. Rev. D* **93**.2 (2016). DOI: 10.1103/physrevd.93.021101

2. I. Riou et al. **A marginally stable optical resonator for enhanced atom interferometry**. In: *J. Phys. B* **50**.15 (2017), p. 155002. DOI: 10.1088/1361-6455/aa7592

3. S. Rota-Rodrigo et al. **Watt-level single-frequency tunable neodymium MOPA fiber laser operating at 915–937 nm**. In: *Opt. Lett.* **42**.21 (2017), p. 4557. DOI: 10.1364/ol.42.004557

4. B. Canuel et al. **Exploring gravity with the MIGA large scale atom interferometer**. In: *Sci. Rep.* **8**.1 (2018), p. 14064. DOI: 10.1038/s41598-018-32165-z

5. J. Junca et al. **Characterizing Earth gravity field fluctuations with the MIGA antenna for future gravitational wave detectors**. In: *Phys. Rev. D* **99**.10 (2019). DOI: 10.1103/physrevd.99.104026

6. A. Bertoldi et al. **A control hardware based on a field programmable gate array for experiments in atomic physics**. In: *Rev. Sci. Instrum.* **91**.3 (Mar. 2020), p. 033203. DOI: 10.1063/1.5129595

7. A. Bertoldi et al. **Atom interferometry in a high finesse cavity**. In: *subm. to Phys. Rev. Lett.* (2019)

8. D. O. Sabulsky et al. **A fibered laser system for the MIGA large scale atom interferometer**. In: *Sci. Rep.* **10**.1 (Feb. 2020). DOI: 10.1038/s41598-020-59971-8

9. B. Canuel et al. **ELGAR - a European Laboratory for Gravitation and Atom-interferometric Research**. In: *subm. to Class. Quantum Grav.* (2019)

10. B. Canuel et al. **Optical resonator with large prope mode for atom interferometry**. France Patent 3054773. 2018

List of my articles related to AI in Space:

1. G. Tino et al. **Precision Gravity Tests with Atom Interferometry in Space**. In: *Nucl. Phys. B Proc. Suppl.* **243-244** (2013), pp. 203–217. DOI: 10.1016/j.nuclphysbps.2013.09.023

2. C. Schubert et al. **Differential atom interferometry with 87 Rb and 85 Rb for testing the WEP in STE-QUEST**. in: (2013). arXiv: 1312.5963 [physics.atom-ph]

3. D. N. Aguilera et al. **STE-QUEST—test of the universality of free fall using cold atom interferometry**. In: *Class. Quantum Grav.* **31**.11 (2014), p. 115010. DOI: 10.1088/0264-9381/31/11/115010

4. T. Schuldt et al. **Design of a dual species atom interferometer for space**. In: *Exp. Astron.* **39**.2 (2015), pp. 167–206. DOI: 10.1007/s10686-014-9433-y

5. A. Trimeche et al. **Concept study and preliminary design of a cold atom interferometer for space gravity gradiometry**. In: *Class. Quantum Grav.* **36**.21 (Oct. 2019), p. 215004. DOI: 10.1088/1361-6382/ab4548

6. Y. El-Neaj, C. Alpigiani, and S. A.-P. et al. **AEDGE: Atomic Experiment for Dark Matter and Gravity Exploration in Space**. In: *EPJ Quantum Technol.* **7** (6 2020). White Paper in response to ESA Science Programm call "Voyage 2050". DOI: 10.1140/epjqt/s40507-020-0080-0

7. L. Blanchet et al. **Exploring the Foundations of the Physical Universe with Space Tests of the Equivalence Principle**. In: (2019). White Paper in response to ESA Science Programm call "Voyage 2050". arXiv: 1908.11785 [physics.space-ph]

8. G. Condon et al. **All-Optical Bose-Einstein Condensates in Microgravity**. In: *Phys. Rev. Lett.* **123**.24 (Dec. 2019), p. 240402. DOI: 10.1103/physrevlett.123.240402

List of my articles related to the AI phase:

1. A. Bertoldi, F. Minardi, and M. Prevedelli. **Phase shift in atom interferometers: Corrections for nonquadratic potentials and finite-duration laser pulses**. In: *Phys. Rev. A* **99**.2 (3 2019), p. 033619. DOI: 10.1103/PhysRevA.99.033619

Chapter 2

Quantum Measurements with Cold Atoms

Cerca una maglia rotta nella rete
che ci stringe, tu balza fuori, fuggi!
Va, per te l'ho pregato, - ora la sete
mi sarà lieve, meno acre la ruggine...

[Look for a flaw in the net that binds us
tight, burst through, break free!
Go, I've prayed for this for you–now my thirst
will be easy, my rancor less bitter...]

— Eugenio Montale, In limine [Threshold]

Ch. 2 describes how atomic sensors can exploit intrinsically quantum features to obtain an increased sensitivity with respect to protocols based on classical properties only. The sensitivity boost over classical statistic granted by quantum mechanics would be of immediate advantage in atom interferometry, as proven in proof-of-concept experiments surpassing the SQL [12, 13, 14, 15]. After making the distinction between quantum-enhanced measurements exploiting entanglement [16] or alternative mechanisms [17], I will present related work I realized with a cavity QED experiment at the Institut d'Optique first in Palaiseau and then in Talence. We studied theoretically how to achieve spin squeezing in an atomic ensemble, and then built a weak, non-destructive probe that we exploited to implement pioneer experiments in quantum feedback and phase locking using an atomic quantum state as a reference.

The research activity described in Ch. 2–4 is based on the high finesse ring cavity I built during my "QNDINTERF" Marie-Curie fellowship. The main targets consisted in developing new techniques for atom interferometry, exploiting non-classical input states and BEC to enhance the instrument sensitivity.

2.1 Quantum-enhanced measurements

Quantum-enhanced measurements rely on quantum mechanical effects to increase the measurement sensitivity beyond what allowed by purely classical means, and represent an obvious edge for both

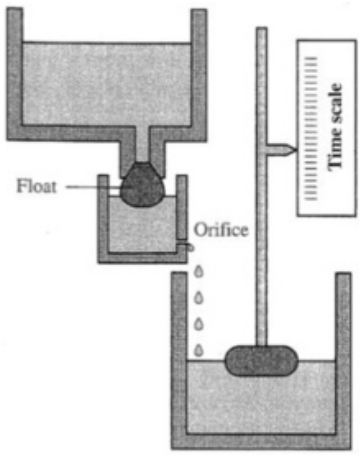

FIGURE 2.1 — [from [226]] Water clock, with the float allowing the automatic control of water level in the intermediate tank.

fundamental and applied science. To date the field has been dominated by the adoption of highly entangled states [16], which are thoroughly studied in diverse contexts ranging from computing, communication, and metrology. A plurality of approaches have been demonstrated to generate entangled states in AMO physics: different kinds of nonlinearity, like those caused by collisions (see [213] and references therein) or atom-light interactions which can be sub-divided in those obtained with: quantum non-demolition (QND) measurements [214, 152]; transfer of non-classical photon states to atoms [215]; light mediated effective interactions of separated atoms [13]. A novel and and yet non-exploited method to generate entanglement between atoms of different species is based on Feshbach resonances [216]: molecular degenerate gases [26] can be obtained via the coherent adiabatic association in a deeply degenerate atomic mixture, but the inversion of the process will produce a massive number of entangled atom pairs suitable to test quantum mechanics in a novel fashion [217].

The multitude of cooling and trapping techniques developed for atoms, ions, and molecules, as well as those for their precision detection and counting, are at the basis of many experiments where highly non-classical states have been demonstrated [13, 213, 152] and are planned to be adopted to boost instrument sensitivity. Atomic inertial sensors and clocks, already representing the state-of-the-art in terms of precision and accuracy, are expected to improve their sensitivity manifold by a massive adoption of entanglement [218, 152].

Despite all these appealing features, highly non-classical states are challenging to generate and extremely fragile: even the scattering of a single photon can irremediably destroy a N00N-state [219]! Nevertheless, multi-particle entanglement is only one of the methods by which quantum mechanics can determine an advantage over classical approaches in measuring: alternative resources that can be harnessed are more general quantum correlations as is the case of quantum discord [220], particle indistinguishability [221], fast scaling of parameters introduced by non-linear Hamiltonians [222, 223, 224] or non-equilibrium steady states [225], as is the case of phase transitions.

2.2 Quantum Feedback on an atomic state

During my Marie-Curie fellowship as a postdoc in the group of Prof. A. Aspect in Palaiseau (France), I developed a cavity experiment to improve quantum sensors by exploiting Bose-condensed and non-classical input states. On this experimental setup we obtained a series of results, described also in the following chapters, like the non-destructive characterization of the cavity geometry using a light

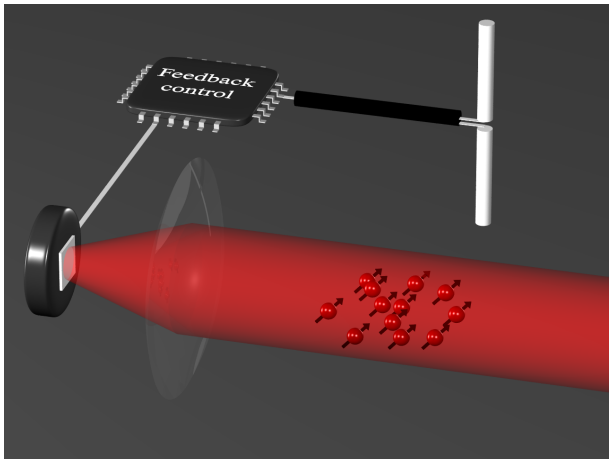

FIGURE 2.2 — Graphical view of our measurement-and-correction experiment: a CSS is probed with laser implementing a WM; the partial information retrieved on the atomic state is used to compute a correction signal, which is applied through a RF antenna. The signal perturbing the atomic state is also sent via the same RF antenna.

shift engineering technique [184] (Sec. 3.1), and the first all-optical BEC and BEC array completely realized in a resonator [227] (Sec. 3.2). The original research line on which is focused this chapter started with the development of a heterodyne non-demolition probe targeting spin squeezing [228], and that we employed to follow the internal atomic state dynamics with minimal destructivity [229]. It soon turned out, however, that our weak probe could be used to implement feedback schemes on atomic states, another technique that opens new avenues for atomic sensing thanks to purely quantum features.

Control theory based on feedback is a well established technique, introduced in ancient Greece with the water clock (see Fig. 2.1), whose key element represented by the float strongly increases the instrument accuracy. Control loops based on retro-action are nowadays pervasive, and can be found in diverse contexts like electronics, self-driving vehicles, and high-frequency trading (HFT). All these examples of automatic system control share a few basic elements, which are the access to the system status via a classical measurement, the calculation of an error signal that give a "distance" of the present state from the sought one, the calculation of a correction value using the error signal and its dynamics, and the application of such correction to the system via an actuator.

When one considers feedback loops in a quantum context, things become immediately more complex, in relation to the weird features introduces by the law of quantum mechanics [230]: performing a measurement on a quantum system changes its status, because of the associated state projection and loss of coherence; the measurement process is not instantaneous, but consists of a first phase where the measured system and the "pointer" probing device are entangled, and only later the effective read-out of the pointer projects the status of the entangled system; measuring a specific observable has an effect on the associated non-commuting operators, in what is called back-action noise [231]. Complexity often brings opportunities, and indeed amazing results have been obtained in the field of quantum measurements: quantum phase magnification allows entanglement-enhanced measurement without low noise detection [232]; the average trajectories of single photons have been observed in a two-slit interferometer using weak measurement [233]; photon number states have been prepared and stabilized using real-time quantum feedback [234].

Our contribution to the field builds on QND measurements in the weak regime, in order to control the status of a quantum system. We first proved such a concept in an experiment where we protected a coherent spin state (CSS) against the action of noise. The two key ingredients that we adopted are:

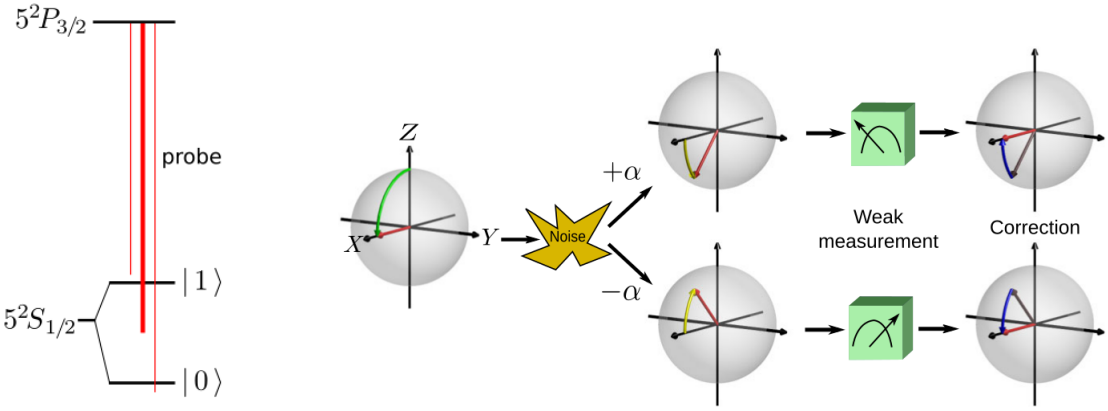

FIGURE 2.3 — [from [190]] (Left) Simplified scheme of the relevant Rb atomic levels and of the heterodyne probe. (Right) Evolution of the collective spin on the Bloch sphere when subject to a binary random collective rotation. A $\pi/2$ rotation around Y prepares a balanced population difference. The state experiences a random rotation of $\pm\alpha$ around Y, which is detected using a weak nondestructive measurement and then corrected.

- QND measurement: process to determine an observable that is an eigenstate of the ideal Hamiltonian of the measured system. Such measurement has an effect on the system only if the system is in a superposition state of the energy operator; after its projection on an eigenstate of H, the QND measurement has no impact on the system, hence it can be repeated at will;

- weak measurement (WM): a measurement whose resolution is far worse than the QPN; whenever a high uncertainty can be tolerated, a WM allows to preserve the initial quantum coherence and induces minimal destructivity.

For a more in depth discussion of quantum noise and measurement one can see [230] and references therein. A graphical view of our quantum measurement-and-correction experiment is shown in Fig. 2.2, where a set of atomic spins are probed with a laser beam, and the measured signal is used to feedback onto the atomic state with an RF antenna.

The observable we chose for the quantum state is the population unbalance $J_z = N_1 - N_2/(N_1+N_2)$ for the ^{87}Rb atomic ensemble, defined with respect to the two magnetically insensitive hyperfine levels $5^2S_{1/2}, F = 1, 2, m_F = 0$. The atoms are coherently manipulated on the Bloch sphere with a RF field produced by an antenna. To measure J_z we implemented a heterodyne non-destructive light probe, which combines a carrier laser on the D2 transition of Rb [235] passing through a high frequency electro-optic modulator (EOM): two sidebands with opposite phase are produced at the modulation frequency. The latter is chosen so that each sideband weakly interacts with the atomic population of one of the two levels of interest (see Fig. 2.3, left), which determines a dispersive dephasing of the beam with J_z. The population unbalance signal encoded in the sidebands is obtained by demodulating the readout of a fast photodiode. The scheme has two major advantages over a Mach-Zehnder interferometer, where reference and probe beam are geometrically separated: first, there is a unique beam, with three frequency components, which determines a very low sensitivity to path vibrations that are commonly rejected; second, the system can work at the shot noise for the weak sideband thanks to the presence of the strong, far-off-resonance carrier. The measurement is realized in AC at a high modulation frequency, which cancels the 1/f noise issue, but requires a demanding

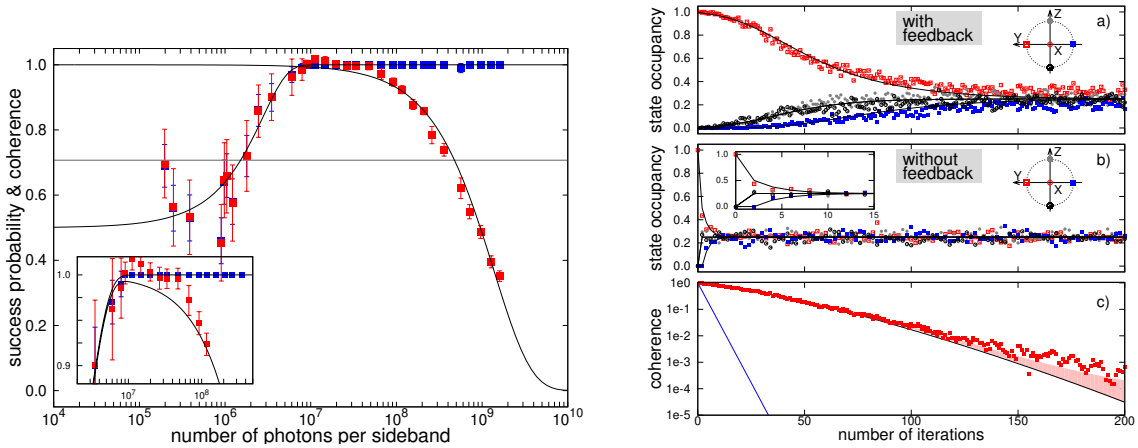

FIGURE 2.4 — [from [190]] (Left) Effect of the cycle consisting of binary collective noise, measurement and correction as a function of the number of photon per sideband in the probe pulse: in solid squares the residual coherence, and in open circles the success probability. An optimal coherence recovery of 0.993 is achieved with 9.1×10^6 photons. (Right) State occupancy as a function of the number of cycles: the measurement-and-correction approach slows the state diffusion and the coherence loss.

high frequency detection electronics. We theoretically studied the spin-squeezing and Dicke state preparation using such heterodyne detection [228], and adopted it experimentally to non-destructively measure Rabi oscillations induced with microwave radiation [229].

To probe trapped ensembles we had to solve the problem represented by the differential light shift induced by the dipole trap at 1560 nm, which induces an inhomogeneous shift on atoms sitting at different trap positions. To this aim we locked a second laser to the cavity, but on the blue side of the $5^2P_{3/2}$–$4^2D_{3/2,5/2}$ transitions at 1529 nm; this allows to engineer the atomic light shift, and in particular to make it homogeneous on the D2 transition.

Probing the atoms confined in the cavity-enhanced dipole trap, allows one to exploit the improved coupling strength provided by the higher optical density; this in turn determines a bigger phase signal on the probe photons for a fixed destructivity, i.e. spontaneous emission. Moreover, the complications related to probing an expanding cloud are completely avoided. We used the improved detection to demonstrate the feedback control of the internal states of an atomic ensemble and its protection against synthetic collective noise [190, 236]: the CSS is rotated by a fixed angle α and random direction around a fixed axis, the resulting state is weakly probed to infer the direction sign and apply a correction (see Fig. 2.3, right). The efficiency of the feedback is studied for such binary noise model and characterized in terms of the trade-off between information retrieval and destructivity from the optical probe: the left side Fig. 2.4 remarkably shows how the final coherence of the atomic ensemble after one measurement-and-correction cycle grows initially with an erf-like shape, and then decreases exponentially as a function of the sideband intensity. The optimal condition is found for 9.1×10^6 photons per sideband, where the ensemble coherence, reduced by the noise from unity to $1/\sqrt{2}\sim0.7$, is recovered to 99.3(1)%. We also implemented more complex feedback scenarios which provide a way towards novel atom interferometry schemes using repeated measurements and feedback: first, the cycle made of disturbance-measurement-correction was repeated several times to study the atomic state dynamics (Fig. 2.4, right), which has shown a factor 10 damping of the spin diffusion; second, a more demanding and realistic noise model was adopted, consisting in an analog instead of binary rotation. Also in this configuration we demonstrated a consistent coherence recovery, and thus the robustness of the scheme.

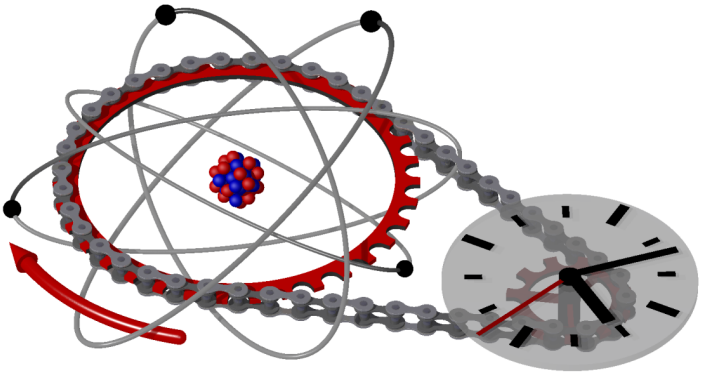

FIGURE 2.5 — Representation of a PLL between a classical oscillator and an atomic reference: their phase dynamics is constrained by the cogwheels and the common transmission belt.

2.3 Atomic phase lock loop

Research activity carried out within the frame of the Euramet JRP project "QESOCAS", and the LAPHIA project "APPL-CLOCK"; they targeted to develop quantum enhanced protocols for atomic clocks and atomic sensors. The enhanced clock protocol is the subject of an international patent [237].

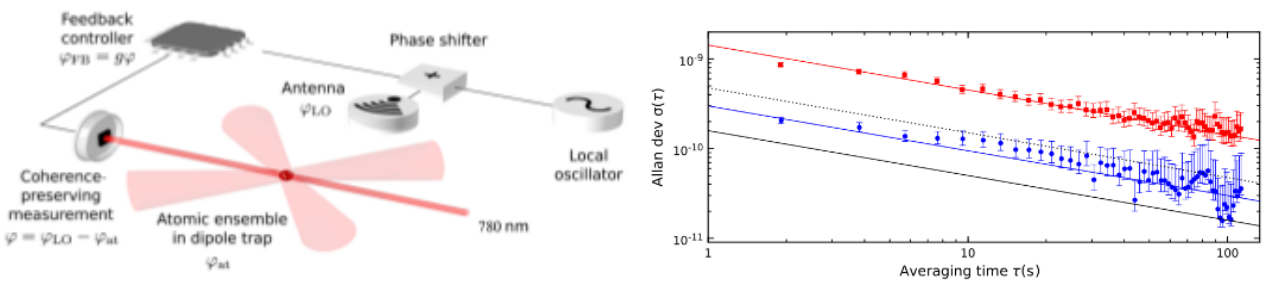

FIGURE 2.6 — [from [191]] (top) Scheme of the experimental setup to interrogate and correct the quantum state of an atomic ensemble, using a weak non-destructive probe and microwave pulses. (bottom) Allan frequency standard deviation for a normal Ramsey clock with interrogation time T=1 ms (red line) and for a clock implementing the phase lock between the LO and the atomic superposition state for 9 successive, correlated interrogations on the same atomic ensemble, for a total interrogation time of 9 ms (blue line). The continuous black line lies a factor 9 below the red curve and represents the theoretically achievable stability level for the phase-lock sequence. The dashed black line lies a factor 3 below the red curve and is the optimum level for nine consecutive but uncorrelated Ramsey measurements with duration T each and the same total cycle time.

We then implemented quantum feedback in a configuration with a much broader and immediate potential impact: a timekeeping device. In standard atomic clocks the frequency of a macroscopic local oscillator (LO) – typically a microwave source or an ultra-stable laser – is periodically compared to an absolute reference, represented by an atomic transition. This is achieved by measuring the phase accumulated during an interrogation interval T that separates two $\pi/2$ pulses in a Ramsey interferometer [238]. The frequency sensitivity scales as 1/T, hence the advantage of having a longer interrogation time. Nevertheless, actual atomic clocks are limited by the LO precision, since it is not possible to detect the relative dephasing unambiguously if the accumulated phase exceeds $\pm\pi/2$. Moreover, the measurement destroys the atomic coherence, hence in this scheme the phase remains

free. With our approach, it is possible to maintain the information on the collective spin phase over many interrogation cycles, which makes feasible to phase-lock-loop (PLL) a LO on an atomic reference, as graphically shown in Fig. 2.5.

First of all we demonstrated that the weak measurement detection allows to follow the spin evolution over several interrogation cycles, shifting the LO frequency and observing the precession. This is possible thanks to the minimal impact of each measurement on the state of the individual spins in the atomic ensemble. We then closed the feedback loop, using the weak signal to control a phase actuator on the LO: we realized in this way the first reported PLL where a classical LO is tightly reference to a quantum state (see Fig. 2.6, top). Last, we implemented an atomic clock with an effective interrogation time increased thanks to repeated WMs of the spin vector [191]; the sensitivity improvement is evident when this scheme is compared to the performance of a standard single Ramsey interrogation clock (Fig. 2.6, bottom). The resulting gain improvement for N=9 successive measurements in terms of the Allan deviation, is equal to 4.75(0.25), which is more than $\sqrt{9}$, i.e. the maximum enhancement classically achievable by averaging over the samples. This result demonstrates an at least partial correlation between the successive measurements. Remarkably, our protocol has been partly implemented at NIST, in a spectroscopic measurement enhanced via a two-ensembles correlated measurement [239]. Our quantum enhancement technique harnesses correlation in time as a quantum resource, and we postulated in [191] that it could be then combined with particle entanglement to obtain a twofold sensitivity boost; such idea has been later developed in [240], where they introduced the Quantum Allan variance as a general measure to describe the instability of quantum frequency standards.

List of my articles related to this chapter:

1. T. Vanderbruggen et al. **Spin-squeezing and Dicke-state preparation by heterodyne measurement**. In: *Phys. Rev. A* **83**.1 (2011). DOI: 10.1103/physreva.83.013821

2. S. Bernon et al. **Heterodyne non-demolition measurements on cold atomic samples: towards the preparation of non-classical states for atom interferometry**. In: *New J. Phys.* **13**.6 (2011), p. 065021. DOI: 10.1088/1367-2630/13/6/065021

3. T. Vanderbruggen et al. **Feedback Control of Trapped Coherent Atomic Ensembles**. In: *Phys. Rev. Lett.* **110**.21 (2013). DOI: 10.1103/physrevlett.110.210503

4. T. Vanderbruggen et al. **Feedback control of coherent spin states using weak nondestructive measurements**. In: *Phys. Rev. A* **89**.6 (2014). DOI: 10.1103/physreva.89.063619

5. R. Kohlhaas et al. **Phase Locking a Clock Oscillator to a Coherent Atomic Ensemble**. In: *Phys. Rev. X* **5**.2 (2015). DOI: 10.1103/physrevx.5.021011

6. B. Barrett, A. Bertoldi, and P. Bouyer. **Inertial quantum sensors using light and matter**. In: *Phys. Scr.* **91**.5 (2016), p. 053006. DOI: 10.1088/0031-8949/91/5/053006

7. A. Bertoldi et al. **Coherent spectroscopic methods with extended interrogation times and systems implementing such methods**. WO Patent WO/2016/097332, US20170356803 , EU Patent 3233719 , Japan Patent JP2018508749. 2017

Chapter 3

Atom Trapping and Cooling

Only describe, don't explain.
— Ludwig Wittgenstein

Ch. 3 is focused on the results I obtained in the general context of atom trapping and cooling, often for the specific configuration of cavity QED. I will present an enhanced imaging technique exploiting light-shift engineering (Sec. 3.1), the direct production of an array of BECs in the high order transverse cavity modes of a resonator (Sec. 3.2), the progress towards a cavity based matter wave beamsplitter (Sec. 3.3) and the dark state loading and cooling in a dipole trap (Sec. 3.4, which has been key to realize an all-optical BEC in microgravity.

3.1 Light shift tomography of an optical cavity

The experimental setup on which is focused this chapter and next one is the traveling wave cavity that I constructed during my Marie-Curie fellowship. The resonator has a bow-tie geometry, and is resonant both at 1560 nm and 780 nm (see Fig. 4.2, left), wavelengths used for trapping the atoms and probing them, respectively. The experiment adopts a few very innovative solutions: it uses a traveling resonator to optically trap the atoms, feature that motivates the present research line concerning non-trivial emergent phenomena within the frame of an ANR-FWF project just financed (Ch. 4); it adopts light in the telecom C band at 1560 nm to trap the atoms, which produces a strong differential light shift on the two levels of the Rb D_2 transition at 780 nm used to probe the atoms. The latter effect is due to the upper transitions $5^2P_{3/2}$–$4^2D_{3/2,5/2}$ at 1529 nm, whose relevant atomic levels are strongly shifted by the trapping light (see Fig. 4.2, right).

Atoms at different locations, i.e. potential depths, can thus be selectively imaged by changing the 780 nm probe detuning with regard to the atomic resonance. Such tomographic technique to image the trapping potential using light shift has been introduced by Brantut *et al.* in [241]. We exploited this effect to precisely map *in situ* and non-destructively the cavity optical potential [184]. We could thus infer the cavity geometry with a micrometric accuracy, finding a remarkable agreement between the realized optical setup and the design specifications. Since the cavity is non degenerate, its transverse modes are separated in frequency, and it is possible to selectively pump each of them by adopting the right frequency shift and a suitable phase mask on the injection laser. As a result we could map

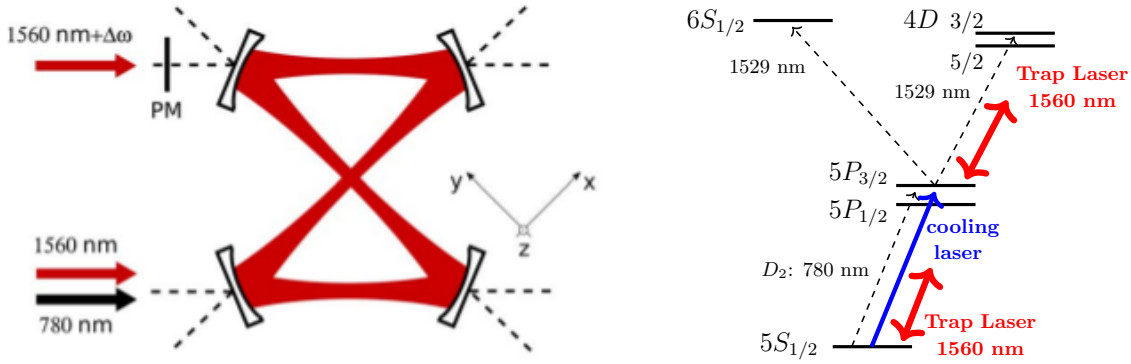

FIGURE 3.1 — (left) [from [227]] Scheme of the bow-tie traveling cavity, injected with light at 1.5 μm and 780 nm, both on the fundamental and high order transverse modes. (right) [from [210]] Lowest energy levels of ^{87}Rb. The transitions at 1529 nm are responsible $m_{F'}$-dependent excited state light shifts to the $5P_{3/2}$ excited state.

the potential profile of the first 3 Hermite-Gauss modes with nodes along the horizontal direction, i.e. $\mathrm{TEM}_{00,10,20}$, as shown in Fig. 3.2.

This initial study of light shift engineering has been followed by several other specific applications, as is the case of the homogeneous probing of Rb atoms trapped in a 1560 nm beam by using a light-shift compensation beam at 1529 nm (technique described in Sec. 2.2), or the possibility to realize AI in a narrow cavity linewidth (technique described in Sec. 1.4.4). Recently a dedicated research line has been devoted to the subject at LP2N, with the target of achieving sub-wavelength lattices structures and probing [242].

3.2 BEC array in a non-degenerate cavity

After characterizing the geometry of the high order transverse cavity modes, we could load cold rubidium atoms in them. Pumping the generic TEM_{nm} mode with telecom radiation gives rise to an array of $(n+1)^2\times(m+1)$ trapping nodes, and such scalability is at the basis of several applications described in the following: we trapped and later condensed atoms in higher modes, obtaining an array of simultaneous BECs [227]; we changed the trap geometry for thermal atoms from a single-well to a four-well one, and we plan to study the process in its coherent version for AI (Sec. 3.3); we are studying the possibility to couple different BECs in a high order mode using the cavity, to generate massive entanglement or a PLL based on superradiance (Ch. 4).

The realization of Bose-Einstein condensation in the cavity required a careful study of the evaporative process dynamics, in relation to the constraint of using a crossed dipole trap with the same beam on the two arms. Such configuration forbids the separate control of the trap depth and curvature, which in turn prevents a run-away evaporation [243]. The solution we adopted to keep a good collisional rate – hence thermalization – along all the process, relies on placing a vertical dimple crossing the cavity in its central region. In the final part of the evaporation the dimple has the role of maintaining almost fixed the horizontal frequencies, while the evaporation becomes vertically driven: in this way BEC is obtained in about 2 s, with a transition temperature $T_c = 190$ nK, and $N_0 = 5\cdot10^4$.

In the next step we repeated the evaporation process after loading the TEM_{01} mode, which shows two trapping regions on top of each other: in this way we simultaneously obtain two BECs (Fig. 4.2, left), and more complex array geometries can be created by using other cavity modes. As described

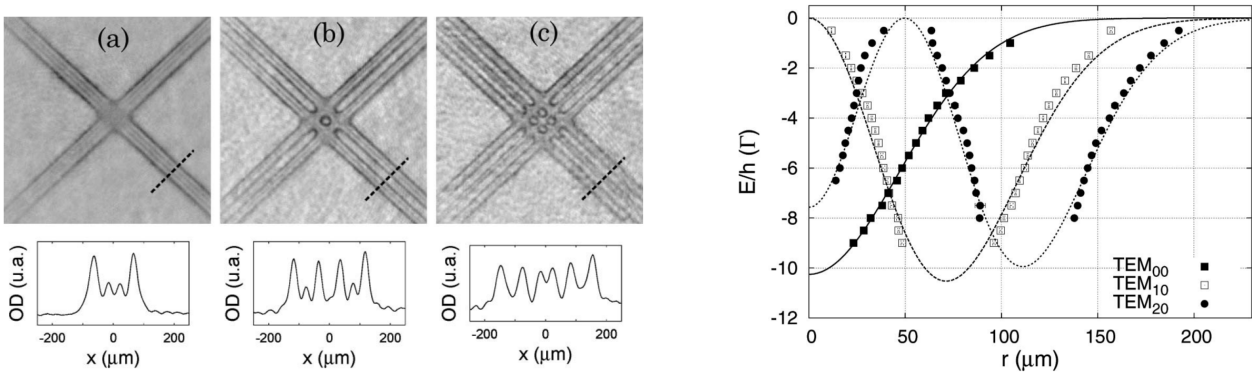

FIGURE 3.2 — [from [184]] (3 on the left, top line) Absorption images with the 1560 nm laser locked to the TEM_{00} (a), TEM_{10} (b), and TEM_{20} (c) mode of the cavity, with the detuning of the probe light set to 5Γ to the red of the transition. (3 on the left, bottom line) Integral optical density obtained by projecting the upper images on the 45° dashed line crossing one arm of the cavity. (right) Optical potential depth induced by the laser at 1560 nm locked to the first three transverse modes of the cavity. Each series of points is fitted with the corresponding Hermite-Gauss mode.

in [227], we plan to exploit this unique feature of our experiment in three original ways:

- implementing homogeneous trapping potentials by simultaneously injecting a well defined combination of high order modes – solution that would allow to eliminate the shift generated by the harmonic potential in several experiments studying condensed matter phenomena and gauge fields;

- obtaining cavity aided atom optics elements (Sec. 3.3);

- couple different BECs via the same cavity mode using self-ordering phenomena (Ch. 4), to implement a quantum network of Bose-condensed samples [244]. The scheme could have potential applications in quantum computing and communication.

3.3 Cavity based matter wave beamsplitter

Research activity being carried out within the frame of the project TAIOL, financed by European Union with the program QuantERA 2018.

BECs are the ultimate sources of coherent matter waves, thanks to their very low temperature and high phase space density, which in turn are at the basis of the very high brilliance of atom lasers and ultra-low expansion rates of delta-kick collimated samples. The field of applications is immense, and ranges from quantum sensing, to studies of extreme consequences of general relativity [245] or quantum field theory effects [246] with analogue systems. The application of coherent matter waves in phase sensitive experiments, like interferometers, requires the coherent splitting of a BEC into a double well. Standard matter-wave beamsplitters rely on optical potentials [8] or RF-dressed potentials on an atom chip [247]. The latter have shown promising results but suffer from three problems: (i) magnetic fields cannot be modulated quickly; (ii) spurious effects due to switching of the magnetic fields; (iii)

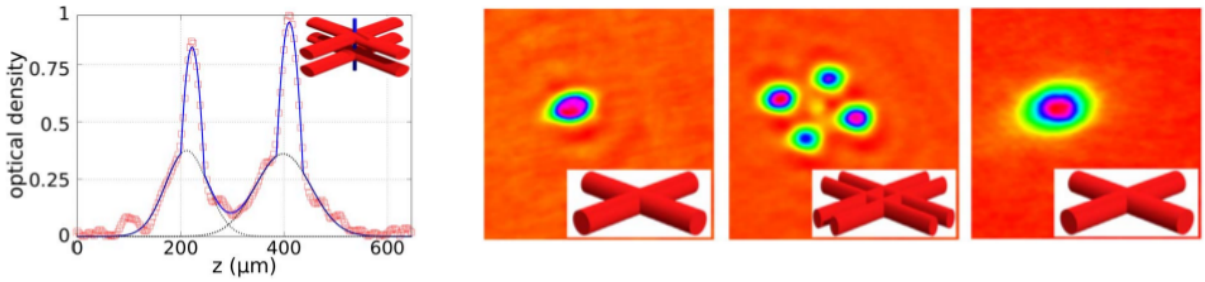

FIGURE 3.3 — [from [227] (left) Optical density profile showing 2 BECs obtained in the TEM_{01} transverse cavity mode. (right) By switching between TEM_{00}, TEM_{10} and back we split in 4 and recombined an atomic ensemble.

undesirable effects of the magnetic fields on the atomic transitions. Optical potentials bypass these problems, but are complex, requiring multiple carefully aligned beams in conjunction with advanced optics, and high power to effectively confine the atoms.

The cavity-based method we propose is all-optical, avoids the problems with RF-dressed potentials, and allows a simple optical arrangement with lower input power due to cavity buildup effects. To perform the beamsplitting operation, we first load 10^6 atoms in the TEM_{00} mode, and then adiabatically inject the TEM_{10} mode with a laser beam with the right frequency and phase profile, obtained with a phase mask. This operation deforms the initial single well in four distinct trapping region, where the atoms are separated (Fig. 4.2, right). A major advantage of our cavity beam-splitter scheme is that during the entire process, odd-powered potential components are suppressed by the cavity mode structure; this is a necessary condition for achieving coherent beam-splitting operations. Odd-powered spatial geometries during the splitting phase mix center-of-mass and internal relative degrees of freedom, leading to mixing of internal modes, and causing both decoherence and heating. The splitting process can eventually be reversed to recombine the 4 atomic clouds. The overall efficiency of the process in terms of atom transfer is greater than 95%, whereas a factor 2 increase in the temperature has been measured.

In collaboration with Dr. Gaaloul at LUH (Hannover, Germany), we are studying ho to implement optimized ramp based on optimal control theory [248] to obtain the coherent splitting and recombination of a BEC using the cavity modes. The preliminary numerical results provided by the German colleagues indicate that the objective is feasible.

3.4 Dark state loading and cooling in a dipole trap

At the end of 2018 we have been financed by ANR (project "EOSBECMR") and LAPHIA (project "OE-TWR") for the study of self-organisation phenomena in a traveling wave cavity configuration (see Ch. 4). Such research activity is carried out together with the theoretical group of Helmut Ritsch (Innsbruck, Austria), pioneer of self-ordering and superradiance in optical resonators, and expert of cavity optomechanics and cavity cooling. Before tackling the fundamental physics questions of order emergence and induced crystallization in the resonator, we decided to improve the quality of the atomic source, i.e. the single - or multiple - BEC obtained in the cavity. Such optimization phase took more time than initially foreseen, but brought also an unexpected insight into the loading and cooling of atoms in a dipole trap by exploiting dark states.

Producing a BEC requires the previous preparation of a cold, high density atomic sample. Typical

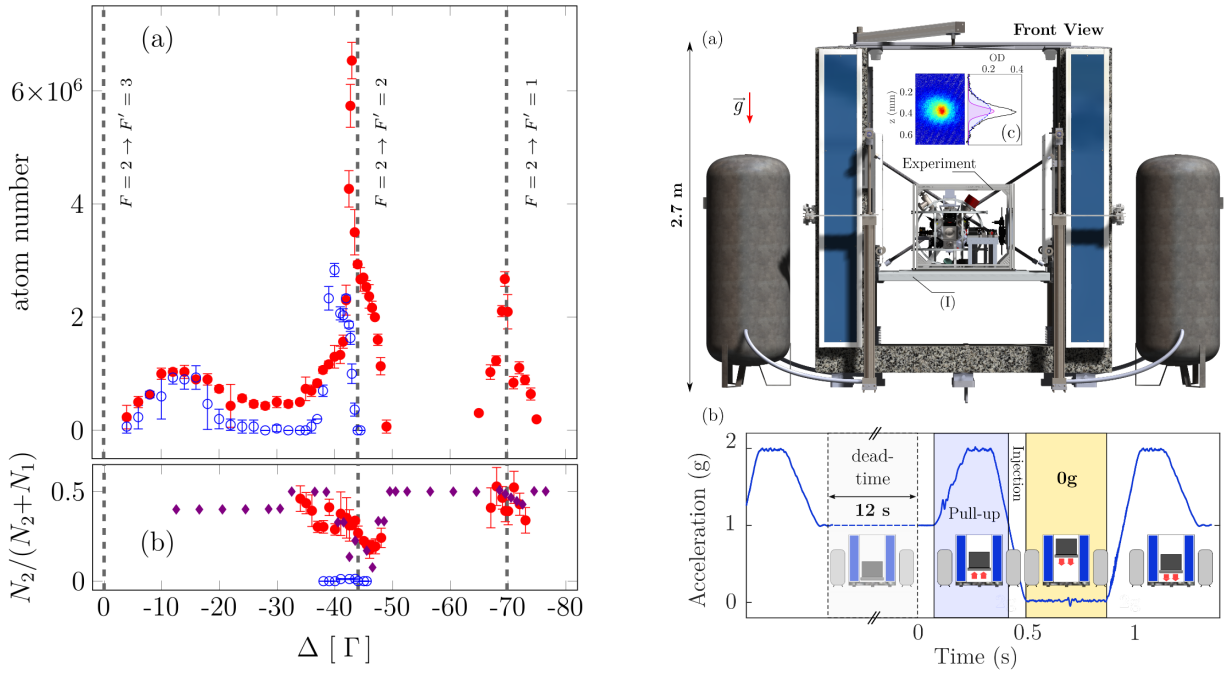

FIGURE 3.4 — (left) [from [210]] (a) Atoms loaded into the FORT as a function of the cooling laser detuning from the $F = 2 \to F' = 3$ resonance during the sub-Doppler cooling phase, for an independent repumper (empty blue circles), and for a repumper in Raman condition with the cooler (filled red circles). (b) Population fraction of atoms in $F = 2$ with the repumper in the two configurations as above; $N_{1,2}$ indicate the atomic populations of the $F = 1, 2$ manifolds. The violet points result from a numerical evaluation of the DSs forming at each detuning (right) [from [104]] (a) Schematic of the Einstein elevator. The payload (I), including the science chamber, cooling beam optics and imaging system, is driven vertically along two air-bearing translation stages. (b) Acceleration profile of the science chamber for sequential parabolas of 400 ms, separated by a dead time of 12 s required to let the motors cool down. (c) Absorption image of the BEC transition after a time-of-flight of 50 ms in 0-g. The projection of the vertical axis shows the typical double structure of the cloud.

protocols are based on a multi-stage cooling process, beginning with laser cooling in a MOT, sub-Doppler cooling, loading into a conservative magnetic or optical dipole trap, followed by evaporative cooling. Although quite efficient, this is only possible for a small subset of alkali and alkali-earth-like atoms that can be initially cooled to low temperature by optical means.

The sub-Doppler cooling phase uses light red detuned from a cycling transition, and exploits laser polarization gradient to produce dissipation mechanisms based on optical pumping or population unbalance between different ground levels [249]; in both cases one obtains efficient friction forces, determined respectively by light lift or radiation pressure. Coupling polarization gradient cooling to the presence of dark states [250] is known as *gray molasses* (GM) [251]; the dark states decoupled from the optical field are coherent superpositions of internal states and external momentum states for the atoms. Remarkably, their creation does not require cycling $F \to F' = F + 1$ transitions, but can rely on any transitions of the $F \to F' \leq F$ form. As a consequence, GM cooling can be applied to a broad class of neutral particles; just to give an example it has been crucial to recently obtain a degenerate Fermi gas of polar potassium-rubidium molecules [26].

To prevent expansion of the cold atom cloud, it is tempting to combine dark-state sub-Doppler cooling with spatial confinement in a far-off resonant optical dipole trap (FORT). However, standard dark states composed by superposing different momenta [252] are eigenstates of the free Hamiltonian but not of the Hamiltonian in the trapped case. This leads to a finite lifetime of the dark states and

their eventual coupling to the light field, i.e. excitation and heating, while the spatial dependence of the trapping potential complicates polarization gradient cooling mechanisms. We were able to efficiently couple GM cooling with direct loading in a dipole trap, on two different rubidium experiments: the ICE experiment run on an Einstein Elevator, lead by Dr. Battelier, where the technique has been crucial to obtain the first reported BEC in microgravity [104]; the cavity QED experiment described in Ch. 2 and Ch. 4, where we actually developed the technique [210].

Whereas GM have been typically performed on the D1 transition in alkali, we adopted a recent protocol demonstrated in [253] to implement dark state cooling on the D2 transition of ^{87}Rb: "quasi-dark" state cooling is feasible thanks to the large hyperfine structure separation. The two mechanisms that we devised to couple the high and quickly achievable atomic phase-space density with the loading in the optical trap are very different: in the ICE setup, GM cooling provides the cold and dense atomic reservoir nearby a 1550 nm FORT, whose strong light shifts generates a transparency volume where atoms can be stored without interacting with the near-resonant photons. On top of this, the FORT beam is spatially modulated to create a time-averaged (or painted) potential, which grants a high capture volume and fast evaporative cooling with a high collision rate. In this way we can produce a BEC in 1.4 s with a critical temperature of 140 nK before the Einstein elevator reaches the 0-g, i.e microgravity, phase of its trajectory (see Fig. 3.4, right).

The GM cooling mechanism adopted on ICE is the same as in [253], namely it exploits dark states that combines Zeeman states of the same hyperfine manifold (Zeeman dark states or ZDSs); the spatial modulation of the FORT allows then the accumulation of the cold atoms in the region where they are uncoupled to the light. On the cavity QED experiment the approach is different: it adapts GM to the presence of the FORT, and brings to a tenfold increase in the loaded atom number. The FORT strongly modifies the relative energy of the Rb levels on the D2 transition, in relation to the presence of a doublet at 1529 nm from the excited $3P_{3/2}$ state (see Fig. 4.2, right). As a consequence the sub-Doppler cooling mechanisms are complicated, but dark states exist that make use of both ground state hyperfine manifolds [250] (Hypefine dark states or HDSs).

GM cooling reposes on the coherent coupling between the levels forming the dark state; HDSs exploiting both ground states of the hyperfine manifold require thus the phase lock of the cooling and repump light. To achieve such configuration, we installed an EOM on the cooling laser, and produce the repumper by modulating the crystal at the hyperfine splitting frequency, equal to ω_{hf}=6.834 GHz. Such repumper replaces the standard one, locked on the $F = 1 \rightarrow F' = 2$ transition, at the end on the MOT phase and when begins the sub-Doppler cooling phase. At this point the depth of the FORT is increased up to 170 μK to trap atoms and, simultaneously the red detuning δ_{Raman} of the two lasers in Λ configuration from the $F' = 3$ level is shifted to the desired value. This operation is actuated in 200 μs and the beams remain illuminated for only 1 ms. The frequency δ_{Raman} has been scanned from -4 Γ to -75 Γ, and each time the loading efficiency in the FORT evaluated using the number of trapped atoms as as a figure of merit, as shown on the left side of Fig. 3.4 with the red points. The comparison with the blue points, obtained repeating the procedure with the standard repumper shows:

- a generally similar behavior between the two regimes, with the loading exploiting GM (red points) always more efficient than the standard molasse (blue points). However, two striking features described next stand out for the dark state cooling;

- for GM-based loading, a sharp optimal peak at -43.5 Γ, close to the $F' = 2$ resonance, and in coincidence to the peak in atomic density reported for Λ-enhances cooling in free space [253]. Optimal HDS cooling condition for atoms outside and on the edges of the FORT provides at once the ideal atomic bath for the FORT loading, and a dissipation mechanism to slow the atoms entering the conservative potential;

- the optimal GM-based loading peak sits atop a broader shape present also for the standard molasse case. However, that broader shape does not abruptly end at the position of the $F = 2 \rightarrow F' = 2$ resonance, and is explained in terms of atoms being loaded from within the trapping volume of the FORT. We verified this hypothesis by varying the FORT power, and observing the related behavior of the broad peak [210], which can be resumed in a wider width with deeper FORT. At the same time, the sharp peak at -43.5 Γ changes only in amplitude, but not in position;

- a similar loading behavior is observed when δ_{Raman} is tuned nearby the $F' = 1$ resonance, only with a lower efficiency, explained in term of a loss determined by the sweeping of the laser frequency through the resonance with the $F' = 2$ level, which causes atomic heating;

- the explanation of the experimental observations in terms of cooling and loading enhanced by the presence of HDSs has found confirmation with the measured behavior of the population fraction of atoms in the $F = 2$ manifold, in good agreement with the results of a numerical evaluation of the dark states forming at each detuning (see left, upper Fig. 3.4, comparison of red and violet points).

3.4.1 Optical cooling in the dipole trap

Optically trapped atoms experience position dependent excited state light shifts, in relation to the local FORT power. Changing the detuning of HDS cooling will hence address atoms at different places in the optical potential creating spatially dependent HDSs. The position of an atom within a conservative trap is also energy dependent, with higher momentum/energy states spending more time near the edges - where the light shift is smaller - and lower momentum/energy states residing near the center - where the light shift is larger. Therefore at any particular detuning only atoms of a particular momentum/energy will be optimally cooled. This opens up the possibility of a novel type of cooling: by starting with small detunings hotter atoms at the edges of the FORT will be selectively cooled, falling into the FORT where a further shift in the Raman beams to larger detunings will cool the atoms to even lower momentum/energy states. A single sweep on the Raman beam detuning can progressively cool all the atoms in the FORT, potentially up to the recoil temperature $\hbar^2 k^2/(2mk_{\text{B}})$. Excited state effects will be minimized, since the protocol relies on dark states, and remarkably, no atoms are lost in the process, given that the energy is carried away via spontaneous emission and not by evaporation.

We tested the protocol on the atoms loaded in the FORT by sweeping δ_{Raman} in 6 ms from -55 Γ to -68 Γ, and then measuring the temperature in time-of-flight: the temperature drops from the initial value of 198 μK to 48 μK (Fig. 3.5). If the detuning is further increased, all atoms are lost as the laser frequency becomes resonant with the $F = 2 \rightarrow F' = 2$ transition at the center of the FORT, where the detuning is maximal. We plan to push forward these very encouraging preliminary results, having the all-optical cooling to BEC as the ultimate target. Some guidelines can be already drawn:

- the dissipative mechanism removes energy via exchange with the Raman lasers, not by removing the high energy tail of the momentum distribution. GM cooling in the FORT does not determine atom loss, unlike evaporation;

- GM cooling is based on a coherent process, and result hence orders of magnitude faster than standard molasses cooling. The result is cooling without a significant expansion of the atomic ensemble, and brings thus to higher phase space densities. This feature is of key importance

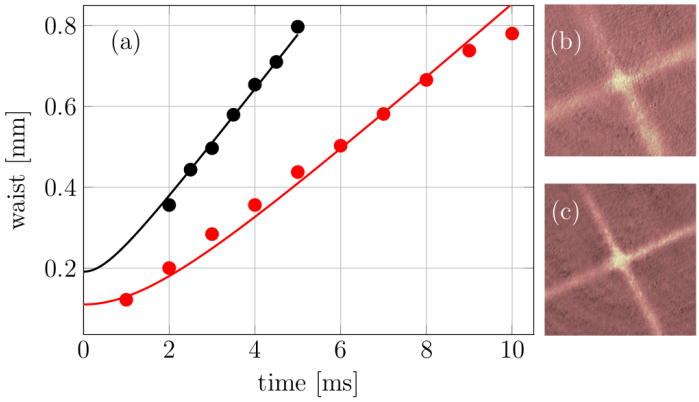

FIGURE 3.5 — [from [210]] (a) Ballistic expansion of the atomic cloud released from the FORT: the temperature is 198 μK before the cooling sweep (black points) and 48 μK after it (red points). The solid lines are time-of-flight fits to the experimental data. Absorption images of the atoms 700 μs after the release from the FORT before (b) and after (c) the cooling sweep: the atoms become more confined to the center of the trap, both in the wings and in the crossing region.

in several contexts, like loading in a narrow potential, later achievement of BEC, realization of non-classical states at high optical density;

- the same laser system adopted for the MOT phase can be used for loading in the FORT and the successive cooling inside it;

- no cycling transition is needed, which opens towards cooling of different atoms and molecules that cannot yet exploit laser cooling;

- a higher momentum/energy selectivity, and then efficiency for the cooling protocol, can be achieved inside the trap by increasing the FORT depth, so as to create larger excited state light shifts;

- the main limitation on the FORT power and then of the cooling protocol is given by the presence of the $F = 2 \rightarrow F' = 3$ transition: its light shift must be smaller than $45\,\Gamma$, to avoid heating the cold atoms at the center of the trap when acting on its flanks. The straightforward solution consists in performing the GM scheme on the D1 transition, which has no $F' = 3$ state. We predict that recoil atomic temperatures in timescales of a few ms would be feasible without loss of atoms by adopting GM on the D1 line.

We have demonstrated the potential of a new type of all-optical cooling performed inside an optical trap using HDSs. The method could open new avenues in the production of ultra-cold atomic and molecular gases in relation to its key features: high speed, minimal scattering, no atom loss and no need of cycling transitions. Remarkably, cooling and loading happen simultaneously, which solves the mode matching issue for the atomic transfer in the final conservative potential and skips altogether the intermediate step often relying on magnetic trapping. The cooling scheme looks optimal for the rapid production of ultra-cold gases in unusual geometries, like in hollow-core crystal fibers [122, 254], and environments, like on satellites [74, 106, 97].

List of my articles related to this chapter:

1. L. Ricci, D. Bassi, and A. Bertoldi. **Combined static potentials for confinement of neutral species**. In: *Phys. Rev. A* **76**.2 (2007). DOI: 10.1103/physreva.76.023428

2. A. Bertoldi and L. Ricci. **Gravito-magnetic trapping of ^{87}Rb**. In: *J. Phys. B* **41**.15 (2008), p. 155301. DOI: 10.1088/0953-4075/41/15/155301

3. A. Bertoldi and L. Ricci. **Dynamics of a cold atom cloud in an anharmonic trap**. In: *Phys. Rev. A* **81**.6 (2010). DOI: 10.1103/physreva.81.063415

4. A. Bertoldi et al. **In situ characterization of an optical cavity using atomic light shift**. In: *Opt. Lett.* **35**.22 (2010), p. 3769. DOI: 10.1364/ol.35.003769

5. D. S. Naik et al. **Bose–Einstein condensate array in a malleable optical trap formed in a traveling wave cavity**. In: *Quantum Sci. Technol.* **3**.4 (2018), p. 045009. DOI: 10.1088/2058-9565/aad48e

6. D. S. Naik et al. **Loading and cooling in an optical trap via hyperfine dark states**. In: *Phys. Rev. Res.* **2**.1 (Feb. 2020). DOI: 10.1103/physrevresearch.2.013212

6. G. Condon et al. **All-Optical Bose-Einstein Condensates in Microgravity**. In: *Phys. Rev. Lett.* **123**.24 (Dec. 2019), p. 240402. DOI: 10.1103/physrevlett.123.240402

Chapter 4

Order emergence in a travelling wave cavity

To see a World in a Grain of Sand
And a Heaven in a Wild Flower,
Hold Infinity in the palm of your hand
And Eternity in an hour.
— William Blake, Auguries of Innocence

The subject of Ch. 4 is the present research activity on the cavity QED experiment, targeting the observation of self-organisation phenomena in the traveling wave configuration implemented in the bow-tie cavity. The principal aim is to investigate order emergence in a broader context with respect to what spectacularly demonstrated in the last years in standing wave resonators. The main ingredient characterizing our specific geometry is the absence of boundary conditions on the intra-cavity electric field at the mirrors; as a consequence, the phase of the optical and atomic lattice that should form in the cavity is a free parameter. The second-order phase transition to the ordered configuration is not only described in terms of a continuous phase parameter, but determines as well the entanglement between the atomic and the light component of the system. The scientific program aims to realize other exotic states of matter, like the entanglement between two components of a single BEC, or a network of entangled BECs. The latter is a potential breakthrough for quantum communication protocols.

The research activity is carried out within the frame of two related projects, one financed by ANR ("EOSBECMR") and the other by LAPHIA ("OE-TWR") for the study of self-organisation phenomena in a traveling wave cavity.

Matter–light interaction involves exchange of energy and momentum. In cavity QED with ultracold particles in high Q resonators, only a single photon is needed to confine the motion of an atom [255] and a single atom can significantly change the field dynamics, allowing the recent experimental realization [256] of theoretical models and applications presented almost 20 years ago [257]. Trapping a quantum degenerate gas in a cavity brings a wealth of quantum phenomena, such as atom-field entanglement, with unprecedented control [258]. As the light fields and atoms are dynamical, photon mediated long-range forces generate long range order and phonon-like excitations with widely controllable properties. Experimentally, these features allowed the study of zero temperature opto-mechanics [259], the Dicke

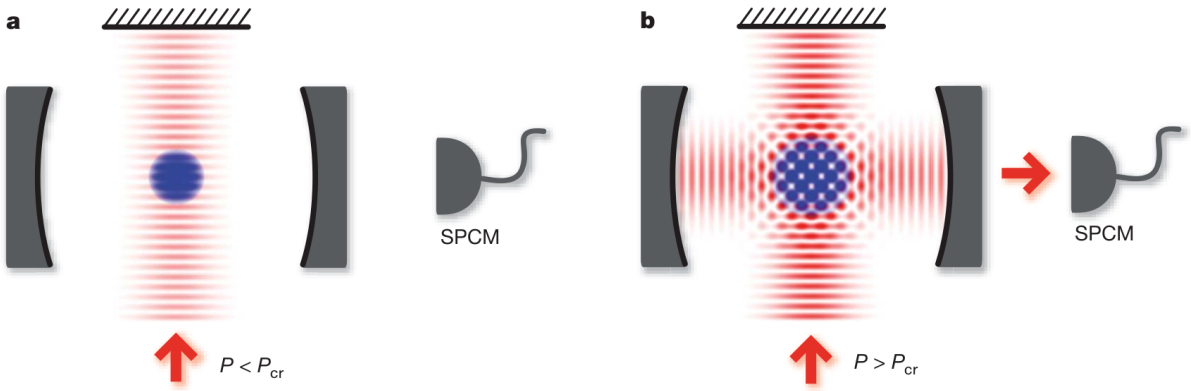

FIGURE 4.1 — [from [256]] Scheme of the Dicke phase transition observed in a BEC trapped in an optical cavity and pumped with a standing-wave laser, whose frequency is far red-detuned with respect to the atomic transition line but close to a particular cavity mode. The photons scattered by the atomic ensemble into the cavity have a phase dependent on the specific atomic position; (a) below a critical power, the build-up of a coherent cavity field is suppressed as a result of destructive interference of the individual scatterers. (b) Above a critical pump power the atoms self-organize onto either the even or odd sites of a chequerboard pattern, thereby maximizing cooperative scattering into the cavity. This dynamical quantum phase transition determines the spontaneous symmetry breaking both in the atomic density and in the relative phase between the pump and cavity fields.

superradiant phase transition [256], the formation of an intra-cavity atom-photon crystal and of an atomic supersolid [260]. Quantum phase diagrams for a BEC in an intra-cavity optical lattice with tunable length, showed photonic interactions exhibiting superfluid, insulating and supersolid regions [261], whereas infinite range interactions demonstrated a superradiant Mott insulating phase [262].

4.1 Self-organisation in a traveling wave cavity

In the past fifteen years, many phenomena of long-standing interest in condensed-matter physics have been realized in ultra-cold atomic settings [263], mainly thanks to the high degree of control attained and their ideal isolation from environment, that allow an efficient description in terms of thoroughly understood tunable Hamiltonians. To date, most ultra-cold atomic realizations have focused on simulating the physics of electrons propagating through static lattices (via, e.g., realizations of the Hubbard model [264]) or on constructing novel quantum fluids (e.g., Tonks-Girardeau gases [265] or unitary Fermi gases [266]). Soft matter issues like supersolidity [267] and glassiness have proven inaccessible to ultra-cold atomic physics because the lasers creating the lattice potentials are insensitive to the atomic motion taking place within those potentials, while they require emergent, compliant lattices capable of exhibiting dynamics, defects, and melting.

A possible approach to realize such phenomena uses atoms interacting with a potential created by dynamic cavity fields instead of static lasers. The physics of many atoms coupled to the electromagnetic cavity modes, i.e., many-body cavity QED, focused first on the novel implications of the atom-cavity coupling for standard ultracold-atomic phenomena such as the superfluid-Mott-insulator transition [268, 269] or the collective excitation of a BEC [270, 271].

More recently a different class of condensed-matter phenomena, involving the dynamics of spatially ordered states, has attracted interest; their experimental realization requires ultra-cold atoms confined in degenerate optical cavities. The presence of more than one electromagnetic mode to interact with opens the possibility to observe Brazovskii transitions [272] to the liquid crystal phase, and then

to investigate a plethora of effects like frustration, dynamics of defects, and supersolidity. The most advanced experiments in this context are represented by the tunable cavity setup of B. Lev in Stanford [273], where interatomic interaction can be varied from short- to long-range [274], and the setup based on two competing cavities of T. Esslinger at ETH in Zurich, implementing two simultaneous order parameters [275].

The many-body cavity QED experiment already adopted for the quantum measurement protocols (Ch. 2) and for the dark-state enhanced cooling (Ch. 3) has a relevant feature to study 'emergent' properties, in the form of spontaneous formation of a patterned atomic structure at a macroscopic level: the bow-tie geometry of the cavity determines its traveling wave configuration, hence there are no boundary conditions for the intra-cavity lattice at the mirrors. This features opens the possibility to study order formation in the presence of a continuous order parameter – the phase of the lattice and also of the atomic pattern. The broad scientific target is to shed light on cooperative effects in atomic systems and order emergence phenomena in new regimes relevant for many effects characterizing glassy materials, like frustration, defect dynamics and melting.

Emergent physics with a BEC in a traveling wave cavity

A cavity held BEC, as we recently obtained [227], will be investigated for observing an emergent crystallization state with a continuous order parameter. An independent pump laser will be incident on the atoms transversely with respect to the cavity plane, and playing with its intensity and detuning with respect to the atomic resonance and to the cavity resonance will unveil the superradiant phase transition. The verification and successive characterization of the cavity induced emergent states will be done by implementing a novel spectroscopy scheme, based on the study of correlation properties (G2 spectroscopy) of both the atomic crystal an the light leaking out of the resonator. The measurement of the statistical correlations in momentum space can be used to investigate cavity mediated momentum correlation/entanglement for the atoms. Cauchy-Schwarz type inequalities for the atoms in momentum space will be adopted and their violation tested to establish the creation of quantum correlated states. An alternative non-destructive approach exploits the correlations of the light emitted from the cavity: at weak coupling, the intracavity-photon correlations are directly related to the atomic momentum correlations, thus measuring two-photon correlations for the photons exiting the cavity should reveal the correlations in the atomic momentum [276]. Such spectroscopic method, introduced first in quantum information and communication, would represent a breakthrough in quantum non-demolition measurements on a cavity QED system.

Two-Component BEC Coupled to a Ring Cavity

The concept of self-ordering can be extended in a ring cavity by adding an extra order of complexity: a multi-component spinor BEC. By adjusting different parameters of the system, we can engineer a variety of phenomena ranging from genuine self-ordering with the spin degree of freedom to cavity-mediated anti-ferromagnetic ordering. Thus far, almost all of the experimental works and most of the theoretical studies of coupled BEC-cavity systems are restricted to single-component – also called scalar – BECs. A two-component BEC coupled to a ring cavity has been recently predicted to exhibit intriguing phenomena: the emergence of a synthetic strong magnetic field and spin-orbit coupling, a cavity-mediated Hofstadter spectrum, disorder-driven density and spin self-ordering, and a variety of spin and magnetic orders [277, 278, 279, 280] to mention a few. With the bow-tie traveling wave resonator we will introduce controllable dynamic spin dependent long-range interactions, and couple multiple BECs to perform cutting edge experiments at the forefront of ultra-cold atomic research.

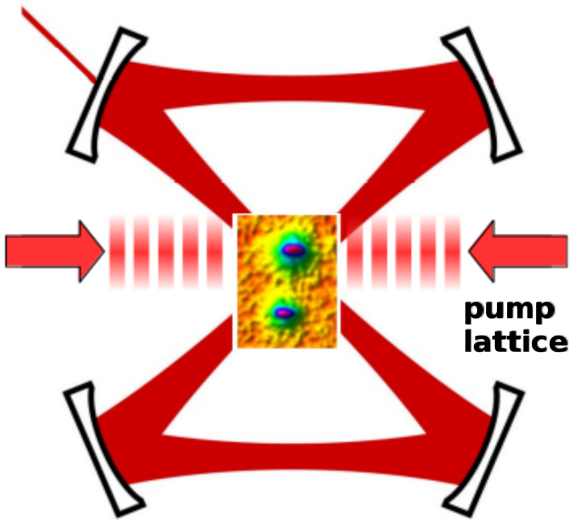

FIGURE 4.2 — The two BECs produced in the bow-tie cavity setup [227] will be phase-locked by using the resonator to transfer the crystallization induced on one condensate via external optical pumping with an optical lattice.

We will experimentally study the dynamics of a two-component BEC coupled to four modes of the ring cavity in opposite and parallel pumping configuration. In both pumping schemes, the system is initially translation invariant, since the two non-degenerate and pumped modes do not interfere with one another, being their polarization orthogonal. The un-pumped degenerate cavity modes are then populated due to the scattering of photons from the pumped modes via two-photon Raman processes. The interference of each pair of degenerate, counter-propagating modes leads to emergence of a dynamical optical potential for each pseudo-spin state, whose position is completely random and independent of the other one. The self-ordering of each component constitutes a real crystallization, accompanied with a genuine translation symmetry breaking, reminiscent of the real crystallization mechanism in solid material, in contrast to a standing wave cavity. Moreover, emergent spin ordering could result due to the pseudo-spin degrees of freedom.

In addition to the cavity inducing a dynamic, compliant light field, the shared light field can also be used to mediate long range interactions between atoms trapped inside a ring cavity. Photon mediated spin-spin interactions can be generated between ultracold-atoms trapped inside a ring cavity [256, 281], with the aim of studying quantum magnetic states of an 'emergent' nature and simulating heavy-fermion materials and metallic spin glasses.

4.1.1 Realize a quantum network of BECs

The non-degenerate resonator implementing our experimental platform can be selectively pumped on its high order transverse modes, which we exploited to obtain an array of BECs [227]. Cavity mediated photons can create long-range interactions between these independent condensates, with a wealth of possible applications: (i) creating correlations between the BECs via a common cavity mode; (ii) achieving entanglement between two independent spinor BECs; (iii) inducing a self-ordering state on one BEC via the cavity-mediated long-range interactions from the second BEC.

The sub-recoil nature of the cavity (≈ 10 kHz vs a recoil frequency $\omega_r = 2\pi \cdot 3.77$ kHz) implies that the light shift per photon exceeds the cavity resonance linewidth, leading to atom-cavity dynamics that are sensitive to the quantized motion of the atoms inside the cavity. For sufficiently large mode

volume or high finesse of the cavity, the otherwise tiny back-action of the moving atoms upon the light field becomes significant. The consequence is an inherently collective character of the atomic motion and a corresponding non-linear dynamics of the intra-cavity field. The resulting multi-BEC system within a single sub-recoil cavity mode coupled to their quantized motion closely resembles the quantum network of cavities connected via optical fibers [282, 283], and will create entangled states between different BECs.

The possibility to transfer the crystallization between two BECs will be investigated, by implementing the following protocol on the two ensembles trapped in the ring cavity (see Fig. 4.2): driving BEC_1 into self-ordered state; the photons scattered into the cavity can interact with BEC_2; two-photon scattering events between the intra-cavity field and BEC_2 can bring it into its own self-ordered state. As both BECs share a common cavity mode, the phase of their ordering should be correlated. Correlations between two independent self-ordered states can thus be created and manipulated: the modulation in phase of the laser pumping BEC_1 should determine the modulation of the phase of the BEC_2 ordering. This can be proved by weakly probing BEC_2 with an external laser and examining the phase of such weak probe with the pump of BEC_1 via homodyne spectroscopy. When the phase of the two self-ordered states are correlated, we should see a defined, constant phase between the weak probe and the pump, which would implement a super-radiance mediated PLL between the BECs.

Chapter 5

Technology for AMO physics

We can only see a short distance ahead, but we can see plenty there that needs to be done.

— Alan Turing, Computing machinery and intelligence

Ch. 5 presents a selection of technological solutions I contributed to develop in the context of AMO physics, ranging from optics, servoing and electronics to generation and control of magnetic fields and exploitation of time and frequency (T/F) signals.

5.1 Serrodyne based Pound-Drever-Hall

The frequency stabilization of lasers is required in a wide range of applications, such as optical atomic clocks [54], gravitational wave detectors [126], and quantum optomechanical setups [284]. In these systems, the correction bandwidth and correction range are two key parameters to reach a low noise stabilization as well as to ensure robustness against perturbations from the environment. Nevertheless, many commonly used lasers, such as fiber, dye, or diode-pumped solid state lasers, have only piezoelectric transducers (PZTs) as a means of frequency correction. Typically, the correction bandwidth is thus limited to a few kilohertz. As a consequence, for higher frequencies, an external actuator is usually needed to extend the correction range. An AOM can only reach a few hundred kHz bandwidth and a dynamic range of up to a few tens of MHz. Instead, an EOM allows a higher correction bandwidth of several MHz, but frequency shifts cannot be sustained for long, hence it operates on a small correction range. An optimal frequency actuator has been proposed that pairs the high bandwidth of an EOM with the large dynamic range of an AOM [285], but its implementation is challenging.

We implemented a novel servo system which uses an EOM as the unique frequency actuator to stabilize a laser on an optical cavity: we can combine a very high dynamic range to the fast response of the EOM thanks to the serrodyne frequency modulation technique. In simple terms, the EOM is driven with a linear phase ramp, to obtain a frequency shift; to avoid the EOM's phase saturation, the accumulated phase value is reset whenever it reaches a fixed integer multiple of 2π. The RF port of the EOM results thus driven by a saw-tooth-like signal, whose slope determines the laser frequency shift. The saw-tooth signal is produced with a non-linear-transmission-line (NLTL), driven by a voltage controlled oscillator (VCO), whose frequency is in turn controlled by a Pound-Drever-Hall error signal

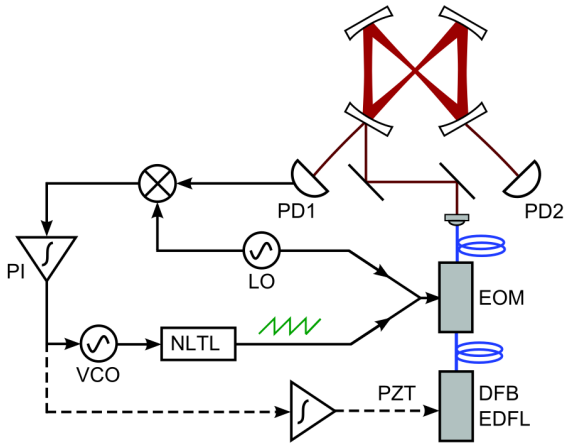

FIGURE 5.1 — (left) [from [286]] Setup of the laser stabilization to the bow-tie optical cavity based on serrodyne frequency shifting. The laser is injected in the cavity after an all-fibered path. The Poud-Drever-Hall correction loop uses the serrodyne frequency and the laser piezoelectric devices as actuators at high (till 2.3 MHz) and low (¡100 Hz) bandwidth.

of the laser/cavity system. The process by which the NLTL produces the saw-tooth-like shape is similar to the wave surging when approaching the seaside: the changing distance of the sea bottom makes the propagation velocity amplitude dependent, and the wave fronts becomes thus steeper.

The microwave NLTL we adopted (Picosecond Pulse Labs, mod. 7112-110) uses an input frequency between 300 MHz and 700 MHz, and generates harmonics till 20 GHz. We obtain with it a 80% transfer of the laser frequency. The laser is servo-controlled to the cavity with 2.3 MHz correction bandwidth and 220 MHz correction range, both about one order of magnitude higher than what achieved with a standard AOM-based correction loop. Moreover, the system is all fibered, which avoids the power loss determined by passing in free space.

5.2 Active control of magnetic field and its bias

Controlling magnetic fields is of fundamental importance in several AMO physics contexts: not only they shift the atomic levels via the Zeeman effect, and result thus crucial to obtain optimally polarized atomic samples, but they permit as well to produce ultracold molecules from atoms [26], and entangled atomic couples from the dissociation of molecules [216] via the Feshbach resonances [289]. Other contexts require the precise measurement of magnetic fields, among the others biological sciences (monitoring of tiny brain or plants magnetic activity), geology (ore prospecting), automotive (proximity sensors). During my first postdoctoral fellowship in Trento I developed first a high bandwidth magnetoresistive magnetometer [290, 291], and then a non–invasive system to simultaneously control the magnetic field strength and its gradient along one direction (Fig. 5.2, left) [287]. To implement the feedback loop we had to solve two problems: first, the sensing system shows a different response with respect to the external and the correction field gradients. An archetypal situation is provided by a feedback loop system that controls the illumination of a room where the external light is predominantly yellow, the compensation lamp predominantly green, and the light level sensor has different efficiencies at different colors. The solution of this problem required the precise characterization of the different sensitivity of the system to: (i) external magnetic fields; (ii) magnetic field generated for

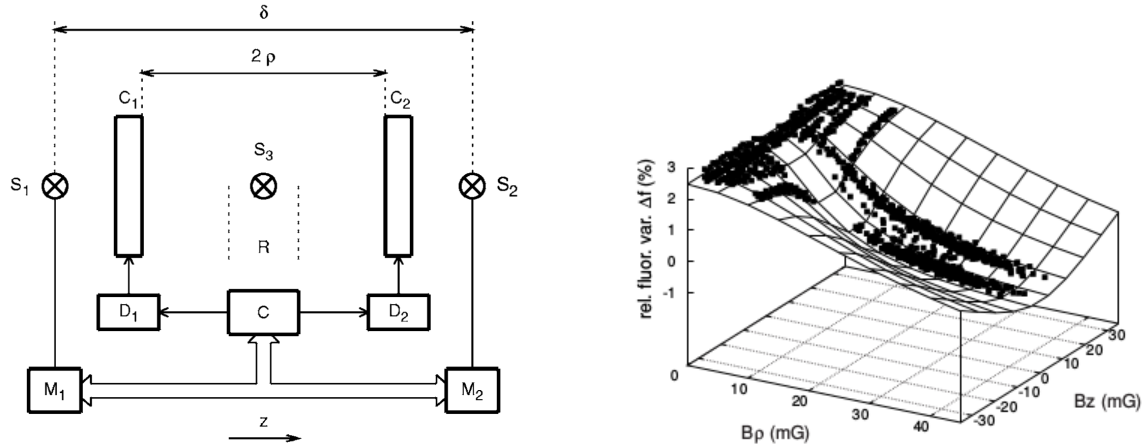

FIGURE 5.2 — (left) [from [287]] Scheme of the system controlling the magnetic field strength and gradient along the z direction. The sensor heads S_i measure the field along the z axis; the field proportional values generated by the consoles M_i are sent to to the controller C. This device real-time processes the readouts and generates two voltage error signals to pilot the current drivers D_i, each feeding a compensation coil C_i. (right) [from [288]] Scan of the atomic fluorescence around a Hanle resonance as a function of the magnetic field components.

the corrections. The second problem is represented by the two quantities to be controlled (B_z and $\partial_z B_z$) not being independent of each other, which required a matrix analysis and implementation of the feedback loop.

The active, simultaneous compensation of field strength and gradient is particularly appropriate whenever the magnetic field cannot be measured *in situ* with a sensor, as well as when a non vanishing magnetic field or a particular gradient is required – these field configurations are not achievable with the standard configurations relying on μ-metal shields, which also determine a consistent reduction of the optical access. As an example, we could produce an uniform field over an extended region, by actively controlling the magnetic field to vanish its gradient; such configuration is of great interest in ground state level crossing resonances experiments, because it can generate not only a specific position where the resonance is obtained, but an entire region. We verified experimentally such configuration, and measured the enhanced absorption Hanle effect resonances in ^{85}Rb (Fig. 5.2, right) [288].

5.3 High efficiency magnetic field sources

Specific configurations of magnetic field must be generated for different purposes in typical cold atom experiments: bias magnetic fields are produced along the three directions to compensate the environmental magnetic field; a magnetic quadrupole is required for the MOT; achieving a BEC in a magnetic trap needs a minimum of the modulus of the magnetic field, with a field far from zero at the trap bottom to avoid Majorana spin-flips. The standard solution to obtain the required field uses a set of circular electromagnets, each with a large number of windings. Additional constraints impose different choices, as is the case of the large amount of power to be dissipated in magnetic traps or in Feshbach coils: the heat produced can be taken away by a coolant flowing in conductive copper tubes with a cylindrical bore. This solution, however, introduces further design concerns due to the viscous resistance R that is opposed by the pipe to the coolant flow, the dependence of R on the pipe length L and bore cross-section σ, and the technical limitation on the coolant pressure. To overcome these difficulties posed by hydrodynamics, we developed a new kind of water-cooled electromagnet in

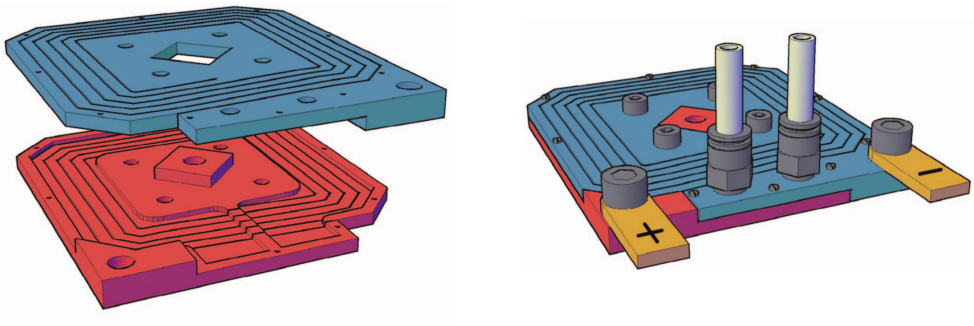

FIGURE 5.3 — [from [292]] Assembly of the two coils (left) to form the final magnet (right). The graphical rendering of the magnet also shows the tightening screws, the electric connections, and the quick release hydraulic couplings with related tubes for the coolant.

which the windings form a single rectangular duct of large section (see Fig. 5.3) [292]. The resulting setup combines an efficient heat removal with low coolant pressure, features that can be exploited to increase the electric current in the electromagnet, so as to optimize the trapping parameters.

On the basis of this prototype, we developed a high performance Ioffe-Pritchard trap [293], which we designed to cope with a set of specific geometric constraints [294]: the shape and size of the glass vacuum cell for the atoms, and other sections of the UHV system make circular electromagnets a sub-optimal choice. To numerically find the best solution to such a multi-parameter problem we used a Monte-Carlo algorithm, which determined the optimal magnet shape. Fig. 5.4 shows the calculated shape of the cloverleaf magnetic trap (left) and its experimental realization (right). The conductive spirals with the calculated shape have been realised by electro–erosion on bulk copper plates, and the sealing of the device required the development of waterproof and insulating layers, realized in Teflon and silicone.

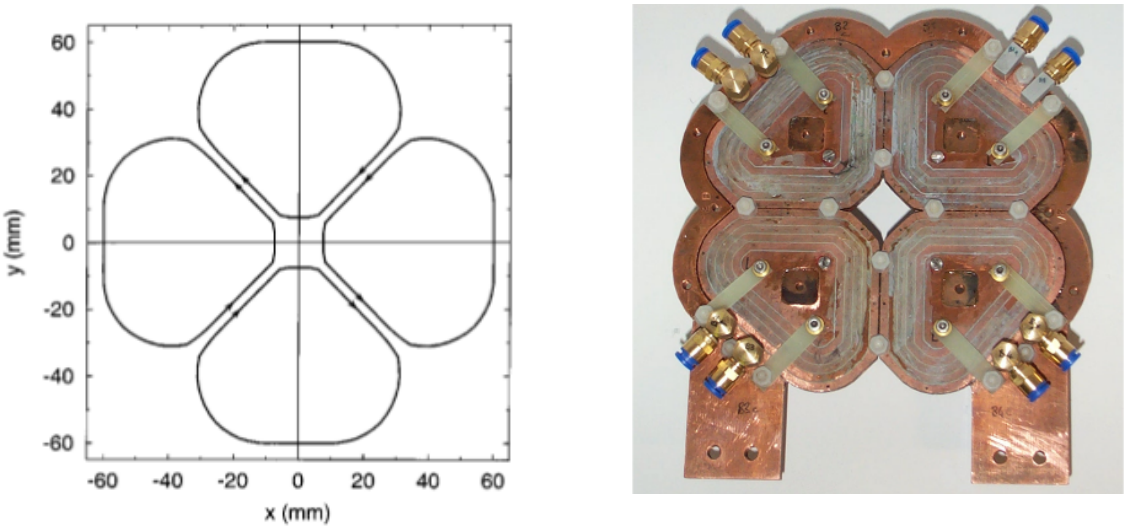

FIGURE 5.4 — (left) [from [294]] Optimized cloverleaf-like magnetic trap configuration obtained with a Monte-Carlo algorithm to cope with the geometrical constraints set by the vacuum setup; (right) its experimental realization.

5.4 Real-time control system for AMO physics experiments

Experiments in AMO physics require precise and accurate control of digital, analog, and radio frequency (RF) signals. During the years, I developed a few different solutions, based on real-time control (RTC) systems like RT-Linux and RTAI. More recently, together with Dr. Prevedelli I developed a hardware control system based on an FPGA core which controls various modules via a simple interface bus [176]. The system supports an operating frequency of 10 MHz and a memory depth of 8 M instructions, both easily scalable. Successive experimental sequences can be stacked with no dead time and synchronized with external events also for specific sub-sequences. Two or more control systems can be cascaded and precisely synchronized, a feature useful to operate large experimental setups in a modular way.

The system is general purpose, and could serve to control a large class of experiments not only in AMO physics. Nevertheless, it has been designed to fulfill the experimental requirements of the three experiments I already described in this manuscript, i.e. the MIGA experiment, the strontium atom interferometer, and the cavity QED experiment adopting a traveling wave resonator.

The strict temporal resolution required, typically of the order of 10 μs or better, determines the RTC character of our system. It is generally not possible to fulfil such a constraint with a modern general purpose multitasking operating system (OS), so dedicated OSs have been developed. The software approach to RTC has certainly the advantage of simplicity, versatility and, in case of open-source solutions, low cost; nevertheless, a hardware approach has generally superior performances in terms of temporal resolution. In our system, the RTC is implemented with a commercial FPGA (Field Programmable Gate Array) board, which sends commands at pre-programmed times on a data bus to which are connected peripherals boards. The large table of time/commands is stored on a SDRAM, and is processed to obtain a maximum rate of one action every 100 ns. The most common peripherals boards we developed are: Digital Outputs, Analog Outputs, DDS-based RF generators, a general purpose Analog I/O module for complex operations. The modular nature of the system makes it easy to adapt parts of it to other applications, or to engineered it to be compatible with portable or space applications in terms of weight, volume, and power consumption.

5.5 Optical clock signal at LP2N

Research activity being carried out within the frame of the project "USOFF", financed by the Aquitaine Region.

The ultimate performance in time and frequency standard in terms of both precision and accuracy[1] is nowadays provided by optical lattice clocks [54, 55]. Realizing and running such an experiment is a complex and expensive task, which requires a noteworthy know-how and is up to now a prerogative of a handful of metrological laboratories in the world. A recent approach to provide the ultra-stable frequency signal of lattice clocks to a wider range of potential users exploits the telecom network to distribute the T/F signal over hundreds and even thousands of km [295]. Several projects at the national and continental scale [296] are developing and implementing the required technology for the capillary distribution of the signals produced at the national metrological labs. Such facility will boost fundamental and applied sciences in several contexts, ranging from geodesy [297], to astronomy [298] and precision gravimetry [299] to mention a few. Another field that will benefit from a wider

[1] Only the intrinsic accuracy is here taken into account; that due to the Cs clock on which the SI time signal is defined is not considered.

dissemination of ultra-stable frequency signal is T/F comparison, which is still a challenging problem, due to the clock signal degradation over large distances. A common technique relies on transmissions using satellites as signal repeaters, but it is limited to 10^{-15} level because of the noise introduced by the atmosphere. Portable clocks are good for specific purposes, but do not represent a solution for a wide signal distribution. Very high quality transfer, compatible with the best existing optical clocks, can instead be realised using the Internet fiber network. The French EquipEx REFIMEVE+ [300] builds on these results, and is making accessible the stable optical clock signal produced by the National Metrological Lab throughout France.

In 2018 I received a grant form the Region Nouvelle-Aquitaine to exploit on the Talence-Bordeaux campus the REFIMEVE+ optical clock signal that will be soon delivered by the Observatoire de Paris. The two main objectives of the project are: (i) to build a metrological laboratory at LP2N, where the optical signal provided by REFIMEVE+ will be referenced to local frequency references (notably: an ultra-stable optical cavity using an optical frequency comb, and the GPS signal); (ii) to implement an embryonic local distribution network, to provide the stabilized signal via optical fiber to several partner laboratories on the Talence-Bordeaux campus. In perspective, the distribution will be made progressively more capillary. Once the infrastructure will be operative, the ultra-stable T/F signals will be exploited by the different partners of the consortium in several contexts, both related to fundamental science and more applied ones:

- (LP2N) implementation of a new class of matter-wave interferometers, for the coherent manipulation of ultra-cold atoms by means of optical cavities (Equipex MIGA), the study of the quantum decoherence for macroscopically delocalised states (ANR ALCALINF), and the measurement of the weak equivalence principle (project ICE);
- (LAB) R&D activity for the synchronization of large networks of radio-telescopes, and to provide the T/F base to the VLBIs;
- (CELIA) development and characterization of high power pulsed lasers;
- (XLIM) development of a new class of highly miniaturized optical reference based on molecular photonic micro-cells for integrated photonic solutions in T/F, space and environmental applications;
- (Companies: ALS, Amplitude Systems, Alphanov, μQuans) development of ultra-fast (femtosecond mode-locked laser) and ultra-stable laser sources, development of opto-electronical systems for the T/F distribution and atomic clocks.

List of my articles related to this chapter:

1. A. Bertoldi et al. **Magnetoresistive magnetometer with improved bandwidth and response characteristics**. In: *Rev. Sci. Instrum.* **76**.6 (2005), p. 065106. DOI: 10.1063/1.1922787

2. A. Bertoldi et al. **Noise and response characterization of an anisotropic magnetoresistive sensor working in a high-frequency flipping regime**. In: *Eur. Phys. J. Appl. Phys.* **33**.1 (2005), pp. 51–57. DOI: 10.1051/epjap:2005088

3. L. Botti et al. **Noninvasive system for the simultaneous stabilization and control of magnetic field strength and gradient**. In: *Rev. Sci. Instrum.* **77**.3 (2006), p. 035103. DOI: 10.1063/1.2173846

4. G. Lamporesi et al. **Source mass and positioning system for an accurate measurement of G**. in: *Rev. Sci. Instrum.* **78**.7 (2007), p. 075109. DOI: 10.1063/1.2751090

5. A. Vilardi et al. **Measurement and modelling of enhanced absorption Hanle effect resonances in ^{85}Rb**. In: *J. Phys. B* **42**.5 (2009), p. 055003. DOI: 10.1088/0953-4075/42/5/055003

6. R. Kohlhaas et al. **Robust laser frequency stabilization by serrodyne modulation**. In: *Opt. Lett.* **37**.6 (2012), p. 1005. DOI: 10.1364/ol.37.001005

7. L. Ricci et al. **A current-carrying coil design with improved liquid cooling arrangement**. In: *Rev. Sci. Instrum.* **84**.6 (2013), p. 065115. DOI: 10.1063/1.4811666

8. S. Rota-Rodrigo et al. **Watt-level single-frequency tunable neodymium MOPA fiber laser operating at 915–937 nm**. In: *Opt. Lett.* **42**.21 (2017), p. 4557. DOI: 10.1364/ol.42.004557

9. A. Bertoldi et al. **A control hardware based on a field programmable gate array for experiments in atomic physics**. In: *Rev. Sci. Instrum.* **91**.3 (Mar. 2020), p. 033203. DOI: 10.1063/1.5129595

10. D. O. Sabulsky et al. **A fibered laser system for the MIGA large scale atom interferometer**. In: *Sci. Rep.* **10**.1 (Feb. 2020). DOI: 10.1038/s41598-020-59971-8

Chapter 6

Curriculum Vitae

Place and date of birth:	Trento (Italy), 13/04/1977
Nationality:	Italian and French
Postal Address:	Institut d'Optique d'Aquitaine, LP2N – UMR5298 rue François Mitterrand F–33400 Talence (France)
Tel:	+33 (0)5 57 01 72 03
E-mail:	andrea.bertoldi@institutoptique.fr
ORCID:	0000-0002-4839-0947
ResearchGate:	https://www.researchgate.net/profile/Andrea_Bertoldi

6.1 Professional experience

- **Laboratoire Photonique, Numérique et Nanosciences (LP2N), France – 2013 - Present**
  Research Engineer IOGS, topics: AI and GWD, cavity QED, AI space missions, metrology
- **Laboratoire Charles Fabry de l'Institut d'Optique (LCFIO), Palaiseau France – 2009 - 2013**
  Post-doctoral and Marie-Curie fellow in the group of Prof. A. Aspect, topics: quantum measurements, cavity QED, AI
- **Università Studi Firenze, Italy – 2005 - 2008**
  Post-doctoral fellow and Research Assistant in the group of Prof. G. Tino, topics: AI, measurement of G
- **Università Studi Trento, Italy – 2005**
  Post-doctoral fellow in the group of Prof. D. Bassi, topics: gravito-magnetic atom trapping

6.2 Education

- **University of Bordeaux, École Doctorale SPI, Bordeaux France – 2017**
  Autorisation à Diriger une Thèse (ADT)
- **Università Studi Trento, Italy – 2004**
  PhD in Physics, Advisor: Dr. L. Ricci, Dissertation: Trapping of neutral atoms by static, combined potentials, Thesis Committee: Prof. S. Stringari, Prof. G. M. Tino, Prof. M. Prevedelli.

- **Università Studi Trento, Italy – 2000**
  M.Sc. (Laurea) degree in Physics, 110/110 cum laude, Advisor: Dr. L. Ricci, Thesis: Magneto-optic and magnetic trapping of rubidium atoms.
- **G. Galilei high school, Trento, Italy – 1996**
  Scientific lyceum degree, score 60/60, in Trento (Italy).

6.3 Honors, grants and appointments

- **From 2019 – member of the Fundamental Physics Advisory Group at CNES**
- **2019 QuantERA Call – member of the Scientific Evaluation Panel**
- **2018–21 Expert Member of COST Action AtomQT CA16221**
- **2018 Laureate of the ANR program, project EOSBECMR**
- **2018 Laureate of the LAPHIA Risky program, project OE-TWR**
- **2018 Laureate of the AAP Région Nouvelle-Aquitaine, project USOFF**
- **2015 Laureate of the AAP Région Nouvelle-Aquitaine, project IASIG-3D**
- **2014 Laureate of the LAPHIA Passeport program, project APLL-CLOCK**
- **2009-11 Marie Curie Individual Fellowship, IEF Grant No. PIEF-GA-2009-235375**
- **2009 EOS Prize** for the article *Precision measurements of gravity using cold atom sensors*, Journal of the European Optical Society – Rapid Comm. 4, 09025 (2009).
- **2001/02/03/04 – PhD fellowship of the Physics Department, Trento University, Italy**
- **1997/98/99/2000 – Fellowship from Trento University, Italy**
- **1998/99/2000 – Fellowship from Cassa Rurale Pinetana e Fornace, Italy**
- **1997 – Prof. F. Clauser Grant** from Lyceum 'G. Galilei', Trento, Italy

---

6.3.1 Supervision of students

• **Direction of Ph.D. students**:
- 2018– Hodei Eneriz Imaz – co-direction with P. Bouyer - *[1 art., 2 subm. art.]*
- 2017– Chen-Hao Feng – direction - *[3 subm. art.]*
- 2016–19 Max Carey – co-direction with Dr. T. Freegarde at Univ. Southampton (UK) - *[2 subm. art.]*

• **Supervision of Ph.D. students**:
- 2015–19 Gregoire Lefèvre – encadrement (dir. P. Bouyer) - *[3 art., 1 pat., 2 proc.]*
- 2014–18 Grigor Kujumjyan (now Scientist at CGI, France) – encadrement (dir. P. Bouyer) - *[1 pat., 1 proc.]*
- 2014–17 Isabelle Riou (now at E2V in Chelmsford – UK) – encadrement (dir. P. Bouyer) - *[2 art., 1 pat., 4 proc.]*
- 2013–15 Etienne Cantin (now postdoc at SYRTE, Paris) – encadrement (dir. P. Bouyer) - *[2 art., 2 proc.]*
- 2011–13 Ralf Kohlhaas (now Instrument Scientist at SRON Netherlands Institute for Space Research – NL) – encadrement (dir. P. Bouyer) - *[5 art., 1 pat., 1 proc.]*
- 2010-12 Thomas Vanderbruggen (co-founder of Koheron, Paris) – encadrement (dir. P. Bouyer) - *[6 art.]*
- 2008-11 Simon Bernon (now MdC at LP2N-IOGS in Bordeaux) – encadrement (dir. P. Bouyer) - *[5 art.]*
- 2005-08 Giacomo Lamporesi (now researcher at CNR-INO Trento – Italy) – encadrement (dir. G. Tino) - *[4 art., 3 proc.]*

• **Supervision of Master students**:
- 2019 Patrick Banon (M2)
- 2018 Jean-Philippe Volkaert (M1)
- 2018 Hassan Rammal (M2)
- 2017 Reza Khoshtinat Nikkhouy (M2)
- 2017 Jordan Heraud (M2)
- 2013 Gabriel Marty (M1)
- 2011 Dorian Grosso (M1, now PhD in the group of S. Haroche at LKB Paris)
- 2011 Ralf Kohlhaas (M2, now at SRON - NL)
- 2008 Manuele Landini (M2, now researcher in the group of H.C. Nägerl at IQOQI Innsbruck)

• **Supervision of Engineer**:
- 2016–now Arnaud Tizon (AI in micro-electronics at LP2N)

6.4 Research funding and participation

6.4.1 Research funding as PI

• **2019–21 EOSBECMR – Emergent Orders of Spinor BECs in a Multimode Ring Resonator**
ANR–FWF PRCI (PI at LP2N: Dr. A. Bertoldi; PI at Univ. Innsbruck: Dr. F. Mivehvar) – **ANR: 345 k€; FWF: 200 k€**
To demonstrate self-organization in a traveling wave cavity, order transfer between two BECs, macroscopic entanglement of BECs via cavity coupling.

• **2018–21 USOFF – Ultra Stable Optical Frequency Fibre distribution network**
Region Nouvelle Aquitaine Project – **506 k€**
To develop a metrological laboratory at LP2N to receive and treat optical clock signal from LNE-SYRTE; redistribute REFIMEVE+ on the Talence-Bordeaux campus for scientific applications in AI, radio-astronomy and laser development.

• **2018–19 OE-TWR – Order Emergence in a Traveling Wave Resonator**
LAPHIA IdEx Risky Project – **65 k€**
To observe atom-cavity coupling and emergent phenomena in traveling wave cavity.

• **2016 Ultra-stable clock laser for strontium atom interferometer**
LAPHIA scholarship for Invited Professor at LP2N. PIs: Dr. M. Prevedelli (Univ. Bologna), Dr. A. Bertoldi – **30 k€**
To develop a clock laser at 698 nm, stabilized on a cavity reference.

• **2015–18 Quantum coherent enhancement of atom interferometric inertial sensors**
UK-France joint PhD program. PIs: Dr. T. Freegarde (Univ. Southampton, UK) and Dr. A. Bertoldi – **160 k£**
To study pulse shaping techniques in AI, and measurement-and-correction protocols in atomic gyroscopes.

• **2015–16 IASIG-3D – Interférométrie Atomique avec du Strontium et Imagerie Gravitationnelle 3D**
Project Region Aquitaine – **220 k€**
With this project we introduced the GGN mitigation technique based on arrays of atom interferometers, and developed a fibered solution for the blue light at 461 nm used for the first laser cooling stage of strontium.

• **2014–15 APLL-CLOCK – Atomic phase-locked loop for timekeeping**
LAPHIA IdEx Passport Project – **72 k€**
This project allowed to implement an enhanced atomic clock exploiting coherence preserving measurements on the same atomic state.

• **2009 - 2011 - QNDINTERF (Quantum Non Demolition INTERFerometry)**
Marie Curie Individual Fellowship, IEF Grant No. PIEF-GA-2009-235375 – **184 k€**.
To develop a cavity QED setup for quantum measurements on rubidium atoms, and to study non-classical input states to enhance AI.

6.4.2 Research funding as PI at LP2N

• **2018–21 TAIOL – Trapped Atom Interferometry in Optical Lattice**
QuantERA 2018. Coordinator: Dr. F. Pereira dos Santos (SYRTE, Paris, France); PI at LP2N: Dr. A. Bertoldi – **LP2N: 150 k€**.
To develop coherent splitting and recombination of BECs on the high order cavity modes of a traveling wave cavity.

• **2014–17 GG-ITT – Gradiometry in space**
ESA ITT 2014. Coordinator: Dr. F. Pereira dos Santos (SYRTE, Paris, France); PIs at LP2N: Dr. A. Bertoldi and Dr. B. Battelier – **LP2N: 60 k€**.
To study the experimental setup and related requirements of a satellite based AI gravity-gradiometer to measure the Earth gravity field.

• **2013–15 QESOCAS – Quantum Engineered States for Optical Clocks and Atomic Sensors**
EMRP JRP-EXL01. Coordinator: Sebastien Bize (SYRTE, France); PIs at IOGS: Dr. A. Bertoldi and Dr. P. Bouyer – **(LP2N: 170 k€)**.
To study advanced techniques for atomic clock; at LP2N we developed a clock relying on successive phase coherent measurements on the same quantum state.

• **2012–13 AI-ISS (QWEP) – Quantum test of the Weak Equivalence Principle in space**
ESA ITT 2011. Coordinator: Astrium Gmbh (Germany); PIs for France: Dr. A. Bertoldi and Dr. P. Bouyer – **LP2N: 50 k€**.
To study the feasibility of a weak equivalence test at 10^{-14} on the International Space Station.

6.4.3 Participation to Scientific Projects

• **2017–20 ALCALINF – Atom Interferometry with Alkaline-Earth atoms**
ANR Project. Coordinator: Dr. P. Bouyer.
Realization of an atom interferometer with strontium atoms, to perform single photon Aton Interferometry.

• **2015–16 MIGA-PHYS – Physics beyond MIGA**
LAPHIA Collaborative Project. Coordinator: Dr. P. Bouyer(LP2N, Bordeaux, France).
To study correlated interferometry with arrays of gravity-gradiometers.

• **2012–16 STE–QUEST (Space–Time Explorer and Quantum Equivalence Principle Space Test)**
class M3 mission proposal for Cosmic Vision 2015-2025, reached Q3 phase. PI: Dr. E. Rasel (University of Hanover, Germany)
This study considered the feasibility of a weak equivalence test at 10^{-15} on the International Space Station.

• **from 2012 MIGA (Matter wave - laser based Interferometer Gravitation Antenna)**
EQUIPEX 2011. PI: Dr. P. Bouyer (LP2N, Bourdeaux, France).
To develop a demonstrator for GW detection with AI at the underground site of LSBB.

• **2010–15 - iSENSE (Integrated Quantum Sensors)**
STREP project, 7th EU Framework Program. Coordinator: Prof. K. Bongs (University of Birmingham, UK).
To develop an integrated, portable gravimeter for applied sciences.

• **from 01/05/2008 - BIARO (Bose-Einstein Condensation and Quantum Non Demolition measurements in a high finesse resonator)**
IFRAF project (French Institute for Cold Atoms). PIs: Dr. P. Bouyer (Institut d'Optique, France), Dr. A. Landragin (SYRTE, France).
To develop a cavity QED experiment for the study of non-classical states for AI.

• **2005 - 2008 - FINAQS (Future Inertial Atomic Quantum Sensors)**
STREP project within NEST-2003-1 ADVENTURE, 6th EU Framework Program. Coordinator: Prof. W. Ertmer (Institute für Quantenoptik, Universität Hanover, Germany).
To develop AI techniques in several European laboratories, both targeting metrological applications and fundamental physics.

• **2005 - 2008 - MAGIA (Accurate Measurement of G by Atom Interferometry)**
INFN (National Institute for Nuclear Science) project. PI: Prof. G. M. Tino (University of Firenze, Italy).
To develop an atomic gravity-gradiometer for the determination of the Newtonian constant G.

• **2006 - 2007 - SLCA (Space Source for Laser Cooled Atoms)**
ESA project, n. 18330/05/NL/PM.
To develop a space qualified atomic source for AI.

• **2000 - 2003 - PHOTON MATTER**
INFN PRA (Advanced Research Project). Coordinator: Prof. M. Inguscio (LENS and University of Florence, Italy).
To develop atom cooling and trapping techniques.

6.5 Scientific production

Google Scholar profile: https://scholar.google.com/citations?user=MEzqBsoAAAAJ&hl

6.5.1 Peer reviewed articles

[1] Y. El-Neaj, C. Alpigiani, and S. A.-P. et al. **AEDGE: Atomic Experiment for Dark Matter and Gravity Exploration in Space**. In: *EPJ Quantum Technol.* **7** (6 2020). White Paper in response to ESA Science Programm call "Voyage 2050". DOI: 10.1140/epjqt/s40507-020-0080-0

[2] D. O. Sabulsky, J. Junca, et al. **A fibered laser system for the MIGA large scale atom interferometer**. In: *Sci. Rep.* **10**.1 (Feb. 2020). DOI: 10.1038/s41598-020-59971-8

[3] D. S. Naik, H. Eneriz-Imaz, et al. **Loading and cooling in an optical trap via hyperfine dark states**. In: *Phys. Rev. Res.* **2**.1 (Feb. 2020). DOI: 10.1103/physrevresearch.2.013212

[4] A. Bertoldi, C.-H. Feng, et al. **A control hardware based on a field programmable gate array for experiments in atomic physics**. In: *Rev. Sci. Instrum.* **91**.3 (Mar. 2020), p. 033203. DOI: 10.1063/1.5129595

[5] G. Condon, M. Rabault, et al. **All-Optical Bose-Einstein Condensates in Microgravity**. In: *Phys. Rev. Lett.* **123**.24 (Dec. 2019), p. 240402. DOI: 10.1103/physrevlett.123.240402

[6] A. Trimeche, B. Battelier, et al. **Concept study and preliminary design of a cold atom interferometer for space gravity gradiometry**. In: *Class. Quantum Grav.* **36**.21 (Oct. 2019), p. 215004. DOI: 10.1088/1361-6382/ab4548

[7] J. Junca, A. Bertoldi, et al. **Characterizing Earth gravity field fluctuations with the MIGA antenna for future gravitational wave detectors**. In: *Phys. Rev. D* **99**.10 (2019). DOI: 10.1103/physrevd.99.104026

[8] A. Bertoldi, F. Minardi, and M. Prevedelli. **Phase shift in atom interferometers: Corrections for nonquadratic potentials and finite-duration laser pulses**. In: *Phys. Rev. A* **99**.2 (3 2019), p. 033619. DOI: 10.1103/PhysRevA.99.033619

[9] D. S. Naik, G. Kuyumjyan, et al. **Bose–Einstein condensate array in a malleable optical trap formed in a traveling wave cavity**. In: *Quantum Sci. Technol.* **3**.4 (2018), p. 045009. DOI: 10.1088/2058-9565/aad48e

[10] B. Canuel, A. Bertoldi, et al. **Exploring gravity with the MIGA large scale atom interferometer**. In: *Sci. Rep.* **8**.1 (2018), p. 14064. DOI: 10.1038/s41598-018-32165-z

[11] S. Rota-Rodrigo, B. Gouhier, et al. **Watt-level single-frequency tunable neodymium MOPA fiber laser operating at 915–937 nm**. In: *Opt. Lett.* **42**.21 (2017), p. 4557. DOI: 10.1364/ol.42.004557

[12] I. Riou, N. Mielec, et al. **A marginally stable optical resonator for enhanced atom interferometry**. In: *J. Phys. B* **50**.15 (2017), p. 155002. DOI: 10.1088/1361-6455/aa7592

[13] B. Barrett, A. Bertoldi, and P. Bouyer. **Inertial quantum sensors using light and matter**. In: *Phys. Scr.* **91**.5 (2016), p. 053006. DOI: 10.1088/0031-8949/91/5/053006

[14] W. Chaibi, R. Geiger, et al. **Low frequency gravitational wave detection with ground-based atom interferometer arrays**. In: *Phys. Rev. D* **93**.2 (2016). DOI: 10.1103/physrevd.93.021101

[15] B. Barrett, L. Antoni-Micollier, et al. **Correlative methods for dual-species quantum tests of the weak equivalence principle**. In: *New J. Phys.* **17**.8 (2015), p. 085010. DOI: 10.1088/1367-2630/17/8/085010

[16] R. Kohlhaas, A. Bertoldi, et al. **Phase Locking a Clock Oscillator to a Coherent Atomic Ensemble**. In: *Phys. Rev. X* **5**.2 (2015). DOI: 10.1103/physrevx.5.021011

[17] T. Schuldt, C. Schubert, et al. **Design of a dual species atom interferometer for space**. In: *Exp. Astron.* **39**.2 (2015), pp. 167–206. DOI: 10.1007/s10686-014-9433-y

[18] T. Vanderbruggen, R. Kohlhaas, et al. **Feedback control of coherent spin states using weak nondestructive measurements**. In: *Phys. Rev. A* **89**.6 (2014). DOI: 10.1103/physreva.89.063619

[19] D. N. Aguilera, H. Ahlers, et al. **STE-QUEST—test of the universality of free fall using cold atom interferometry**. In: *Class. Quantum Grav.* **31**.11 (2014), p. 115010. DOI: 10.1088/0264-9381/31/11/115010

[20] G. Tino, F. Sorrentino, et al. **Precision Gravity Tests with Atom Interferometry in Space**. In: *Nucl. Phys. B Proc. Suppl.* **243-244** (2013), pp. 203–217. DOI: 10.1016/j.nuclphysbps.2013.09.023

[21] L. Ricci, L. M. Martini, et al. **A current-carrying coil design with improved liquid cooling arrangement**. In: *Rev. Sci. Instrum.* **84**.6 (2013), p. 065115. DOI: 10.1063/1.4811666

[22] T. Vanderbruggen, R. Kohlhaas, et al. **Feedback Control of Trapped Coherent Atomic Ensembles**. In: *Phys. Rev. Lett.* **110**.21 (2013). DOI: 10.1103/physrevlett.110.210503

[23] F. Sorrentino, A. Bertoldi, et al. **Simultaneous measurement of gravity acceleration and gravity gradient with an atom interferometer**. In: *Appl. Phys. Lett.* **101**.11 (2012), p. 114106. DOI: 10.1063/1.4751112

[24] R. Kohlhaas, T. Vanderbruggen, et al. **Robust laser frequency stabilization by serrodyne modulation**. In: *Opt. Lett.* **37**.6 (2012), p. 1005. DOI: 10.1364/ol.37.001005

[25] S. Bernon, T. Vanderbruggen, et al. **Heterodyne non-demolition measurements on cold atomic samples: towards the preparation of non-classical states for atom interferometry**. In: *New J. Phys.* **13**.6 (2011), p. 065021. DOI: 10.1088/1367-2630/13/6/065021

[26] T. Vanderbruggen, S. Bernon, et al. **Spin-squeezing and Dicke-state preparation by heterodyne measurement**. In: *Phys. Rev. A* **83**.1 (2011). DOI: 10.1103/physreva.83.013821

[27] A. Bertoldi, S. Bernon, et al. **In situ characterization of an optical cavity using atomic light shift**. In: *Opt. Lett.* **35**.22 (2010), p. 3769. DOI: 10.1364/ol.35.003769

[28] A. Bertoldi. **Flattening Earth acceleration in atomic fountains**. In: *Phys. Rev. A* **82**.1 (2010). DOI: 10.1103/physreva.82.013622

[29] A. Bertoldi and L. Ricci. **Dynamics of a cold atom cloud in an anharmonic trap**. In: *Phys. Rev. A* **81**.6 (2010). DOI: 10.1103/physreva.81.063415

[30] F. Sorrentino, M. de Angelis, et al. **Precision measurements of gravity using cold atom sensors**. In: *J. of the Europ. Opt. Soc. – Rapid Comm.* **4** (2009). DOI: 10.2971/jeos.2009.09025

[31] A. Vilardi, D. Tabarelli, et al. **Measurement and modelling of enhanced absorption Hanle effect resonances in ^{85}Rb**. In: *J. Phys. B* **42**.5 (2009), p. 055003. DOI: 10.1088/0953-4075/42/5/055003

[32] M. de Angelis, A. Bertoldi, et al. **Precision gravimetry with atomic sensors**. In: *Meas. Sci. Technol.* **20**.2 (2008), p. 022001. DOI: 10.1088/0957-0233/20/2/022001

[33] A. Bertoldi and L. Ricci. **Gravito-magnetic trapping of ^{87}Rb**. In: *J. Phys. B* **41**.15 (2008), p. 155301. DOI: 10.1088/0953-4075/41/15/155301

[34] G. Lamporesi, A. Bertoldi, et al. **Determination of the Newtonian Gravitational Constant Using Atom Interferometry**. In: *Phys. Rev. Lett.* **100**.5 (2008). DOI: 10.1103/physrevlett.100.050801

[35] L. Ricci, D. Bassi, and A. Bertoldi. **Combined static potentials for confinement of neutral species**. In: *Phys. Rev. A* **76**.2 (2007). DOI: 10.1103/physreva.76.023428

[36] G. Lamporesi, A. Bertoldi, et al. **Source mass and positioning system for an accurate measurement of G**. in: *Rev. Sci. Instrum.* **78**.7 (2007), p. 075109. DOI: 10.1063/1.2751090

[37] A. Bertoldi, G. Lamporesi, et al. **Atom interferometry gravity-gradiometer for the determination of the Newtonian gravitational constant G**. in: *Eur. Phys. J. D* **40**.2 (2006), pp. 271–279. DOI: 10.1140/epjd/e2006-00212-2

[38] L. Botti, R. Buffa, et al. **Noninvasive system for the simultaneous stabilization and control of magnetic field strength and gradient**. In: *Rev. Sci. Instrum.* **77**.3 (2006), p. 035103. DOI: 10.1063/1.2173846

[39] A. Bertoldi, L. Botti, et al. **Noise and response characterization of an anisotropic magnetoresistive sensor working in a high-frequency flipping regime**. In: *Eur. Phys. J. Appl. Phys.* **33**.1 (2005), pp. 51–57. DOI: 10.1051/epjap:2005088

[40] A. Bertoldi, D. Bassi, et al. **Magnetoresistive magnetometer with improved bandwidth and response characteristics**. In: *Rev. Sci. Instrum.* **76**.6 (2005), p. 065106. DOI: 10.1063/1.1922787

[41] L. Ricci, A. Bertoldi, and D. Bassi. "A Toroidal Magnetic Guide for Neutral Atoms". In: *Laser Physics at the Limits*. Springer Berlin Heidelberg, 2002, pp. 477–485. DOI: 10.1007/978-3-662-04897-9_44

[42] L. Ricci, A. Bertoldi, and D. Bassi. **Winding shape optimization for asymmetric confinement magnets**. In: *Rev. Sci. Instrum.* **73**.9 (2002), pp. 3181–3186. DOI: 10.1063/1.1499209

6.5.2 Patents

[1] B. Canuel, A. Bertoldi, et al. **Optical resonator with large prope mode for atom interferometry**. France Patent 3054773. 2018

[2] A. Bertoldi, R. Kohlhaas, et al. **Coherent spectroscopic methods with extended interrogation times and systems implementing such methods**. WO Patent WO/2016/097332, US20170356803 , EU Patent 3233719 , Japan Patent JP2018508749. 2017

6.5.3 Hardware & Software Repository

[1] M. Prevedelli, A. Bertoldi, C.-H. Feng, H. Eneriz Imaz, M. Carey, D. S. Naik, and P. Bouyer, ˇ201cYet another control system for AMO physics,ˇ201d Zenodo, December 2019, https://doi.org/10.5281/zenodo.3571496.

Articles in Review

[1] L. Blanchet, K. Bongs, et al. **Exploring the Foundations of the Physical Universe with Space Tests of the Equivalence Principle**. In: (2019). White Paper in response to ESA Science Programm call "Voyage 2050". arXiv: 1908.11785 [physics.space-ph]

[2] B. Canuel et al. **ELGAR - a European Laboratory for Gravitation and Atom-interferometric Research**. In: *subm. to Class. Quantum Grav.* (2019)

[3] C. Schubert, J. Hartwig, et al. **Differential atom interferometry with 87 Rb and 85 Rb for testing the WEP in STE-QUEST**. in: (2013). arXiv: 1312.5963 [physics.atom-ph]

6.5.4 Peer Reviewed Conference Proceedings

[1] S. Rota-Rodrigo, B. Gouhier, et al. **Watt-level single-frequency tunable neodymium MOPA fiber laser operating at 915-937 nm**. In: *Fiber Lasers XV: Technology and Systems*. Ed. by A. L. Carter and I. Hartl. SPIE, 2018. DOI: 10.1117/12.2287133

[2] G. Lefevre, G. Condon, et al. **Studies of general relativity with quantum sensors**. In: *Prooc. 52th rencontres de Moriond, La Thuile, Aosta Valley, Italy (21-28 March 2017)*. 2017. arXiv: 1705.10475 [physics.atom-ph]

[3] I. Riou, G. Lefèvre, et al. **High resolution atom interferometry with optical resonators**. In: *International Conference on Space Optics — ICSO 2016*. Ed. by N. Karafolas, B. Cugny, and Z. Sodnik. SPIE, 2017. DOI: 10.1117/12.2296221

[4] A. Bertoldi, R. Kohlhaas, et al. **Phase locking an atom interferometer**. In: *2016 European Frequency and Time Forum (EFTF)*. IEEE, 2016. DOI: 10.1109/eftf.2016.7477819

[5] B. Canuel, S. Pelisson, et al. **MIGA: combining laser and matter wave interferometry for mass distribution monitoring and advanced geodesy**. In: *Quantum Optics*. Ed. by J. Stuhler and A. J. Shields. SPIE, Apr. 2016. DOI: 10.1117/12.2228825. arXiv: 1604.02072 [physics.atom-ph]

[6] R. Geiger, L. Amand, et al. **Matter-wave laser Interferometer Gravitation Antenna (MIGA): New perspectives for fundamental physics and geosciences**. In: *Prooc. 50th rencontres de Moriond, La Thuile, Aosta Valley, Italy (21–28 March 2015)*. 2015. arXiv: 1505.07137 [physics.atom-ph]

[7] B. Canuel, L. Amand, et al. **The matter-wave laser interferometer gravitation antenna (MIGA): New perspectives for fundamental physics and geosciences**. In: *E3S Web of Conferences* **4** (2014). Ed. by P. Febvre, E. P. di Borgo, and K. Coulié-Castellani, p. 01004. DOI: 10.1051/e3sconf/20140401004

[8] K. Bongs, J. Malcolm, et al. **iSense: A Technology Platform for Cold Atom Based Quantum Technologies**. In: *Research in Optical Sciences*. OSA, 2014. DOI: 10.1364/qim.2014.qtu3b.1

[9] B. Barrett, P.-A. Gominet, et al. **Mobile and remote inertial sensing with atom interferometers**. In: *Proceedings of the International School of Physics "Enrico Fermi"* **188**.Atom Interferometry (2014), pp. 493–555. ISSN: 0074-784X. DOI: 10.3254/978-1-61499-448-0-493

[10] M. de Angelis, M. Angonin, et al. **iSense: A Portable Ultracold-Atom-Based Gravimeter**. In: *Procedia Computer Science* **7** (2011), pp. 334–336. DOI: 10.1016/j.procs.2011.09.067

[11] G. M. Tino, A. Alberti, et al. **Precision gravity tests by atom interferometry**. In: *Laser Spectroscopy*. World Scientific Publishing Company, 2008. DOI: 10.1142/9789812813206_0008

[12] A. Bertoldi, L. Cacciapuoti, et al. **Atom interferometry for precision tests of gravity: Measurement of G and test of Newtonian law at micrometric distances**. In: *The Eleventh Marcel Grossmann Meeting*. World Scientific Publishing Company, 2008. DOI: 10.1142/9789812834300_0449

[13] G. Ferrari, A. Bertoldi, et al. **Atom interferometry for precision tests of gravity: Measurement of G and test of Newtonian law at micrometric distances**. In: *XII SIGRAV Conference, Torino, Italy (2006)*

6.5.5 Oral presentations at conferences and workshops

• ***(INVITED)*** **Atomic Experiment for Dark Matter and Gravity Exploration in Space**, invited discussion leader on "Probes of particle physics with high-precision optics" at the workshop "Gravitational Wave Probes of Fundamental Physics", EuCAPT Amsterdam (The Netherlands), November 11-13, 2019.

• ***(INVITED)*** **Dark state cooling of Rb in a telecom dipole trap**, workshop "Hollow core Fiber Key enabling technology for time/frequency applications", Xlim in Limoges (France), November 19-20, 2019.

• **Atom Interferometry based GW detection in the mid-band**, workshop "Hollow core Fiber Key enabling technology for time/frequency applications", Xlim in Limoges (France), November 19-20, 2019.

• ***(INVITED)*** **MIGA, ELGAR and Gravitational Wave detection at low frequency with Atom Interferometry**, Workshop on "Terrestrial infrasound gravitational wave detection with atom interferometry", Hanover (Germany), February 25-27, 2019.

• ***(INVITED)*** **Measurement-and-correction schemes in Atom Interferometry**, Workshop on Atom Interferometry GDR cold atoms, Toulouse (France), December 05-06, 2018.

• ***(INVITED)*** **Atom Interferometers and GW detection**, 3 hours lecture at "Gravitational Waves 2018", Physics School in Les Houches (France), July 25-26, 2018.

• ***(INVITED)*** **MIGA and Atom Interferometry for Gravitational Wave Detection**, 15th Marcel Grossmann Meeting, University Roma "La Sapienza" (Roma–Italy), July 3, 2018.

• ***(INVITED)*** **Atomic physics and Gravitational Wave detection**, AtomQT workshop, Heraklion (Crete-Greece), April 18, 2018.

• ***(INVITED)*** **Phase-locking an atomic clock**, 5th LAPHIA Symposium 2017, Talence (France), December 11-13, 2017.

• ***(INVITED)*** **Matter wave interferometry for GW detection**, GWPAW 2017, Annecy (France), May 30-June 2, 2017.

• ***(INVITED)*** **Phase-locking an atomic clock**, AIV XXIII Conference, Florence (Italy), April 5-7, 2017.

• ***(INVITED)*** **MIGA and very long baseline atom interferometry at LSBB**, iDUST, Rustrel, June 1-3, 2016.

• **Phase locking an atom interferometer**, EFTF, York (UK), 7 April 2016.

• **Gravitational Wave physics and geoscience with the MIGA instrument**, LSBB Days Workshop, Rustrel, June 3-4, 2015.

• **MIGA installation at LSBB**, LSBB Days Workshop, Rustrel, June 3-4, 2015.

• **Improving atomic clocks using coherence preserving measurements**, LP2N Days Workshop, Talence, May 26-27, 2014.

• ***(INVITED)*** **Weak measurements and feedback control of trapped atomic ensembles**, QMAP Workshop, GRDI Franco-Chinois "Quantum Manipulation of Atoms and Photons", Palaiseau, September 25, 2013.

• ***(INVITED)*** **Atom Interferometry for STE-QUEST**, CNES review of the Cosmic Vision M3 Proposals, Paris, June 13, 2013.

• ***(INVITED)*** **Atom Interferometry test of the Weak Equivalence Principle**, MICROSCOPE II Workshop, Palaiseau, January 29-30, 2013.

• **Weak measurements and feedback to protect atomic coherence**, iSENSE meeting workshop, Paris (France), 22 Mars 2012.

• **Levitation scheme and vacuum chamber for iSENSE**, iSENSE yearly meeting workshop, Brussels (Belgium), 14 September 2011.

• **Vacuum setup and levitating gravity sensor for iSENSE project**, iSENSE workshop, Birmingham University (UK), 06 October 2010.

• **A toroidal magneto–optical trap for neutral atoms**, INFN School, Capri (Italy), October 2001.

6.5.6 Invited Colloquia

• **Low frequency Gravitational Wave detection with Atom Interferometry**, Albert Einstein Institute (AEI), MPQ Postdam (Germany), 15 May 2019.

• **MIGA and Gravitational Wave Detection at low frequency with Atom Interferometry**, XLim, Limoges (France), 25 April 2019.

• **MIGA and Gravitational Wave detection at low frequency with Atom Interferometry**, IQOQI Innsbruck (Austria), 21 March 2019.

• **MIGA and Gravitational Wave detection at low frequency with Atom Interferometry**, Bordeaux Laboratory for Astrophysics (LAB), Pessac (France), 5 December 2018.

• **MIGA and Atom Interferometry for low frequency Gravitational Wave detection**, ARTEMIS, Nice (France), 26 November 2018.

• **MIGA and Atom Interferometry for low frequency Gravitational Wave detection**, Amsterdam (The Netherlands), 7 November 2018.

• **MIGA and Atom Interferometry for low frequency Gravitational Wave detection**, Trento (Italy), 31 October 2018.

• **MIGA and Atom Interferometry for Gravitational Wave detection at low frequency**, ICFO, Barcelone (Spain), 7 September 2018.

• **MIGA and Gravitational Wave detection with atom interferometry at low frequency**, Nanyang Technological University, Singapore, 13 February 2018.

• **Multiband GW astronomy coupling atomic and optical interferometers**, AEI (Albert Einstein Institute) Max Planck Institute for Gravitational Physics, Hannover, Germany, 9 November 2017.

• **MIGA and GW detection with atom interferometry at low frequency**, School of Physics and Astronomy, Birmingham, UK, 3 October 2017.

• **MIGA gravity gradiometer for infrasound GW detection**, LAPP, Annecy, France, 30 May 2017.

• **Atom interferometry with feedback and phase lock loops**, Universidad del Pais Vasco UPV/EHU, Leioa - Bilbao, Spain, 20 December 2016.

• **Phase locking in atom interferometry**, School of Physics and Astronomy, University of Southampton, Southampton (UK) 21 July 2016.

• **Cold atoms, weak measurements and feedback for timekeeping**, Lectio Magistralis at the opening of the Academic year, PhD School, University of Trento, Italy, 27 February 2013.

• **Protecting ensemble atomic coherence with weak measurements and feedback**, Graduate College course in cold atoms and metrology, University of Hannover, Germany, 13 December 2012.

• **Heterodyne non-demolition measurements on cold atoms**, Imperial College, London (UK), 21 July 2011.

• **Heterodyne non-demolition measurements on cold atoms**, Observatoire de Paris, Paris (France), 09 June 2011.

• **Cold atoms, quantum non demolition measurements, and squeezing in a high finesse optical cavity**, BEC–INFM – Trento University, Trento (Italy), 13 October 2009.

• **Measuring G by atom interferometry**, IOTA – Institut d'Optique, Paris–Sud XI University, Paris (France), 15 February 2008.

• **Measurement of the gravitational constant G by atom interferometry**, ICFO – Institut de Ciències Fotòniques, Castelldefels (Spain), July 2007.

• **Combined static potentials for confinement of neutral species**, LENS, Florence (Italy), 11/2004.

6.5.7 In the press

• November 2019, PhysicsWorld, "European physicists propose huge underground gravitational-wave laboratory".

• November 2016, La Revue Parlementaire, "La France à la pointe des technologies quantiques", Les Dossier de la RP, Nouvelle Aquitaine, p. 13.

• November 2016, Institut de physique - actualité scientifiques, www.cnrs.fr/inp, "Vers un détecteur d'ondes gravitationnelles terrestre à basse fréquence utilisant l'interférométrie atomique".

• 20 october 2016, Le Monde - Sciences et Techno, "Les secousses souterraines de l'espace-temps".

• June 2015, Institut de physique - actualité scientifiques, www.cnrs.fr/inp, "Synchroniser les oscillations d'un quartz avec un système quantique".

6.6 Teaching

During my Ph.D. I started to teach different courses at the Bachelor of Science in Mathematics (**Computer science, algorithms and data structures**) and Physics (**Advanced Electronics** and **Laboratory of solid matter physics**).

In the last few years I am in charge of the "Travaux Dirigés" at the Institut d'Optique in Bordeaux (LP2N) for **Radiometry and photometry** and **Optical reflection and anamorphosis**, and in the last couple of years of the course **Quantum Optics and Cold Atoms** at the Master Degree of the Univ. of Bordeaux. Since 2019 I teach part of the course **Coherent manipulation of matter with light** at the Master Degree of the Univ. of Bordeaux.

I gave a few lectures to Ph.D schools in Trento (**Neutral atom cooling and Matter Wave Interferometry**), at the Leibniz University of Hanover (**Protecting ensemble atomic coherence with weak measurements and feedback**) and at Les Houches (**Atom Interferometers and GW detection**).

• Member of the PhD Committee of S. Coop (06/09/2018) – ICFO Barcelone (Spain); G. Lefèvre (10/05/2019), G. Kuyumjyan (11/12/2017), I. Riou (25/04/2017), E. Cantin (03/11/2015) at LP2N (France).

• **2019** Teaching of **Coherent manipulation of matter with light**, Master Degree "Laser Matière et Nanosciences" at the Univ. Bordeaux, France — (6 h/year).

• **July 2018** 3 hours lecture on **Atom Interferometers and GW detection** at "Gravitational Waves 2018", Physics School in Les Houches (France), July 25-26, 2018.

• **2017** "Autorisation à diriger une thèse" (ADT).

• **2012 and 2018** Qualification aux fonctions de maître de conférences, section 30 (Milieux dilués et optique).

• **2017 / 2018** Teaching assistance for the course **Quantum Optics and Cold Atoms**, Master Degree "Laser Matière et Nanosciences" at the Univ. Bordeaux, France — (12 h/year).

• **2016** Teaching assistance for the course **Optical reflection and anamorphosis**, Master Degree at the Institut d'Optique Graduate School, France — (20h).

• **2015 / 2016 / 2017 / 2018 / 2019** Teaching assistance for the course **Radiometry and photometry**, Master Degree at the Institut d'Optique Graduate School, France — (15 h/year).

• **December 2012** 2 hour course on **Protecting ensemble atomic coherence with weak measurements and feedback** at Graduate College course in Cold Atoms and Metrology, University of Hanover, Germany.

• **2008** Doctoral School in Physics (University of Trento, Italy), lecturer for the course **Neutral atom cooling techniques and Matter Wave Interferometry** — 9 h.

• **2003** Teaching assistance for the course **Advanced electronics**, B.Sc. Degree in Physics (University of Trento) — 25 h.

• **2002** Teaching assistance for the course **Laboratory of solid matter physics**, B.Sc. Degree in Physics (University of Trento) — 50 h.

• **2001 and 2002** Teaching assistance for the course **Computer science: algorithms and data structures**, B.Sc. Degree in Mathematics (University of Trento) — 50 h/year.

• **1999 and 2000** Tutorship of Physics, Mathematics, and Statistics at the Economy Department (University of Trento) — 70 h + 20 h.

• **1998** Organization of the showing **The Laser**, for the *Scientific and Technological Week*, University of Trento.

6.7 Science Review Activity and other Responsabilities

6.7.1 Academic Referee for scientific journals

Publons profile: https://publons.com/author/1324730/andrea-bertoldi#profile

• **APS** (Phys. Rev. Lett. – 2009, Phys. Rev. Appl. – 2016, Phys Rev. A – 2012, Phys Rev. D – 2015)

• **OSA** (Opt. Expr. – 2015, Opt. Lett. – 2010, Appl. Opt. – 2012)

• **Springer** (Experimental Astronomy – 2011)

• **IOP** (New J. Physics – 2013, Meas. Sci. Technol. – 2015)

• **Nature Pub. Group** (Sci. Rep. – 2017)

6.7.2 Project reviewer

• Scientific Evaluation Panel QuantERA - 2019

• EURAMET (European Association of National Metrology Institutes) - 2014

• ANR (Agence Nationale de la Recherche) France - 2018

• MIUR (Ministero dell'Istruzione dell'Università e della Ricerca) Italy - 2018

• FWF (The Austrian Science Fund) Austria - 2019

6.7.3 Organization of events

• LAPHIA Seminar of Prof. B. Allen from Albert Einstein Institute (Hanover–Germany) **The direct observation of gravitational waves**, Talence, France, 16 May 2018.

• **International School and Conference on *Frontiers on Matter Wave Optics FOMO 2016***, Archachon, France, 3–10 and 10–17 September 2016.

• **SIGRAV Graduate School on *Experimental gravitation in space***, Firenze, Italy, 25–27 September 2006.

• **International Workshop on *Advances in precision tests and experimental gravitation in space***, Firenze, Italy, 28–30 September 2006 (ESA, University of Firenze, GREX, SIGRAV).

6.7.4 Responsibilities

• **2013–19** In charge of the Formation at the Institut d'Optique d'Aquitanie – LP2N, Talence, France.

• **2016–19** Supervision of the activity of A. Tizon, engineer expert in digital electronics at LP2N, Talence, France.

• **2015–16** Organization of the **weekly meeting in the Cold Atom in Bordeaux group** (LP2N, Talence, France).

• **2011/12/13** Organization of the **weekly meeting in the Atom Optics group** (Institut d'Optique, Palaiseau, France).

Bibliography

[1] L. de Broglie. **Waves and Quanta**. In: *Nature* **112** (2815 1923), pp. 540–540. DOI: 10.1038/112540a0.

[2] M. H. Anderson, J. R. Ensher, M. R. Matthews, C. E. Wieman, and E. A. Cornell. **Observation of Bose-Einstein Condensation in a Dilute Atomic Vapor**. In: *Science* **269** (5221 1995), pp. 198–201. DOI: 10.1126/science.269.5221.198.

[3] K. B. Davis, M.-O. Mewes, M. R. Andrews, N. J. van Druten, D. S. Durfee, D. M. Kurn, and W. Ketterle. **Bose-Einstein Condensation in a Gas of Sodium Atoms**. In: *Phys. Rev. Lett.* **75** (22 1995), pp. 3969–3973. DOI: 10.1103/PhysRevLett.75.3969.

[4] C. C. Bradley, C. A. Sackett, J. J. Tollett, and R. G. Hulet. **Evidence of Bose-Einstein Condensation in an Atomic Gas with Attractive Interactions**. In: *Phys. Rev. Lett.* **75** (9 1995), pp. 1687–1690. DOI: 10.1103/PhysRevLett.75.1687.

[5] O. Carnal and J. Mlynek. **Young's double-slit experiment with atoms: A simple atom interferometer**. In: *Phys. Rev. Lett.* **66** (21 1991), pp. 2689–2692. DOI: 10.1103/PhysRevLett.66.2689.

[6] D. W. Keith, C. R. Ekstrom, Q. A. Turchette, and D. E. Pritchard. **An interferometer for atoms**. In: *Phys. Rev. Lett.* **66** (21 1991), pp. 2693–2696. DOI: 10.1103/PhysRevLett.66.2693.

[7] F. Riehle, T. Kisters, A. Witte, J. Helmcke, and C. J. Bordé. **Optical Ramsey spectroscopy in a rotating frame: Sagnac effect in a matter-wave interferometer**. In: *Phys. Rev. Lett.* **67** (2 1991), pp. 177–180. DOI: 10.1103/PhysRevLett.67.177.

[8] M. Kasevich and S. Chu. **Atomic interferometry using stimulated Raman transitions**. In: *Phys. Rev. Lett.* **67** (2 1991), pp. 181–184. DOI: 10.1103/PhysRevLett.67.181.

[9] P. R. Berman. *Atom Interferometry*. New York: Academic Press, 1997. ISBN: 9780120924608.

[10] A. Bertoldi, G. Lamporesi, L. Cacciapuoti, M. de Angelis, M. Fattori, T. Petelski, A. Peters, M. Prevedelli, J. Stuhler, and G. M. Tino. **Atom interferometry gravity-gradiometer for the determination of the Newtonian gravitational constant G**. In: *Eur. Phys. J. D* **40** (2 2006), pp. 271–279. DOI: 10.1140/epjd/e2006-00212-2.

[11] G. Lamporesi, A. Bertoldi, L. Cacciapuoti, M. Prevedelli, and G. M. Tino. **Determination of the Newtonian Gravitational Constant Using Atom Interferometry**. In: *Phys. Rev. Lett.* **100** (5 2008), p. 239. DOI: 10.1103/PhysRevLett.100.050801.

[12] J. Appel, P. J. Windpassinger, D. Oblak, U. B. Hoff, N. Kjaergaard, and E. S. Polzik. **Mesoscopic atomic entanglement for precision measurements beyond the standard quantum limit**. In: *Proc. Natl. Acad. Sci. U.S.A.* **106**.27 (June 2009), pp. 10960–10965. DOI: 10.1073/pnas.0901550106.

[13] I. D. Leroux, M. H. Schleier-Smith, and V. Vuletić. **Orientation-Dependent Entanglement Lifetime in a Squeezed Atomic Clock**. In: *Phys. Rev. Lett.* **104**.25 (June 2010). DOI: 10.1103/physrevlett.104.250801.

[14] B. Lucke, M. Scherer, J. Kruse, L. Pezze, F. Deuretzbacher, P. Hyllus, O. Topic, J. Peise, W. Ertmer, J. Arlt, L. Santos, A. Smerzi, and C. Klempt. **Twin Matter Waves for Interferometry Beyond the Classical Limit**. In: *Science* **334**.6057 (Oct. 2011), pp. 773–776. DOI: 10.1126/science.1208798.

[15] I. Kruse, K. Lange, J. Peise, B. Lücke, L. Pezzè, J. Arlt, W. Ertmer, C. Lisdat, L. Santos, A. Smerzi, and C. Klempt. **Improvement of an Atomic Clock using Squeezed Vacuum**. In: *Phys. Rev. Lett.* **117**.14 (Sept. 2016). DOI: 10.1103/physrevlett.117.143004.

[16] L. Pezzè, A. Smerzi, M. K. Oberthaler, R. Schmied, and P. Treutlein. **Quantum metrology with nonclassical states of atomic ensembles**. In: *Rev. Mod. Phys.* **90** (3 2018), p. 99. DOI: 10.1103/RevModPhys.90.035005.

[17] D. Braun, G. Adesso, F. Benatti, R. Floreanini, U. Marzolino, M. W. Mitchell, and S. Pirandola. **Quantum-enhanced measurements without entanglement**. In: *Rev. Mod. Phys.* **90** (3 2018), p. 44. DOI: 10.1103/RevModPhys.90.035006.

[18] M. Planck. **Ueber das Gesetz der Energieverteilung im Normalspectrum**. In: *Ann. Phys.* **309**.3 (1901), pp. 553–563. DOI: 10.1002/andp.19013090310.

[19] A. Einstein. **Über einen die Erzeugung und Verwandlung des Lichtes betreffenden heuristischen Gesichtspunkt**. In: *Ann. Phys.* **322**.6 (1905), pp. 132–148. DOI: 10.1002/andp.19053220607.

[20] R. A. Millikan. **A Direct Determination of "*h*."**. In: *Phys. Rev.* **4**.1 (July 1914), pp. 73–75. DOI: 10.1103/physrev.4.73.2.

[21] E. Schrödinger. **An Undulatory Theory of the Mechanics of Atoms and Molecules**. In: *Phys. Rev.* **28**.6 (Dec. 1926), pp. 1049–1070. DOI: 10.1103/physrev.28.1049.

[22] G. Thomson and A. Reid. **Diffraction of Cathode Rays by a Thin Film**. In: *Nature* **119**.3007 (June 1927), pp. 890–890. DOI: 10.1038/119890a0.

[23] C. J. Davisson and L. H. Germer. **Reflection of Electrons by a Crystal of Nickel**. In: *Proc. Natl. Acad. Sci. U.S.A.* **14**.4 (Apr. 1928), pp. 317–322. DOI: 10.1073/pnas.14.4.317.

[24] E. Fermi and L. Marshall. **Interference Phenomena of Slow Neutrons**. In: *Phys. Rev.* **71**.10 (May 1947), pp. 666–677. DOI: 10.1103/physrev.71.666.

[25] T. Kovachy, J. M. Hogan, A. Sugarbaker, S. M. Dickerson, C. A. Donnelly, C. Overstreet, and M. A. Kasevich. **Matter Wave Lensing to Picokelvin Temperatures**. In: *Phys. Rev. Lett.* **114**.14 (Apr. 2015). DOI: 10.1103/physrevlett.114.143004.

[26] L. De Marco, G. Valtolina, K. Matsuda, W. G. Tobias, J. P. Covey, and J. Ye. **A degenerate Fermi gas of polar molecules**. In: *Science* **363**.6429 (Jan. 2019), pp. 853–856. DOI: 10.1126/science.aau7230.

[27] R. P. Feynman, A. R. Hibbs, and D. F. Styer. *Quantum mechanics and path integrals*. New York, NY, USA: Dover, 2010. ISBN: 0-486-47722-3.

[28] P. Storey and C. Cohen-Tannoudji. **The Feynman path integral approach to atomic interferometry. A tutorial**. In: *J. Phys. II* **4** (1994), pp. 1999–2027. DOI: 10.1051/jp2:1994103.

[29] C. Antoine and C. Bordé. **Exact phase shifts for atom interferometry**. In: *Phys. Lett. A* **306**.5-6 (Jan. 2003), pp. 277–284. DOI: 10.1016/s0375-9601(02)01625-0.

[30] K. Bongs, R. Launay, and M. A. Kasevich. **High-order inertial phase shifts for time-domain atom interferometers**. In: *Appl. Phys. B* **84** (2006), p. 599. DOI: 10.1007/s00340-006-2397-5.

[31] M. Cadoret, N. Zahzam, Y. Bidel, C. Diboune, A. Bonnin, F. Théron, and A. Bresson. **Phase shift formulation for N-light-pulse atom interferometers: application to inertial sensing**. In: *J. Opt. Soc. Am. B* **33** (2016), p. 1777. DOI: 10.1364/josab.33.001777.

[32] B. Dubetsky and M. A. Kasevich. **Atom interferometer as a selective sensor of rotation or gravity**. In: *Phys. Rev. A* **74** (2006), p. 023615. DOI: 10.1103/physreva.74.023615.

[33] B. Cheng, P. Gillot, S. Merlet, and F. Pereira Dos Santos. **Influence of chirping the Raman lasers in an atom gravimeter: Phase shifts due to the Raman light shift and to the finite speed of light**. In: *Phys. Rev. A* **92** (2015), p. 063617. DOI: 10.1103/physreva.92.063617.

[34] V. Schkolnik, B. L. M. Hauth, C. Freier, and A. Peters. **The effect of wavefront aberrations in atom interferometry**. In: *Appl. Phys. B* **120** (2015), pp. 311–316. DOI: 10.1007/s00340-015-6138-5.

[35] C. J. Bordé. **Quantum Theory of Atom-Wave Beam Splitters and Application to Multidimensional Atomic Gravito-Inertial Sensors**. In: *Gen. Rel. Gravit.* **36**.3 (Mar. 2004), pp. 475–502. DOI: 10.1023/b:gerg.0000010726.64769.6d.

[36] S. Dimopoulos, P. W. Graham, J. M. Hogan, and M. A. Kasevich. **General relativistic effects in atom interferometry**. In: *Phys. Rev. D* **78**.4 (Aug. 2008), p. 042003. DOI: 10.1103/physrevd.78.042003.

[37] K.-P. Marzlin and J. Audretsch. **"Freely" falling two-level atom in a running laser wave**. In: *Phys. Rev. A* **53** (1996), pp. 1004–1013. DOI: 10.1103/physreva.53.1004.

[38] A. Bertoldi, F. Minardi, and M. Prevedelli. **Phase shift in atom interferometers: Corrections for non-quadratic potentials and finite-duration laser pulses**. In: *Phys. Rev. A* **99** (3 2019), p. 033619. DOI: 10.1103/PhysRevA.99.033619.

[39] J. J. Sakurai and J. J. Napolitano. *Modern Quantum Mechanics*. 2nd Ed. Addison–Wesley, San Francisco, 2011. DOI: 10.1017/9781108499996.

[40] S. Blanes, F. Casas, J. A. Oteo, and J. Ros. **The Magnus expansion and some of its applications**. In: *Phys. Rep.* **470** (2009), pp. 151–238. DOI: 10.1016/j.physrep.2008.11.001.

[41] S. Blanes, F. Casas, J. A. Oteo, and J. Ros. **A pedagogical approach to the Magnus expansion**. In: *Eur. J. Phys.* **31** (2010), p. 907. DOI: 10.1088/0143-0807/31/4/020.

[42] D. F. Walls and G. J. Milburn. *Quantum Optics*. Springer–Verlag, Berlin, 2008. ISBN: 9783540285731. DOI: 10.1007/978-3-540-28574-8.

[43] C. Cohen–Tannoudji, J. Dupont–Roc, and G. Grynberg. *Atom–Photon Interactions*. J. Wiley & Sons, New York, 2008. DOI: 10.1002/9783527617197.

[44] A. Roura, W. Zeller, and W. P. Schleich. **Overcoming loss of contrast in atom interferometry due to gravity gradients**. In: *New J. Phys.* **16** (2014), p. 123012. DOI: 10.1088/1367-2630/16/12/123012.

[45] A. Roura. **Circumventing Heisenberg's Uncertainty Principle in Atom Interferometry Tests of the Equivalence Principle**. In: *Phys. Rev. Lett.* **118** (2017), p. 160401. DOI: 10.1103/PhysRevLett.118.160401.

[46] G. D'Amico, G. Rosi, S. Zhan, L. Cacciapuoti, M. Fattori, and G. M. Tino. **Canceling the Gravity Gradient Phase Shift in Atom Interferometry**. In: *Phys. Rev. Lett.* **119** (2017), p. 253201. DOI: 10.1103/PhysRevLett.119.253201.

[47] C. Overstreet, P. Asenbaum, T. Kovachy, R. Notermans, J. M. Hogan, and M. A. Kasevich. **Effective Inertial Frame in an Atom Interferometric Test of the Equivalence Principle**. In: *Phys. Rev. Lett.* **120** (18 2018), p. 183604. DOI: 10.1103/PhysRevLett.120.183604.

[48] P. Cheinet, B. Canuel, F. Pereira Dos Santos, A. Gauguet, F. Yver-Leduc, and A. Landragin. **Measurement of the Sensitivity Function in a Time-Domain Atomic Interferometer**. In: *IEEE Trans. Instrum. Meas.* **57** (2008), pp. 1141–1148. DOI: 10.1109/tim.2007.915148.

[49] C. Antoine and C. Bordé. **Quantum theory of atomic clocks and gravito-inertial sensors: an update**. In: *J. Opt. B: Quantum Semiclass. Opt.* **5** (2003), S199. DOI: 10.1088/1464-4266/5/2/380.

[50] S.-w. Chiow, T. Kovachy, H.-C. Chien, and M. A. Kasevich. **102 $\hbar$k Large Area Atom Interferometers**. In: *Phys. Rev. Lett.* **107** (13 2011), p. 130403. DOI: 10.1103/PhysRevLett.107.130403.

[51] B. Plotkin-Swing, D. Gochnauer, K. E. McAlpine, E. S. Cooper, A. O. Jamison, and S. Gupta. **Three-Path Atom Interferometry with Large Momentum Separation**. In: *Phys. Rev. Lett.* **121**.13 (Sept. 2018), p. 133201. DOI: 10.1103/physrevlett.121.133201.

[52] P. W. Graham, J. M. Hogan, M. A. Kasevich, and S. Rajendran. **Resonant mode for gravitational wave detectors based on atom interferometry**. In: *Phys. Rev. D* **94** (10 2016), p. 104022. DOI: 10.1103/PhysRevD.94.104022.

[53] A. D. Cronin, J. Schmiedmayer, and D. E. Pritchard. **Optics and interferometry with atoms and molecules**. In: *Rev. Mod. Phys.* **81** (3 2009), pp. 1051–1129. DOI: 10.1103/RevModPhys.81.1051.

[54] A. D. Ludlow, M. M. Boyd, J. Ye, E. Peik, and P. Schmidt. **Optical atomic clocks**. In: *Rev. Mod. Phys.* **87** (2 2015), pp. 637–701. DOI: 10.1103/RevModPhys.87.637.

[55] E. Oelker, R. B. Hutson, C. J. Kennedy, L. Sonderhouse, T. Bothwell, A. Goban, D. Kedar, C. Sanner, J. M. Robinson, G. E. Marti, D. G. Matei, T. Legero, M. Giunta, R. Holzwarth, F. Riehle, U. Sterr, and J. Ye. **Demonstration of 4.8×10^{-17} stability at 1 s for two independent optical clocks**. In: *Nature Photon.* **13**.10 (July 2019), pp. 714–719. DOI: 10.1038/s41566-019-0493-4.

[56] H. Marion, F. Pereira Dos Santos, M. Abgrall, S. Zhang, Y. Sortais, S. Bize, I. Maksimovic, D. Calonico, J. Grünert, C. Mandache, P. Lemonde, G. Santarelli, P. Laurent, A. Clairon, and C. Salomon. **Search for Variations of Fundamental Constants using Atomic Fountain Clocks**. In: *Phys. Rev. Lett.* **90**.15 (Apr. 2003). DOI: 10.1103/physrevlett.90.150801.

[57] P. Wcisło, P. Ablewski, K. Beloy, S. Bilicki, M. Bober, R. Brown, R. Fasano, R. Ciuryło, H. Hachisu, T. Ido, J. Lodewyck, A. Ludlow, W. McGrew, P. Morzyński, D. Nicolodi, M. Schioppo, M. Sekido, R. L. Targat, P. Wolf, X. Zhang, B. Zjawin, and M. Zawada. **New bounds on dark matter coupling from a global network of optical atomic clocks**. In: *Sci. Adv.* **4**.12 (Dec. 2018), eaau4869. DOI: 10.1126/sciadv.aau4869.

[58] W. B. Cairncross and J. Ye. **Atoms and molecules in the search for time-reversal symmetry violation**. In: *Nat. Rev. Phys.* **1**.8 (July 2019), pp. 510–521. DOI: 10.1038/s42254-019-0080-0.

[59] A. Peters, K. Y. Chung, and S. Chu. **Measurement of gravitational acceleration by dropping atoms**. In: *Nature* **400**.6747 (Aug. 1999), pp. 849–852. DOI: 10.1038/23655.

[60] M. Snadden, J. McGuirk, P. Bouyer, K. Haritos, and M. Kasevich. **Measurement of the Earth's Gravity Gradient with an Atom Interferometer-Based Gravity Gradiometer**. In: *Phys. Rev. Lett.* **81**.5 (Aug. 1998), pp. 971–974. DOI: 10.1103/physrevlett.81.971.

[61] B. Canuel, F. Leduc, D. Holleville, A. Gauguet, J. Fils, A. Virdis, A. Clairon, N. Dimarcq, C. J. Bordé, A. Landragin, and P. Bouyer. **Six-Axis Inertial Sensor Using Cold-Atom Interferometry**. In: *Phys. Rev. Lett.* **97**.1 (July 2006). DOI: 10.1103/physrevlett.97.010402.

[62] D. Savoie, M. Altorio, B. Fang, L. A. Sidorenkov, R. Geiger, and A. Landragin. **Interleaved atom interferometry for high-sensitivity inertial measurements**. In: *Sci. Adv.* **4**.12 (Dec. 2018), eaau7948. DOI: 10.1126/sciadv.aau7948.

[63] P. Asenbaum, C. Overstreet, T. Kovachy, D. D. Brown, J. M. Hogan, and M. A. Kasevich. **Phase Shift in an Atom Interferometer due to Spacetime Curvature across its Wave Function**. In: *Phys. Rev. Lett.* **118** (18 2017), p. 183602. DOI: 10.1103/PhysRevLett.118.183602.

[64] J. B. Fixler, G. T. Foster, J. M. McGuirk, and M. A. Kasevich. **Atom Interferometer Measurement of the Newtonian Constant of Gravity**. In: *Science* **315**.5808 (Jan. 2007), pp. 74–77. DOI: 10.1126/science.1135459.

[65] M. A. Hohensee, B. Estey, P. Hamilton, A. Zeilinger, and H. Müller. **Force-Free Gravitational Redshift: Proposed Gravitational Aharonov-Bohm Experiment**. In: *Phys. Rev. Lett.* **108** (23 2012), p. 38. DOI: 10.1103/PhysRevLett.108.230404.

[66] P. Haslinger, M. Jaffe, V. Xu, O. Schwartz, M. Sonnleitner, M. Ritsch-Marte, H. Ritsch, and H. Müller. **Attractive force on atoms due to blackbody radiation**. In: *Nature Phys.* **14** (3 2018), pp. 257–260. DOI: 10.1038/s41567-017-0004-9.

[67] C. Burrage, E. J. Copeland, and E. Hinds. **Probing dark energy with atom interferometry**. In: *J. Cosmol. Astropart. Phys.* **2015**.03 (Mar. 2015), pp. 042–042. DOI: 10.1088/1475-7516/2015/03/042.

[68] M. Jaffe, P. Haslinger, V. Xu, P. Hamilton, A. Upadhye, B. Elder, J. Khoury, and H. Müller. **Testing sub-gravitational forces on atoms from a miniature in-vacuum source mass**. In: *Nature Phys* **13** (10 2017), pp. 938–942. DOI: 10.1038/nphys4189.

[69] D. Sabulsky, I. Dutta, E. Hinds, B. Elder, C. Burrage, and E. J. Copeland. **Experiment to Detect Dark Energy Forces Using Atom Interferometry**. In: *Phys. Rev. Lett.* **123**.6 (Aug. 2019). DOI: 10.1103/physrevlett.123.061102.

[70] A. Arvanitaki, S. Dimopoulos, A. A. Geraci, J. Hogan, and M. Kasevich. **How to Test Atom and Neutron Neutrality with Atom Interferometry**. In: *Phys. Rev. Lett.* **100** (12 2008), p. 120407. DOI: 10.1103/PhysRevLett.100.120407.

[71] R. Bouchendira, P. Cladé, S. Guellati-Khélifa, F. Nez, and F. Biraben. **New Determination of the Fine Structure Constant and Test of the Quantum Electrodynamics**. In: *Phys. Rev. Lett.* **106** (8 2011), p. 287. DOI: 10.1103/PhysRevLett.106.080801.

[72] S. Dimopoulos, P. W. Graham, J. M. Hogan, and M. A. Kasevich. **Testing General Relativity with Atom Interferometry**. In: *Phys. Rev. Lett.* **98** (11 2007), p. 111102. DOI: 10.1103/PhysRevLett.98.111102.

[73] M. Nauenberg. **Einstein's equivalence principle in quantum mechanics revisited**. In: *Am. J. Phys.* **84** (11 2016), pp. 879–882. DOI: 10.1119/1.4962981.

[74] D. N. Aguilera, H. Ahlers, B. Battelier, A. Bawamia, A. Bertoldi, R. Bondarescu, K. Bongs, P. Bouyer, C. Braxmaier, L. Cacciapuoti, C. Chaloner, M. Chwalla, W. Ertmer, M. Franz, N. Gaaloul, M. Gehler, D. Gerardi, L. Gesa, N. Gürlebeck, J. Hartwig, M. Hauth, O. Hellmig, W. Herr, S. Herrmann, A. Heske, A. Hinton, P. Ireland, P. Jetzer, U. Johann, M. Krutzik, A. Kubelka, C. Lämmerzahl, A. Landragin, I. Lloro, D. Massonnet, I. Mateos, A. Milke, M. Nofrarias, M. Oswald, A. Peters, K. Posso-Trujillo, E. Rasel, E. Rocco, A. Roura, J. Rudolph, W. Schleich, C. Schubert, T. Schuldt, S. Seidel, K. Sengstock, C. F. Sopuerta, F. Sorrentino, D. Summers, G. M. Tino, C. Trenkel, N. Uzunoglu, W. von Klitzing, R. Walser, T. Wendrich, A. Wenzlawski, P. Weßels, A. Wicht, E. Wille, M. Williams, P. Windpassinger, and N. Zahzam. **STE-QUEST—test of the universality of free fall using cold atom interferometry**. In: *Class. Quantum Grav.* **31** (11 2014), p. 115010. DOI: 10.1088/0264-9381/31/11/115010.

[75] L. Zhou, S. Long, B. Tang, X. Chen, F. Gao, W. Peng, W. Duan, J. Zhong, Z. Xiong, J. Wang, Y. Zhang, and M. Zhan. **Test of Equivalence Principle at 10^{-8} Level by a Dual-Species Double-Diffraction Raman Atom Interferometer**. In: *Phys. Rev. Lett.* **115** (1 2015), p. 3. DOI: 10.1103/PhysRevLett.115.013004.

[76] J. Williams, S.-w. Chiow, N. Yu, and H. Müller. **Quantum test of the equivalence principle and space-time aboard the International Space Station**. In: *New J. Phys.* **18** (2 2016), p. 025018. DOI: 10.1088/1367-2630/18/2/025018.

[77] G. Rosi, G. D'Amico, L. Cacciapuoti, F. Sorrentino, M. Prevedelli, M. Zych, Č. Brukner, and G. M. Tino. **Quantum test of the equivalence principle for atoms in coherent superposition of internal energy states**. In: *Nat. Commun.* **8** (2017), p. 15529. DOI: 10.1038/ncomms15529.

[78] R. Geiger and M. Trupke. **Proposal for a Quantum Test of the Weak Equivalence Principle with Entangled Atomic Species**. In: *Phys. Rev. Lett.* **120** (4 2018), p. 043602. DOI: 10.1103/PhysRevLett.120.043602.

[79] S. Dimopoulos, P. W. Graham, J. M. Hogan, M. A. Kasevich, and S. Rajendran. **Gravitational wave detection with atom interferometry**. In: *Phys. Lett. B* **678** (1 2009), pp. 37–40. DOI: 10.1016/j.physletb.2009.06.011.

[80] T. Kovachy, P. Asenbaum, C. Overstreet, C. A. Donnelly, S. M. Dickerson, A. Sugarbaker, J. M. Hogan, and M. A. Kasevich. **Quantum superposition at the half-metre scale**. In: *Nature* **528** (7583 2015), pp. 530–533. DOI: 10.1038/nature16155.

[81] L. Diósi. **A universal master equation for the gravitational violation of quantum mechanics**. In: *Phys. Lett. A* **120** (8 1987), pp. 377–381. DOI: 10.1016/0375-9601(87)90681-5.

[82] R. Penrose. **On Gravity's role in Quantum State Reduction**. In: *Gen. Relat. Gravit.* **28** (5 1996), pp. 581–600. DOI: 10.1007/BF02105068.

[83] I. Pikovski, M. Zych, F. Costa, and Č. Brukner. **Universal decoherence due to gravitational time dilation**. In: *Nature Phys.* **11** (8 2015), pp. 668–672. DOI: 10.1038/nphys3366.

[84] R. H. Parker, C. Yu, W. Zhong, B. Estey, and H. Müller. **Measurement of the fine-structure constant as a test of the Standard Model**. In: *Science* **360**.6385 (Apr. 2018), pp. 191–195. DOI: 10.1126/science.aap7706.

[85] P. Hamilton, A. Zhmoginov, F. Robicheaux, J. Fajans, J. S. Wurtele, and H. Müller. **Antimatter Interferometry for Gravity Measurements**. In: *Phys. Rev. Lett.* **112**.12 (Mar. 2014). DOI: 10.1103/physrevlett.112.121102.

[86] C. Freier, M. Hauth, V. Schkolnik, B. Leykauf, M. Schilling, H. Wziontek, H.-G. Scherneck, J. Müller, and A. Peters. **Mobile quantum gravity sensor with unprecedented stability**. In: *J. Phys.: Conf. Ser.* **723** (2016), p. 012050. DOI: 10.1088/1742-6596/723/1/012050.

[87] Z. Jiang, V. Pálinkáš, F. E. Arias, J. Liard, S. Merlet, H. Wilmes, L. Vitushkin, L. Robertsson, L. Tisserand, F. Pereira Dos Santos, Q. Bodart, R. Falk, H. Baumann, S. Mizushima, J. Mäkinen, M. Bilker-Koivula, C. Lee, I. M. Choi, B. Karaboce, W. Ji, Q. Wu, D. Ruess, C. Ullrich, J. Kostelecký, D. Schmerge, M. Eckl, L. Timmen, N. Le Moigne, R. Bayer, T. Olszak, J. Ågren, C. Del Negro, F. Greco, M. Diament, S. Deroussi, S. Bonvalot, J. Krynski, M. Sekowski, H. Hu, L. J. Wang, S. Svitlov, A. Germak, O. Francis, M. Becker, D. Inglis, and I. Robinson. **The 8th International Comparison of Absolute Gravimeters 2009: the first Key Comparison (CCM.G-K1) in the field of absolute gravimetry**. In: *Metrologia* **49** (6 2012), pp. 666–684. DOI: 10.1088/0026-1394/49/6/666.

[88] F. Sorrentino, A. Bertoldi, Q. Bodart, L. Cacciapuoti, M. de Angelis, Y.-H. Lien, M. Prevedelli, G. Rosi, and G. M. Tino. **Simultaneous measurement of gravity acceleration and gravity gradient with an atom interferometer**. In: *Appl. Phys. Lett.* **101** (11 2012), p. 114106. DOI: 10.1063/1.4751112.

[89] T. L. Gustavson, P. Bouyer, and M. A. Kasevich. **Precision Rotation Measurements with an Atom Interferometer Gyroscope**. In: *Phys. Rev. Lett.* **78** (11 1997), pp. 2046–2049. DOI: 10.1103/PhysRevLett.78.2046.

[90] J. K. Stockton, K. Takase, and M. A. Kasevich. **Absolute Geodetic Rotation Measurement Using Atom Interferometry**. In: *Phys. Rev. Lett.* **107** (13 2011), p. 133001. DOI: 10.1103/PhysRevLett.107.133001.

[91] R. Caldani, K. X. Weng, S. Merlet, and F. Pereira Dos Santos. **Simultaneous accurate determination of both gravity and its vertical gradient**. In: *Phys. Rev. A* **99** (3 2019), p. 033601. DOI: 10.1103/PhysRevA.99.033601.

[92] X. Wu, F. Zi, J. Dudley, R. J. Bilotta, P. Canoza, and H. Müller. **Multiaxis atom interferometry with a single-diode laser and a pyramidal magneto-optical trap**. In: *Optica* **4** (12 2017), p. 1545. DOI: 10.1364/OPTICA.4.001545.

[93] P. Cheiney, L. Fouché, S. Templier, F. Napolitano, B. Battelier, P. Bouyer, and B. Barrett. **Navigation-Compatible Hybrid Quantum Accelerometer Using a Kalman Filter**. In: *Phys. Rev. Appl.* **10** (3 2018), p. 344. DOI: 10.1103/PhysRevApplied.10.034030.

[94] C.-C. Chen, S. Bennetts, R. G. Escudero, B. Pasquiou, and F. Schreck. **Continuous Guided Strontium Beam with High Phase-Space Density**. In: *Phys. Rev. Appl.* **12**.4 (Oct. 2019). DOI: 10.1103/physrevapplied.12.044014.

[95] H. J. McGuinness, A. V. Rakholia, and G. W. Biedermann. **High data-rate atom interferometer for measuring acceleration**. In: *Appl. Phys. Lett.* **100** (1 2012), p. 011106. DOI: 10.1063/1.3673845.

[96] A. V. Rakholia, H. J. McGuinness, and G. W. Biedermann. **Dual-Axis High-Data-Rate Atom Interferometer via Cold Ensemble Exchange**. In: *Phys. Rev. Appl.* **2** (5 2014), p. 054012. DOI: 10.1103/PhysRevApplied.2.054012.

[97] A. Trimeche, B. Battelier, D. Becker, A. Bertoldi, P. Bouyer, C. Braxmaier, E. Charron, R. Corgier, M. Cornelius, K. Douch, N. Gaaloul, S. Herrmann, J. Müller, E. Rasel, C. Schubert, H. Wu, and F. P. dos Santos. **Concept study and preliminary design of a cold atom interferometer for space gravity gradiometry**. In: *Class. Quantum Grav.* **36**.21 (Oct. 2019), p. 215004. DOI: 10.1088/1361-6382/ab4548.

[98] M. de Angelis, A. Bertoldi, L. Cacciapuoti, A. Giorgini, G. Lamporesi, M. Prevedelli, G. Saccorotti, F. Sorrentino, and G. M. Tino. **Precision gravimetry with atomic sensors**. In: *Meas. Sci. Technol.* **20** (2 2009), p. 022001. DOI: 10.1088/0957-0233/20/2/022001.

[99] V. Ménoret, P. Vermeulen, N. L. Moigne, S. Bonvalot, P. Bouyer, A. Landragin, and B. Desruelle. **Gravity measurements below 10^{-9} g with a transportable absolute quantum gravimeter**. In: *Sci. Rep.* **8**.1 (Aug. 2018). DOI: 10.1038/s41598-018-30608-1.

[100] Y. Bidel, N. Zahzam, C. Blanchard, A. Bonnin, M. Cadoret, A. Bresson, D. Rouxel, and M. F. Lequentrec-Lalancette. **Absolute marine gravimetry with matter-wave interferometry**. In: *Nat. Commun.* **9** (1 2018), p. 65. DOI: 10.1038/s41467-018-03040-2.

[101] M. A. Kasevich and B. Dubetsky. ***Kinematic sensors employing atom interferometer phases***. US Patent 7317184B2. Nov. 2006.

[102] B. Barrett, P. Cheiney, B. Battelier, F. Napolitano, and P. Bouyer. **Multidimensional Atom Optics and Interferometry**. In: *Phys. Rev. Lett.* **122** (4 2019), p. 043604. DOI: 10.1103/PhysRevLett.122.043604.

[103] H. Müntinga, H. Ahlers, M. Krutzik, A. Wenzlawski, S. Arnold, D. Becker, K. Bongs, H. Dittus, H. Duncker, N. Gaaloul, C. Gherasim, E. Giese, C. Grzeschik, T. W. Hänsch, O. Hellmig, W. Herr, S. Herrmann, E. Kajari, S. Kleinert, C. Lämmerzahl, W. Lewoczko-Adamczyk, J. Malcolm, N. Meyer, R. Nolte, A. Peters, M. Popp, J. Reichel, A. Roura, J. Rudolph, M. Schiemangk, M. Schneider, S. T. Seidel, K. Sengstock, V. Tamma, T. Valenzuela, A. Vogel, R. Walser, T. Wendrich, P. Windpassinger, W. Zeller, T. van Zoest, W. Ertmer, W. P. Schleich, and E. M. Rasel. **Interferometry with Bose-Einstein Condensates in Microgravity**. In: *Phys. Rev. Lett.* **110** (9 2013), p. 3. DOI: 10.1103/PhysRevLett.110.093602.

[104] G. Condon, M. Rabault, B. Barrett, L. Chichet, R. Arguel, H. Eneriz-Imaz, D. Naik, A. Bertoldi, B. Battelier, P. Bouyer, and A. Landragin. **All-Optical Bose-Einstein Condensates in Microgravity**. In: *Phys. Rev. Lett.* **123**.24 (Dec. 2019), p. 240402. DOI: 10.1103/physrevlett.123.240402.

[105] B. Barrett, L. Antoni-Micollier, L. Chichet, B. Battelier, T. Lévèque, A. Landragin, and P. Bouyer. **Dual matter-wave inertial sensors in weightlessness**. In: *Nat. Commun.* **7** (2016), p. 13786. DOI: 10.1038/ncomms13786.

[106] D. Becker, M. D. Lachmann, S. T. Seidel, H. Ahlers, A. N. Dinkelaker, J. Grosse, O. Hellmig, H. Müntinga, V. Schkolnik, T. Wendrich, A. Wenzlawski, B. Weps, R. Corgier, T. Franz, N. Gaaloul, W. Herr, D. Lüdtke, M. Popp, S. Amri, H. Duncker, M. Erbe, A. Kohfeldt, A. Kubelka-Lange, C. Braxmaier, E. Charron, W. Ertmer, M. Krutzik, C. Lämmerzahl, A. Peters, W. P. Schleich, K. Sengstock, R. Walser, A. Wicht, P. Windpassinger, and E. M. Rasel. **Space-borne Bose–Einstein condensation for precision interferometry**. In: *Nature* **562** (7727 2018), pp. 391–395. DOI: 10.1038/s41586-018-0605-1.

[107] E. R. Elliott, M. C. Krutzik, J. R. Williams, R. J. Thompson, and D. C. Aveline. **NASA's Cold Atom Lab (CAL): system development and ground test status**. In: *npj Micrograv.* **4**.1 (Aug. 2018). DOI: 10.1038/s41526-018-0049-9.

[108] S. M. Dickerson, J. M. Hogan, A. Sugarbaker, D. M. S. Johnson, and M. A. Kasevich. **Multiaxis Inertial Sensing with Long-Time Point Source Atom Interferometry**. In: *Phys. Rev. Lett.* **111** (8 2013), p. 083001. DOI: 10.1103/PhysRevLett.111.083001.

[109] L. Ricci, D. Bassi, and A. Bertoldi. **Combined static potentials for confinement of neutral species**. In: *Phys. Rev. A* **76**.2 (Aug. 2007). DOI: 10.1103/physreva.76.023428.

[110] K. J. Hughes, J. H. T. Burke, and C. A. Sackett. **Suspension of Atoms Using Optical Pulses, and Application to Gravimetry**. In: *Phys. Rev. Lett.* **102** (15 2009), p. 150403. DOI: 10.1103/PhysRevLett.102.150403.

[111] K. Shibata, H. Ikeda, R. Suzuki, and T. Hirano. **Compensation of gravity on cold atoms by a linear optical potential**. In: *Phys. Rev. Res.* **2**.1 (Jan. 2020). DOI: 10.1103/physrevresearch.2.013068.

[112] J. Stuhler, M. Fattori, T. Petelski, and G. M. Tino. **MAGIA using atom interferometry to determine the Newtonian gravitational constant**. In: *J. Opt. B* **5**.2 (Apr. 2003), S75–S81. DOI: 10.1088/1464-4266/5/2/361.

[113] P. J. Mohr, B. N. Taylor, and D. B. Newell. **CODATA recommended values of the fundamental physical constants: 2006**. In: *Rev. Mod. Phys.* **80**.2 (June 2008), pp. 633–730. DOI: 10.1103/revmodphys.80.633.

[114] G. Lamporesi, A. Bertoldi, A. Cecchetti, B. Duhlach, M. Fattori, A. Malengo, S. Pettorruso, M. Prevedelli, and G. M. Tino. **Source mass and positioning system for an accurate measurement of G**. In: *Rev. Sci. Instrum.* **78**.7 (July 2007), p. 075109. DOI: 10.1063/1.2751090.

[115] G. Rosi, F. Sorrentino, L. Cacciapuoti, M. Prevedelli, and G. M. Tino. **Precision measurement of the Newtonian gravitational constant using cold atoms**. In: *Nature* **510** (2014), pp. 518–521. DOI: 10.1038/nature13433.

[116] P. J. Mohr, D. B. Newell, and B. N. Taylor. **CODATA Recommended Values of the Fundamental Physical Constants: 2014**. In: *J. Phys. Chem. Ref. Data* **45**.4 (Dec. 2016), p. 043102. DOI: 10.1063/1.4954402.

[117] K. Horstman and V. Trimble. **A citation history of measurements of Newton's constant of gravity**. In: *Scientometrics* **119**.1 (Feb. 2019), pp. 527–541. DOI: 10.1007/s11192-019-03031-0.

[118] C. Rothleitner and S. Schlamminger. **Invited Review Article: Measurements of the Newtonian constant of gravitation, G**. In: *Rev. Sci. Instrum.* **88**.11 (Nov. 2017), p. 111101. DOI: 10.1063/1.4994619.

[119] J. P. Schwarz, D. S. Robertson, T. M. Niebauer, and J. E. Faller. **A Free-Fall Determination of the Newtonian Constant of Gravity**. In: *Science* **282**.5397 (Dec. 1998), pp. 2230–2234. DOI: 10.1126/science.282.5397.2230.

[120] G. Rosi. **Challenging the 'Big *G*' measurement with atoms and light**. In: *J. Phys. B* **49**.20 (Oct. 2016), p. 202002. DOI: 10.1088/0953-4075/49/20/202002.

[121] G. W. Biedermann, X. Wu, L. Deslauriers, S. Roy, C. Mahadeswaraswamy, and M. A. Kasevich. **Testing gravity with cold-atom interferometers**. In: *Phys. Rev. A* **91** (3 2015), p. 033629. DOI: 10.1103/PhysRevA.91.033629.

[122] M. Xin, W. S. Leong, Z. Chen, and S.-Y. Lan. **An atom interferometer inside a hollow-core photonic crystal fiber**. In: *Sci. Adv.* **4** (1 2018), e1701723. DOI: 10.1126/sciadv.1701723.

[123] K. Kawana and D. Ueda. **Amplification of gravitational motion via quantum weak measurement**. In: *Prog. Theor. Exp. Phys.* **2019**.4 (Apr. 2019). DOI: 10.1093/ptep/ptz019.

[124] J. H. Taylor and J. M. Weisberg. **A new test of general relativity - Gravitational radiation and the binary pulsar PSR 1913+16**. In: *ApJ* **253** (1982), p. 908. DOI: 10.1086/159690.

[125] B. Abbott et al. **Observation of Gravitational Waves from a Binary Black Hole Merger**. In: *Phys. Rev. Lett.* **116** (6 2016), p. 688. DOI: 10.1103/PhysRevLett.116.061102.

[126] B. Abbott et al. **GWTC-1: A Gravitational-Wave Transient Catalog of Compact Binary Mergers Observed by LIGO and Virgo during the First and Second Observing Runs**. In: *Phys. Rev. X* **9**.3 (Sept. 2019). DOI: 10.1103/physrevx.9.031040.

[127] B. Abbott et al. **A gravitational-wave standard siren measurement of the Hubble constant**. In: *Nature* **551** (7678 2017), pp. 85–88. DOI: 10.1038/nature24471.

[128] B. Abbott et al. **GW170817: Observation of Gravitational Waves from a Binary Neutron Star Inspiral**. In: *Phys. Rev. Lett.* **119** (16 2017), p. 61. DOI: 10.1103/PhysRevLett.119.161101.

[129] *Einstein@Home*. https://einsteinathome.org.

[130] J. Harms, B. J. J. Slagmolen, R. X. Adhikari, M. C. Miller, M. Evans, Y. Chen, H. Müller, and M. Ando. **Low-frequency terrestrial gravitational-wave detectors**. In: *Phys. Rev. D* **88** (12 2013), p. 337. DOI: 10.1103/PhysRevD.88.122003.

[131] J. Harms. **Terrestrial Gravity Fluctuations**. In: *Living Rev. Relativ.* **18**.1 (Dec. 2015). DOI: 10.1007/lrr-2015-3.

[132] F. Badaracco and J. Harms. **Optimization of seismometer arrays for the cancellation of Newtonian noise from seismic body waves**. In: *Class. Quantum Grav.* **36**.14 (June 2019), p. 145006. DOI: 10.1088/1361-6382/ab28c1.

[133] W. Chaibi, R. Geiger, B. Canuel, A. Bertoldi, A. Landragin, and P. Bouyer. **Low frequency gravitational wave detection with ground-based atom interferometer arrays**. In: *Phys. Rev. D* **93** (2 2016), p. 173. DOI: 10.1103/PhysRevD.93.021101.

[134] A. Sesana. **Prospects for Multiband Gravitational-Wave Astronomy after GW150914**. In: *Phys. Rev. Lett.* **116** (23 2016), p. 4. DOI: 10.1103/PhysRevLett.116.231102.

[135] C. J. Bordé, J. Sharma, P. Tourrenc, and T. Damour. **Theoretical approaches to laser spectroscopy in the presence of gravitational fields**. In: *J. Phys. Lett.-Paris* **44**.24 (1983), pp. 983–990. DOI: 10.1051/jphyslet:019830044024098300.

[136] R. Y. Chiao and A. D. Speliotopoulos. **Towards MIGO, the matter-wave interferometric gravitational-wave observatory, and the intersection of quantum mechanics with general relativity**. In: *J. Mod. Opt.* **51**.6-7 (Apr. 2004), pp. 861–899. DOI: 10.1080/09500340408233603.

[137] G. M. Tino and F. Vetrano. **Is it possible to detect gravitational waves with atom interferometers?** In: *Class. Quantum Grav.* **24**.9 (Apr. 2007), pp. 2167–2178. DOI: 10.1088/0264-9381/24/9/001.

[138] P. W. Graham, J. M. Hogan, M. A. Kasevich, and S. Rajendran. **New Method for Gravitational Wave Detection with Atomic Sensors**. In: *Phys. Rev. Lett.* **110** (17 2013), p. 171102. DOI: 10.1103/PhysRevLett.110.171102.

[139] S. Kolkowitz, I. Pikovski, N. Langellier, M. Lukin, R. Walsworth, and J. Ye. **Gravitational wave detection with optical lattice atomic clocks**. In: *Phys. Rev. D* **94** (12 2016), p. 13. DOI: 10.1103/PhysRevD.94.124043.

[140] M. A. Norcia, J. R. K. Cline, and J. K. Thompson. **Role of atoms in atomic gravitational-wave detectors**. In: *Phys. Rev. A* **96** (4 2017), p. 042118. DOI: 10.1103/PhysRevA.96.042118.

[141] B. Canuel, A. Bertoldi, L. Amand, E. Pozzo di Borgo, T. Chantrait, C. Danquigny, M. Dovale Álvarez, B. Fang, A. Freise, R. Geiger, J. Gillot, S. Henry, J. Hinderer, D. Holleville, J. Junca, G. Lefèvre, M. Merzougui, N. Mielec, T. Monfret, S. Pelisson, M. Prevedelli, S. Reynaud, I. Riou, Y. Rogister, S. Rosat, E. Cormier, A. Landragin, W. Chaibi, S. Gaffet, and P. Bouyer. **Exploring gravity with the MIGA large scale atom interferometer**. In: *Sci. Rep.* **8** (1 2018), p. 2689. DOI: 10.1038/s41598-018-32165-z.

[142] J. Coleman et al. **MAGIS-100 at Fermilab**. In: *Proceedings of The 39th International Conference on High Energy Physics — PoS(ICHEP2018)*. Sissa Medialab, Aug. 2019. DOI: 10.22323/1.340.0021.

[143] M.-S. Zhan, J. Wang, W.-T. Ni, D.-F. Gao, G. Wang, L.-X. He, R.-B. Li, L. Zhou, X. Chen, J.-Q. Zhong, B. Tang, Z.-W. Yao, L. Zhu, Z.-Y. Xiong, S.-B. Lu, G.-H. Yu, Q.-F. Cheng, M. Liu, Y.-R. Liang, P. Xu, X.-D. He, M. Ke, Z. Tan, and J. Luo. **ZAIGA: Zhaoshan long-baseline Atom Interferometer Gravitation Antenna**. In: *Int. J. Mod. Phys. D* (May 2019), p. 1940005. DOI: 10.1142/s0218271819400054.

[144] *AION project*. https://www.hep.ph.ic.ac.uk/AION-Project/.

[145] B. Canuel et al. **ELGAR - a European Laboratory for Gravitation and Atom-interferometric Research**. In: *in prep.* (2019).

[146] Y. El-Neaj, C. Alpigiani, and S. A.-P. et al. **AEDGE: Atomic Experiment for Dark Matter and Gravity Exploration in Space**. In: *EPJ Quantum Technol.* **7** (6 2020). White Paper in response to ESA Science Programm call "Voyage 2050". DOI: 10.1140/epjqt/s40507-020-0080-0.

[147] I. Mandel, A. Sesana, and A. Vecchio. **The astrophysical science case for a decihertz gravitational-wave detector**. In: *Class. Quantum Grav.* **35** (5 2018), p. 054004. DOI: 10.1088/1361-6382/aaa7e0.

[148] P. W. Graham and S. Jung. **Localizing gravitational wave sources with single-baseline atom interferometers**. In: *Phys. Rev. D* **97** (2 2018), p. 024052. DOI: 10.1103/PhysRevD.97.024052.

[149] Z. Pagel, W. Zhong, R. H. Parker, C. T. Olund, N. Y. Yao, and H. Mueller. **Bloch beamsplitters and dual-lattice methods for atom interferometry**. In: (2019). arXiv: 1907.05994 [physics.atom-ph].

[150] M. Gebbe, S. Abend, J.-N. Siems, M. Gersemann, H. Ahlers, H. Müntinga, S. Herrmann, N. Gaaloul, C. Schubert, K. Hammerer, C. Lämmerzahl, W. Ertmer, and E. M. Rasel. **Twin-lattice atom interferometry**. In: (2019). arXiv: 1907.08416 [quant-ph].

[151] K. C. Cox, G. P. Greve, J. M. Weiner, and J. K. Thompson. **Deterministic Squeezed States with Collective Measurements and Feedback**. In: *Phys. Rev. Lett.* **116**.9 (Mar. 2016). DOI: 10.1103/physrevlett.116.093602.

[152] O. Hosten, N. J. Engelsen, R. Krishnakumar, and M. A. Kasevich. **Measurement noise 100 times lower than the quantum-projection limit using entangled atoms**. In: *Nature* **529** (7587 2016), pp. 505–508. DOI: 10.1038/nature16176.

[153] S. Dimopoulos, P. W. Graham, J. M. Hogan, M. A. Kasevich, and S. Rajendran. **Atomic gravitational wave interferometric sensor**. In: *Phys. Rev. D* **78**.12 (Dec. 2008), p. 122002. DOI: 10.1103/physrevd.78.122002.

[154] K. A. Kuns, H. Yu, Y. Chen, and R. X. Adhikari. **Astrophysics and cosmology with a deci-hertz gravitational-wave detector: TianGO**. In: (2019). arXiv: 1908.06004 [gr-qc].

[155] M. A. Sedda et al. **The missing link in the grawitational wave astronomy: discoveries waiting in the decihertz range**. In: (2019). arXiv: 1908.11375 [gr-qc].

[156] K. Eda, Y. Itoh, S. Kuroyanagi, and J. Silk. **Gravitational waves as a probe of dark matter minispikes**. In: *Phys. Rev. D* **91**.4 (Feb. 2015). DOI: 10.1103/physrevd.91.044045.

[157] B. J. Kavanagh, D. Gaggero, and G. Bertone. **Merger rate of a subdominant population of primordial black holes**. In: *Phys. Rev. D* **98**.2 (July 2018). DOI: 10.1103/physrevd.98.023536.

[158] D. Baumann, H. S. Chia, and R. A. Porto. **Probing ultralight bosons with binary black holes**. In: *Phys. Rev. D* **99**.4 (Feb. 2019). DOI: 10.1103/physrevd.99.044001.

[159] D. J. Weir. **Gravitational waves from a first-order electroweak phase transition: a brief review**. In: *Philos. Trans. Royal Soc. A* **376**.2114 (Jan. 2018), p. 20170126. DOI: 10.1098/rsta.2017.0126.

[160] R. Saito and J. Yokoyama. **Gravitational-Wave Background as a Probe of the Primordial Black-Hole Abundance**. In: *Phys. Rev. Lett.* **102**.16 (Apr. 2009), p. 161101. DOI: 10.1103/physrevlett.102.161101.

[161] B. Allen and J. D. Romano. **Detecting a stochastic background of gravitational radiation: Signal processing strategies and sensitivities**. In: *Phys. Rev. D* **59**.10 (Mar. 1999), p. 102001. DOI: 10.1103/physrevd.59.102001.

[162] P. D. Lasky, C. M. Mingarelli, T. L. Smith, J. T. Giblin, E. Thrane, D. J. Reardon, R. Caldwell, M. Bailes, N. R. Bhat, S. Burke-Spolaor, S. Dai, J. Dempsey, G. Hobbs, M. Kerr, Y. Levin, R. N. Manchester, S. Osłowski, V. Ravi, P. A. Rosado, R. M. Shannon, R. Spiewak, W. van Straten, L. Toomey, J. Wang, L. Wen, X. You, and X. Zhu. **Gravitational-Wave Cosmology across 29 Decades in Frequency**. In: *Phys. Rev. X* **6** (1 2016), p. 293. DOI: 10.1103/PhysRevX.6.011035.

[163] J. Lautier, L. Volodimer, T. Hardin, S. Merlet, M. Lours, F. Pereira Dos Santos, and A. Landragin. **Hybridizing matter-wave and classical accelerometers**. In: *Appl. Phys. Lett.* **105** (14 2014), p. 144102. DOI: 10.1063/1.4897358.

[164] J. M. Hogan, D. M. S. Johnson, S. Dickerson, T. Kovachy, A. Sugarbaker, S.-w. Chiow, P. W. Graham, M. A. Kasevich, B. Saif, S. Rajendran, P. Bouyer, B. D. Seery, L. Feinberg, and R. Keski-Kuha. **An atomic gravitational wave interferometric sensor in low earth orbit (AGIS-LEO)**. In: *Gen. Relativ. Gravit.* **43** (7 2011), pp. 1953–2009. DOI: 10.1007/s10714-011-1182-x.

[165] C. Schubert, D. Schlippert, S. Abend, E. Giese, A. Roura, W. P. Schleich, W. Ertmer, and E. M. Rasel. **Scalable, symmetric atom interferometer for infrasound gravitational wave detection**. In: (2019). arXiv: 1909.01951 [quant-ph].

[166] S.-w. Chiow, J. Williams, and N. Yu. **Laser-ranging long-baseline differential atom interferometers for space**. In: *Phys. Rev. A* **92**.6 (Dec. 2015). DOI: 10.1103/physreva.92.063613.

[167] J. M. Hogan and M. A. Kasevich. **Atom-interferometric gravitational-wave detection using heterodyne laser links**. In: *Phys. Rev. A* **94**.3 (Sept. 2016). DOI: 10.1103/physreva.94.033632.

[168] W. M. Itano, J. C. Bergquist, J. J. Bollinger, J. M. Gilligan, D. J. Heinzen, F. L. Moore, M. G. Raizen, and D. J. Wineland. **Quantum projection noise: Population fluctuations in two-level systems**. In: *Phys. Rev. A* **47**.5 (May 1993), pp. 3554–3570. DOI: 10.1103/physreva.47.3554.

[169] *Earth Gravitational Models 1996*. https://cddis.nasa.gov/926/egm96/egm96.html.

[170] G. Rosi, L. Cacciapuoti, F. Sorrentino, M. Menchetti, M. Prevedelli, and G. M. Tino. **Measurement of the Gravity-Field Curvature by Atom Interferometry**. In: *Phys. Rev. Lett.* **114** (2015), p. 013001. DOI: 10.1103/PhysRevLett.114.013001.

[171] B. Canuel, S. Pelisson, L. Amand, A. Bertoldi, E. Cormier, B. Fang, S. Gaffet, R. Geiger, J. Harms, D. Holleville, A. Landragin, G. Lefèvre, J. Lhermite, N. Mielec, M. Prevedelli, I. Riou, and P. Bouyer. **MIGA: combining laser and matter wave interferometry for mass distribution monitoring and advanced geodesy**. In: *Quantum Optics*. Ed. by J. Stuhler and A. J. Shields. SPIE, Apr. 2016. DOI: 10.1117/12.2228825.

[172] J. Junca, A. Bertoldi, D. Sabulsky, G. Lefèvre, X. Zou, J.-B. Decitre, R. Geiger, A. Landragin, S. Gaffet, P. Bouyer, and B. Canuel. **Characterizing Earth gravity field fluctuations with the MIGA antenna for future gravitational wave detectors**. In: *Phys. Rev. D* **99**.10 (May 2019). DOI: 10.1103/physrevd.99.104026.

[173] L. Zhou, Z. Y. Xiong, W. Yang, B. Tang, W. C. Peng, K. Hao, R. B. Li, M. Liu, J. Wang, and M. S. Zhan. **Development of an atom gravimeter and status of the 10-meter atom interferometer for precision gravity measurement**. In: *Gen. Relat. Gravit.* **43**.7 (Mar. 2011), pp. 1931–1942. DOI: 10.1007/s10714-011-1167-9.

[174] J. Hartwig, S. Abend, C. Schubert, D. Schlippert, H. Ahlers, K. Posso-Trujillo, N. Gaaloul, W. Ertmer, and E. M. Rasel. **Testing the universality of free fall with rubidium and ytterbium in a very large baseline atom interferometer**. In: *New J. Phys.* **17**.3 (Mar. 2015), p. 035011. DOI: 10.1088/1367-2630/17/3/035011.

[175] D. O. Sabulsky, J. Junca, G. Lefèvre, X. Zou, A. Bertoldi, B. Battelier, M. Prevedelli, G. Stern, J. Santoire, Q. Beaufils, R. Geiger, A. Landragin, B. Desruelle, P. Bouyer, and B. Canuel. **A fibered laser system for the MIGA large scale atom interferometer**. In: *Sci. Rep.* **10**.1 (Feb. 2020). DOI: 10.1038/s41598-020-59971-8.

[176] A. Bertoldi, C.-H. Feng, H. Eneriz, M. Carey, D. S. Naik, J. Junca, X. Zou, D. O. Sabulsky, B. Canuel, P. Bouyer, and M. Prevedelli. **A control hardware based on a field programmable gate array for experiments in atomic physics**. In: *Rev. Sci. Instrum.* **91**.3 (Mar. 2020), p. 033203. DOI: 10.1063/1.5129595.

[177] P. Hamilton, M. Jaffe, P. Haslinger, Q. Simmons, H. Muller, and J. Khoury. **Atom-interferometry constraints on dark energy**. In: *Science* **349** (6250 2015), pp. 849–851. DOI: 10.1126/science.aaa8883.

[178] J. L. Hall, C. J. Bordé, and K. Uehara. **Direct Optical Resolution of the Recoil Effect Using Saturated Absorption Spectroscopy**. In: *Phys. Rev. Lett.* **37**.20 (Nov. 1976), pp. 1339–1342. DOI: 10.1103/physrevlett.37.1339.

[179] I. Riou, N. Mielec, G. Lefèvre, M. Prevedelli, A. Landragin, P. Bouyer, A. Bertoldi, R. Geiger, and B. Canuel. **A marginally stable optical resonator for enhanced atom interferometry**. In: *J. Phys. B* **50**.15 (2017), p. 155002. DOI: 10.1088/1361-6455/aa7592.

[180] B. Canuel, A. Bertoldi, I. Riou, P. Bouyer, R. Geiger, and N. Mielec. **Optical resonator with large prope mode for atom interferometry**. France Patent 3054773. 2018.

[181] M. Jaffe, V. Xu, P. Haslinger, H. Müller, and P. Hamilton. **Efficient Adiabatic Spin-Dependent Kicks in an Atom Interferometer**. In: *Phys. Rev. Lett.* **121** (4 2018), p. 040402. DOI: 10.1103/PhysRevLett.121.040402.

[182] H. Katori, M. Takamoto, V. G. Pal'chikov, and V. D. Ovsiannikov. **Ultrastable Optical Clock with Neutral Atoms in an Engineered Light Shift Trap**. In: *Phys. Rev. Lett.* **91**.17 (Oct. 2003), p. 173005. DOI: 10.1103/physrevlett.91.173005.

[183] S. Stellmer, B. Pasquiou, R. Grimm, and F. Schreck. **Laser Cooling to Quantum Degeneracy**. In: *Phys. Rev. Lett.* **110**.26 (June 2013), p. 263003. DOI: 10.1103/physrevlett.110.263003.

[184] A. Bertoldi, S. Bernon, T. Vanderbruggen, A. Landragin, and P. Bouyer. **In situ characterization of an optical cavity using atomic light shift**. In: *Opt. Lett.* **35**.22 (2010), p. 3769. DOI: 10.1364/OL.35.003769.

[185] A. Taichenachev, V. Yudin, C. Oates, C. Hoyt, Z. Barber, and L. Hollberg. **Magnetic Field-Induced Spectroscopy of Forbidden Optical Transitions with Application to Lattice-Based Optical Atomic Clocks**. In: *Phys. Rev. Lett.* **96**.8 (Mar. 2006), p. 083001. DOI: 10.1103/physrevlett.96.083001.

[186] A. Bertoldi, C.-H. Feng, D. S. Naik, B. Canuel, P. Bouyer, and M. Prevedelli. **Atom interferometry in a high finesse cavity**. In: *submitted to Phys. Rev. Lett.* (2019).

[187] *The National Institute of Standards and Technology (NIST) database*. available at http://www.nist.gov/pml/data.

[188] A. D. Ludlow. "The Strontium Optical Lattice Clock: Optical Spectroscopy with Sub-Hertz Accuracy". PhD thesis. Univ. of Colorado, 2008.

[189] G. W. Biedermann, K. Takase, X. Wu, L. Deslauriers, S. Roy, and M. A. Kasevich. **Zero-Dead-Time Operation of Interleaved Atomic Clocks**. In: *Phys. Rev. Lett.* **111**.17 (Oct. 2013). DOI: 10.1103/physrevlett.111.170802.

[190] T. Vanderbruggen, R. Kohlhaas, A. Bertoldi, S. Bernon, A. Aspect, A. Landragin, and P. Bouyer. **Feedback Control of Trapped Coherent Atomic Ensembles**. In: *Phys. Rev. Lett.* **110** (21 2013), p. 210503. DOI: 10.1103/PhysRevLett.110.210503.

[191] R. Kohlhaas, A. Bertoldi, E. Cantin, A. Aspect, A. Landragin, and P. Bouyer. **Phase Locking a Clock Oscillator to a Coherent Atomic Ensemble**. In: *Phys. Rev. X* **5** (2 2015), p. 021011. DOI: 10.1103/PhysRevX.5.021011.

[192] M. Dovale-Álvarez, D. D. Brown, A. W. Jones, C. M. Mow-Lowry, H. Miao, and A. Freise. **Fundamental limitations of cavity-assisted atom interferometry**. In: *Phys. Rev. A* **96** (5 2017), p. 053820. DOI: 10.1103/PhysRevA.96.053820.

[193] N. Hinkley, J. A. Sherman, N. B. Phillips, M. Schioppo, N. D. Lemke, K. Beloy, M. Pizzocaro, C. W. Oates, and A. D. Ludlow. **An Atomic Clock with 10^{-18} Instability**. In: *Science* **341**.6151 (Aug. 2013), pp. 1215–1218. DOI: 10.1126/science.1240420.

[194] B. J. Bloom, T. L. Nicholson, J. R. Williams, S. L. Campbell, M. Bishof, X. Zhang, W. Zhang, S. L. Bromley, and J. Ye. **An optical lattice clock with accuracy and stability at the 10^{-18} level**. In: *Nature* **506**.7486 (Jan. 2014), pp. 71–75. DOI: 10.1038/nature12941.

[195] L. Hu, N. Poli, L. Salvi, and G. M. Tino. **Atom Interferometry with the Sr Optical Clock Transition**. In: *Phys. Rev. Lett.* **119**.26 (Dec. 2017). DOI: 10.1103/physrevlett.119.263601.

[196] T. Akatsuka, T. Takahashi, and H. Katori. **Optically guided atom interferometer tuned to magic wavelength**. In: *Appl. Phys. Expr.* **10**.11 (Oct. 2017), p. 112501. DOI: 10.7567/apex.10.112501.

[197] I. Nosske, L. Couturier, F. Hu, C. Tan, C. Qiao, J. Blume, Y. H. Jiang, P. Chen, and M. Weidemüller. **Two-dimensional magneto-optical trap as a source for cold strontium atoms**. In: *Phys. Rev. A* **96**.5 (Nov. 2017). DOI: 10.1103/physreva.96.053415.

[198] S. Rota-Rodrigo, B. Gouhier, M. Laroche, J. Zhao, B. Canuel, A. Bertoldi, P. Bouyer, N. Traynor, B. Cadier, T. Robin, and G. Santarelli. **Watt-level single-frequency tunable neodymium MOPA fiber laser operating at 915–937 nm**. In: *Opt. Lett.* **42**.21 (2017), p. 4557. DOI: 10.1364/ol.42.004557.

[199] A. E. Leanhardt. **Cooling Bose-Einstein Condensates Below 500 Picokelvin**. In: *Science* **301**.5639 (Sept. 2003), pp. 1513–1515. DOI: 10.1126/science.1088827.

[200] J. M. Reeves, O. Garcia, B. Deissler, K. L. Baranowski, K. J. Hughes, and C. A. Sackett. **Time-orbiting potential trap for Bose-Einstein condensate interferometry**. In: *Phys. Rev. A* **72**.5 (Nov. 2005). DOI: 10.1103/physreva.72.051605.

[201] F. Jendrzejewski, A. Bernard, K. Müller, P. Cheinet, V. Josse, M. Piraud, L. Pezzé, L. Sanchez-Palencia, A. Aspect, and P. Bouyer. **Three-dimensional localization of ultracold atoms in an optical disordered potential**. In: *Nat. Phys.* **8**.5 (Mar. 2012), pp. 398–403. DOI: 10.1038/nphys2256.

[202] V. Xu, M. Jaffe, C. D. Panda, S. L. Kristensen, L. W. Clark, and H. Müller. **Probing gravity by holding atoms for 20 seconds**. In: *Science* **366**.6466 (Nov. 2019), pp. 745–749. DOI: 10.1126/science.aay6428.

[203] M. Robert-de-Saint-Vincent, J.-P. Brantut, C. J. Bordé, A. Aspect, T. Bourdel, and P. Bouyer. **A quantum trampoline for ultra-cold atoms**. In: *EPL (Europhys. Lett.)* **89**.1 (Jan. 2010), p. 10002. DOI: 10.1209/0295-5075/89/10002.

[204] C. A. Sackett. **Limits on weak magnetic confinement of neutral atoms**. In: *Phys. Rev. A* **73**.1 (Jan. 2006). DOI: 10.1103/physreva.73.013626.

[205] H. Ammann and N. Christensen. **Delta Kick Cooling: A New Method for Cooling Atoms**. In: *Phys. Rev. Lett.* **78**.11 (Mar. 1997), pp. 2088–2091. DOI: 10.1103/physrevlett.78.2088.

[206] A. A. Geraci and A. Derevianko. **Sensitivity of Atom Interferometry to Ultralight Scalar Field Dark Matter**. In: *Phys. Rev. Lett.* **117**.26 (Dec. 2016). DOI: 10.1103/physrevlett.117.261301.

[207] L. Blanchet, K. Bongs, P. Bouyer, B. Battelier, A. Bertoldi, C. Braxmaier, L. Wörner, D. Calonico, P. Fayet, A. Hees, C. L. Poncin-Lafitte, P. Jetzer, C. Lämmerzahl, S. Lecomte, G. Métris, E. Rasel, N. Gaaloul, S. Loriani, C. Schubert, S. Reynaud, C. Guerlin, C. Salomon, M. Rodrigues, J. Bergé, M. Rothacher, W. Schleich, A. Roura, S. Schiller, C. Sopuerta, M. Nofrarias, F. Sorrentino, T. Sumner, G. Tino, W. von Klitzing, and M. Zelan. **Exploring the Foundations of the Physical Universe with Space Tests of the Equivalence Principle**. In: (2019). White Paper in response to ESA Science Programm call "Voyage 2050". arXiv: 1908.11785 [physics.space-ph].

[208] G. Tino, F. Sorrentino, D. Aguilera, B. Battelier, A. Bertoldi, Q. Bodart, K. Bongs, P. Bouyer, C. Braxmaier, L. Cacciapuoti, N. Gaaloul, N. Gürlebeck, M. Hauth, S. Herrmann, M. Krutzik, A. Kubelka, A. Landragin, A. Milke, A. Peters, E. Rasel, E. Rocco, C. Schubert, T. Schuldt, K. Sengstock, and A. Wicht. **Precision Gravity Tests with Atom Interferometry in Space**. In: *Nucl. Phys. B Proc. Suppl.* **243-244** (2013), pp. 203–217. DOI: 10.1016/j.nuclphysbps.2013.09.023.

[209] B. Barrett, L. Antoni-Micollier, L. Chichet, B. Battelier, P.-A. Gominet, A. Bertoldi, P. Bouyer, and A. Landragin. **Correlative methods for dual-species quantum tests of the weak equivalence principle**. In: *New J. Phys.* **17** (8 2015), p. 085010. DOI: 10.1088/1367-2630/17/8/085010.

[210] D. S. Naik, H. Eneriz-Imaz, M. Carey, T. Freegarde, F. Minardi, B. Battelier, P. Bouyer, and A. Bertoldi. **Loading and cooling in an optical trap via hyperfine dark states**. In: *Phys. Rev. Res.* **2**.1 (Feb. 2020). DOI: 10.1103/physrevresearch.2.013212.

[211] C. Schubert, J. Hartwig, H. Ahlers, K. Posso-Trujillo, N. Gaaloul, U. Velte, A. Landragin, A. Bertoldi, P. Bouyer, F. S. adn G. M. Tino, M. Krutzik, A. Peters, S. Herrmann, C. Lämmerzahl, L. Cacciapuoti, E. Rocco, K. Bongs, W. Ertmer, and E. M. Rasel. **Differential atom interferometry with 87 Rb and 85 Rb for testing the WEP in STE-QUEST**. In: (2013). arXiv: 1312.5963 [physics.atom-ph].

[212] T. Schuldt, C. Schubert, M. Krutzik, L. G. Bote, N. Gaaloul, J. Hartwig, H. Ahlers, W. Herr, K. Posso-Trujillo, J. Rudolph, S. Seidel, T. Wendrich, W. Ertmer, S. Herrmann, A. Kubelka-Lange, A. Milke, B. Rievers, E. Rocco, A. Hinton, K. Bongs, M. Oswald, M. Franz, M. Hauth, A. Peters, A. Bawamia, A. Wicht, B. Battelier, A. Bertoldi, P. Bouyer, A. Landragin, D. Massonnet, T. Lévèque, A. Wenzlawski, O. Hellmig, P. Windpassinger, K. Sengstock, W. von Klitzing, C. Chaloner, D. Summers, P. Ireland, I. Mateos, C. F. Sopuerta, F. Sorrentino, G. M. Tino, M. Williams, C. Trenkel, D. Gerardi, M. Chwalla, J. Burkhardt, U. Johann, A. Heske, E. Wille, M. Gehler, L. Cacciapuoti, N. Gürlebeck, C. Braxmaier, and E. Rasel. **Design of a dual species atom interferometer for space**. In: *Exp. Astron.* **39**.2 (2015), pp. 167–206. DOI: 10.1007/s10686-014-9433-y.

[213] B. Lücke, J. Peise, G. Vitagliano, J. Arlt, L. Santos, G. Tóth, and C. Klempt. **Detecting Multiparticle Entanglement of Dicke States**. In: *Phys. Rev. Lett.* **112**.15 (Apr. 2014). DOI: 10.1103/physrevlett.112.155304.

[214] A. Kuzmich, N. P. Bigelow, and L. Mandel. **Atomic quantum non-demolition measurements and squeezing**. In: *Europhys. Lett. (EPL)* **42**.5 (June 1998), pp. 481–486. DOI: 10.1209/epl/i1998-00277-9.

[215] J. Hald, J. L. Sørensen, C. Schori, and E. S. Polzik. **Entanglement transfer from light to atoms**. In: *J. Mod. Opt.* **47**.14-15 (Nov. 2000), pp. 2599–2614. DOI: 10.1080/09500340008232184.

[216] C. Gneiting and K. Hornberger. **Molecular Feshbach dissociation as a source for motionally entangled atoms**. In: *Phys. Rev. A* **81**.1 (Jan. 2010). DOI: 10.1103/physreva.81.013423.

[217] C. Gneiting and K. Hornberger. **Bell Test for the Free Motion of Material Particles**. In: *Phys. Rev. Lett.* **101**.26 (Dec. 2008). DOI: 10.1103/physrevlett.101.260503.

[218] D. Meiser, J. Ye, and M. J. Holland. **Spin squeezing in optical lattice clocks via lattice-based QND measurements**. In: *New J. Phys.* **10**.7 (July 2008), p. 073014. DOI: 10.1088/1367-2630/10/7/073014.

[219] J. P. Dowling. **Quantum optical metrology – the lowdown on high-N00N states**. In: *Cont. Phys.* **49**.2 (Mar. 2008), pp. 125–143. DOI: 10.1080/00107510802091298.

[220] H. Ollivier and W. H. Zurek. **Quantum Discord: A Measure of the Quantumness of Correlations**. In: *Phys. Rev. Lett.* **88**.1 (Dec. 2001). DOI: 10.1103/physrevlett.88.017901.

[221] G. Ghirardi and L. Marinatto. **General criterion for the entanglement of two indistinguishable particles**. In: *Phys. Rev. A* **70**.1 (July 2004). DOI: 10.1103/physreva.70.012109.

[222] A. Luis. **Nonlinear transformations and the Heisenberg limit**. In: *Phys. Lett. A* **329**.1-2 (Aug. 2004), pp. 8–13. DOI: 10.1016/j.physleta.2004.06.080.

[223] S. Boixo, S. T. Flammia, C. M. Caves, and J. Geremia. **Generalized Limits for Single-Parameter Quantum Estimation**. In: *Phys. Rev. Lett.* **98**.9 (Feb. 2007). DOI: 10.1103/physrevlett.98.090401.

[224] M. Napolitano, M. Koschorreck, B. Dubost, N. Behbood, R. J. Sewell, and M. W. Mitchell. **Interaction-based quantum metrology showing scaling beyond the Heisenberg limit**. In: *Nature* **471**.7339 (Mar. 2011), pp. 486–489. DOI: 10.1038/nature09778.

[225] T. Prosen. **Matrix product solutions of boundary driven quantum chains**. In: *J. Phys. A* **48**.37 (Aug. 2015), p. 373001. DOI: 10.1088/1751-8113/48/37/373001.

[226] Newton, Gould, and Kaiser. ***Analytical Design of Linear Feedback controls***. Wiley, New York, 1957.

[227] D. S. Naik, G. Kuyumjyan, D. Pandey, P. Bouyer, and A. Bertoldi. **Bose–Einstein condensate array in a malleable optical trap formed in a traveling wave cavity**. In: *Quantum Sci. Technol.* **3** (4 2018), p. 045009. DOI: 10.1088/2058-9565/aad48e.

[228] T. Vanderbruggen, S. Bernon, A. Bertoldi, A. Landragin, and P. Bouyer. **Spin-squeezing and Dicke-state preparation by heterodyne measurement**. In: *Phys. Rev. A* **83**.1 (2011). DOI: 10.1103/physreva.83.013821.

[229] S. Bernon, T. Vanderbruggen, R. Kohlhaas, A. Bertoldi, A. Landragin, and P. Bouyer. **Heterodyne non-demolition measurements on cold atomic samples: towards the preparation of non-classical states for atom interferometry**. In: *New J. Phys.* **13**.6 (2011), p. 065021. DOI: 10.1088/1367-2630/13/6/065021.

[230] A. A. Clerk, M. H. Devoret, S. M. Girvin, F. Marquardt, and R. J. Schoelkopf. **Introduction to quantum noise, measurement, and amplification**. In: *Rev. Mod. Phys.* **82**.2 (Apr. 2010), pp. 1155–1208. DOI: 10.1103/revmodphys.82.1155.

[231] I. Teper, G. Vrijsen, J. Lee, and M. A. Kasevich. **Backaction noise produced via cavity-aided nondemolition measurement of an atomic clock state**. In: *Phys. Rev. A* **78**.5 (Nov. 2008). DOI: 10.1103/physreva.78.051803.

[232] O. Hosten, R. Krishnakumar, N. J. Engelsen, and M. A. Kasevich. **Quantum phase magnification**. In: *Science* **352**.6293 (June 2016), pp. 1552–1555. DOI: 10.1126/science.aaf3397.

[233] S. Kocsis, B. Braverman, S. Ravets, M. J. Stevens, R. P. Mirin, L. K. Shalm, and A. M. Steinberg. **Observing the Average Trajectories of Single Photons in a Two-Slit Interferometer**. In: *Science* **332**.6034 (June 2011), pp. 1170–1173. DOI: 10.1126/science.1202218.

[234] C. Sayrin, I. Dotsenko, X. Zhou, B. Peaudecerf, T. Rybarczyk, S. Gleyzes, P. Rouchon, M. Mirrahimi, H. Amini, M. Brune, J.-M. Raimond, and S. Haroche. **Real-time quantum feedback prepares and stabilizes photon number states**. In: *Nature* **477**.7362 (Aug. 2011), pp. 73–77. DOI: 10.1038/nature10376.

[235] D. A. Steck. **Rubidium 87 D Line Data**. In: available online at http://steck.us/alkalidata (revision 2.1.5,13 January 2015). 2015.

[236] T. Vanderbruggen, R. Kohlhaas, A. Bertoldi, E. Cantin, A. Landragin, and P. Bouyer. **Feedback control of coherent spin states using weak nondestructive measurements**. In: *Phys. Rev. A* **89**.6 (2014). DOI: 10.1103/physreva.89.063619.

[237] A. Bertoldi, R. Kohlhaas, A. Landragin, and P. Bouyer. **Coherent spectroscopic methods with extended interrogation times and systems implementing such methods**. US Patent 20,170,356,803 , EU Patent 3233719 , WO Patent WO/2016/097332, Japan Patent 2017-533335. 2017.

[238] N. F. Ramsey. **The method of successive oscillatory fields**. In: *Physics Today* **66**.1 (Jan. 2013), pp. 36–41. DOI: 10.1063/pt.3.1857.

[239] M. Schioppo, R. C. Brown, W. F. McGrew, N. Hinkley, R. J. Fasano, K. Beloy, T. H. Yoon, G. Milani, D. Nicolodi, J. A. Sherman, N. B. Phillips, C. W. Oates, and A. D. Ludlow. **Ultrastable optical clock with two cold-atom ensembles**. In: *Nat. Photon.* **11**.1 (Nov. 2016), pp. 48–52. DOI: 10.1038/nphoton.2016.231.

[240] K. Chabuda, I. D. Leroux, and R. Demkowicz-Dobrzański. **The quantum Allan variance**. In: *New J. Phys.* **18**.8 (Aug. 2016), p. 083035. DOI: 10.1088/1367-2630/18/8/083035.

[241] J. P. Brantut, J. F. Clément, M. R. de Saint Vincent, G. Varoquaux, R. A. Nyman, A. Aspect, T. Bourdel, and P. Bouyer. **Light-shift tomography in an optical-dipole trap for neutral atoms**. In: *Phys. Rev. A* **78** (3 Sept. 2008), p. 031401. DOI: 10.1103/PhysRevA.78.031401.

[242] M. Bellouvet, C. Busquet, J. Zhang, P. Lalanne, P. Bouyer, and S. Bernon. **Doubly dressed states for near-field trapping and subwavelength lattice structuring**. In: *Phys. Rev. A* **98**.2 (Aug. 2018). DOI: 10.1103/physreva.98.023429.

[243] C.-L. Hung, X. Zhang, N. Gemelke, and C. Chin. **Accelerating evaporative cooling of atoms into Bose-Einstein condensation in optical traps**. In: *Phys. Rev. A* **78**.1 (July 2008). DOI: 10.1103/physreva.78.011604.

[244] A. N. Pyrkov and T. Byrnes. **Entanglement generation in quantum networks of Bose–Einstein condensates**. In: *New J. Phys.* **15**.9 (Sept. 2013), p. 093019. DOI: 10.1088/1367-2630/15/9/093019.

[245] J. Steinhauer. **Observation of self-amplifying Hawking radiation in an analogue black-hole laser**. In: *Nat. Phys.* **10**.11 (Oct. 2014), pp. 864–869. DOI: 10.1038/nphys3104.

[246] J.-C. Jaskula, G. B. Partridge, M. Bonneau, R. Lopes, J. Ruaudel, D. Boiron, and C. I. Westbrook. **Acoustic Analog to the Dynamical Casimir Effect in a Bose-Einstein Condensate**. In: *Phys. Rev. Lett.* **109**.22 (Nov. 2012). DOI: 10.1103/physrevlett.109.220401.

[247] T. Schumm, S. Hofferberth, L. M. Andersson, S. Wildermuth, S. Groth, I. Bar-Joseph, J. Schmiedmayer, and P. Krüger. **Matter-wave interferometry in a double well on an atom chip**. In: *Nat. Phys.* **1**.1 (Sept. 2005), pp. 57–62. DOI: 10.1038/nphys125.

[248] U. Hohenester, P. K. Rekdal, A. Borzı, and J. Schmiedmayer. **Optimal quantum control of Bose-Einstein condensates in magnetic microtraps**. In: *Phys. Rev. A* **75**.2 (Feb. 2007). DOI: 10.1103/physreva.75.023602.

[249] J. Dalibard and C. Cohen-Tannoudji. **Laser cooling below the Doppler limit by polarization gradients: simple theoretical models**. In: *J. Opt. Soc. Am. B* **6**.11 (Nov. 1989), pp. 2023–2045. DOI: 10.1364/JOSAB.6.002023.

[250] D. Finkelstein-Shapiro, S. Felicetti, T. Hansen, T. Pullerits, and A. Keller. **Classification of dark states in multilevel dissipative systems**. In: *Phys. Rev. A* **99**.5 (May 2019), p. 053829. DOI: 10.1103/physreva.99.053829.

[251] M. Weidemüller, T. Esslinger, M. A. Ol'shanii, A. Hemmerich, and T. W. Hänsch. **A Novel Scheme for Efficient Cooling below the Photon Recoil Limit**. In: *Europhys. Lett. (EPL)* **27**.2 (July 1994), pp. 109–114. DOI: 10.1209/0295-5075/27/2/006.

[252] F. Papoff, F. Mauri, and E. Arimondo. **Transient velocity-selective coherent population trapping in one dimension**. In: *J. Opt. Soc. Am. B* **9**.3 (Mar. 1992), pp. 321–331. DOI: 10.1364/JOSAB.9.000321.

[253] S. Rosi, A. Burchianti, S. Conclave, D. S. Naik, G. Roati, C. Fort, and F. Minardi. **Λ-enhanced grey molasses on the D2 transition of Rubidium-87 atoms**. In: *Sci. Rep.* **8**.1 (Jan. 2018), p. 1301. DOI: 10.1038/s41598-018-19814-z.

[254] M. Xin, W. S. Leong, Z. Chen, and S.-Y. Lan. **Transporting Long-Lived Quantum Spin Coherence in a Photonic Crystal Fiber**. In: *Phys. Rev. Lett.* **122**.16 (2019). DOI: 10.1103/physrevlett.122.163901.

[255] C. J. Hood, T. W. Lynn, A. C. Doherty, A. S. Parkins, and H. J. Kimble. **The Atom-Cavity Microscope: Single Atoms Bound in Orbit by Single Photons**. In: *Science* **287**.5457 (2000), pp. 1447–1453. ISSN: 0036-8075. DOI: 10.1126/science.287.5457.1447.

[256] K. Baumann, C. Guerlin, F. Brennecke, and T. Esslinger. **Dicke quantum phase transition with a superfluid gas in an optical cavity**. In: *Nature* **464** (7293 2010), pp. 1301–1306. DOI: 10.1038/nature09009.

[257] P. Horak and H. Ritsch. **Scaling properties of cavity-enhanced atom cooling**. In: *Phys. Rev. A* **64**.3 (2001), p. 033422. DOI: 10.1103/physreva.64.033422.

[258] H. Ritsch, P. Domokos, F. Brennecke, and T. Esslinger. **Cold atoms in cavity-generated dynamical optical potentials**. In: *Rev. Mod. Phys.* **85** (2 2013), pp. 553–601. DOI: 10.1103/RevModPhys.85.553.

[259] M. Aspelmeyer, T. Kippenberg, and F. Marquardt. **Cavity optomechanics**. In: *Rev. Mod. Phys.* **86**.4 (Dec. 2014), pp. 1391–1452. DOI: 10.1103/revmodphys.86.1391.

[260] N. Dogra, F. Brennecke, S. D. Huber, and T. Donner. **Phase transitions in a Bose-Hubbard model with cavity-mediated global-range interactions**. In: *Phys. Rev. A* **94**.2 (2016), p. 023632. DOI: 10.1103/physreva.94.023632.

[261] R. Landig, L. Hruby, N. Dogra, M. Landini, R. Mottl, T. Donner, and T. Esslinger. **Quantum phases from competing short- and long-range interactions in an optical lattices**. In: *Nature* **532** (2016), p. 476. DOI: 10.1038/nature17409.

[262] J. Klinder, H. Keßler, M. R. Bakhtiari, M. Thorwart, and A. Hemmerich. **Observation of a Superradiant Mott Insulator in the Dicke-Hubbard Model**. In: *Phys. Rev. Lett.* **115**.23 (2015), p. 230403. DOI: 10.1103/physrevlett.115.230403.

[263] I. Bloch, J. Dalibard, and W. Zwerger. **Many-body physics with ultracold gases**. In: *Rev. Mod. Phys.* **80** (3 2008), pp. 885–964. DOI: 10.1103/RevModPhys.80.885.

[264] R. Jördens, N. Strohmaier, K. Günter, H. Moritz, and T. Esslinger. **A Mott insulator of fermionic atoms in an optical lattice**. In: *Nature* **455** (7210 2008), pp. 204–207. DOI: 10.1038/nature07244.

[265] B. Paredes, A. Widera, V. Murg, O. Mandel, S. Fölling, I. Cirac, G. V. Shlyapnikov, T. W. Hänsch, and I. Bloch. **Tonks–Girardeau gas of ultracold atoms in an optical lattice**. In: *Nature* **429** (6989 2004), pp. 277–281. DOI: 10.1038/nature02530.

[266] K. M. O'Hara. **Observation of a Strongly Interacting Degenerate Fermi Gas of Atoms**. In: *Science* **298**.5601 (Nov. 2002), pp. 2179–2182. DOI: 10.1126/science.1079107.

[267] E. Kim. **Observation of Superflow in Solid Helium**. In: *Science* **305** (5692 2004), pp. 1941–1944. DOI: 10.1126/science.1101501.

[268] J. Larson, B. Damski, G. Morigi, and M. Lewenstein. **Mott-Insulator States of Ultracold Atoms in Optical Resonators**. In: *Phys. Rev. Lett.* **100** (5 2008), p. 1. DOI: 10.1103/PhysRevLett.100.050401.

[269] S. Fernández-Vidal, G. De Chiara, J. Larson, and G. Morigi. **Quantum ground state of self-organized atomic crystals in optical resonators**. In: *Phys. Rev. A* **81** (4 2010), p. 043407. DOI: 10.1103/PhysRevA.81.043407.

[270] D. Nagy, G. Szirmai, and P. Domokos. **Self-organization of a Bose-Einstein condensate in an optical cavity**. In: *Eur. Phys. J. D* **48** (1 2008), pp. 127–137. DOI: 10.1140/epjd/e2008-00074-6.

[271] F. Brennecke, T. Donner, S. Ritter, T. Bourdel, M. Köhl, and T. Esslinger. **Cavity QED with a Bose–Einstein condensate**. In: *Nature* **450** (7167 2007), pp. 268–271. DOI: 10.1038/nature06120.

[272] S. A. Brazovskiĭ. **Phase transition of an isotropic system to a nonuniform state**. In: *Zh. Eksp. Teor. Fiz.* **68** (1975), pp. 175–185.

[273] A. J. Kollár, A. T. Papageorge, K. Baumann, M. A. Armen, and B. L. Lev. **An adjustable-length cavity and Bose–Einstein condensate apparatus for multimode cavity QED**. In: *New J. Phys.* **17** (4 2015), p. 043012. DOI: 10.1088/1367-2630/17/4/043012.

[274] V. D. Vaidya, Y. Guo, R. M. Kroeze, K. E. Ballantine, A. J. Kollár, J. Keeling, and B. L. Lev. **Tunable-Range, Photon-Mediated Atomic Interactions in Multimode Cavity QED**. In: *Phys. Rev. X* **8** (1 2018), p. 85. DOI: 10.1103/PhysRevX.8.011002.

[275] A. Morales, P. Zupancic, J. Léonard, T. Esslinger, and T. Donner. **Coupling two order parameters in a quantum gas**. In: *Nature Mater.* **17** (8 2018), pp. 686–690. DOI: 10.1038/s41563-018-0118-1.

[276] S. Gopalakrishnan, B. L. Lev, and P. M. Goldbart. **Atom-light crystallization of Bose-Einstein condensates in multimode cavities: Nonequilibrium classical and quantum phase transitions, emergent lattices, supersolidity, and frustration**. In: *Phys. Rev. A* **82** (4 2010), p. 1515. DOI: 10.1103/PhysRevA.82.043612.

[277] Y. Deng, J. Cheng, H. Jing, and S. Yi. **Bose-Einstein Condensates with Cavity-Mediated Spin-Orbit Coupling**. In: *Phys. Rev. Lett.* **112** (14 2014), p. 143007. DOI: 10.1103/PhysRevLett.112.143007.

[278] B. Padhi and S. Ghosh. **Spin-orbit-coupled Bose-Einstein condensates in a cavity: Route to magnetic phases through cavity transmission**. In: *Phys. Rev. A* **90** (2 2014), p. 023627. DOI: 10.1103/PhysRevA.90.023627.

[279] F. Mivehvar, F. Piazza, and H. Ritsch. **Disorder-Driven Density and Spin Self-Ordering of a Bose-Einstein Condensate in a Cavity**. In: *Phys. Rev. Lett.* **119** (6 2017), p. 063602. DOI: 10.1103/PhysRevLett.119.063602.

[280] F. Mivehvar, S. Ostermann, F. Piazza, and H. Ritsch. **Driven-Dissipative Supersolid in a Ring Cavity**. In: *Phys. Rev. Lett.* **120** (12 2018), p. 1107. DOI: 10.1103/PhysRevLett.120.123601.

[281] J. Struck, C. Olschlager, R. Le Targat, P. Soltan-Panahi, A. Eckardt, M. Lewenstein, P. Windpassinger, and K. Sengstock. **Quantum Simulation of Frustrated Classical Magnetism in Triangular Optical Lattices**. In: *Science* **333** (6045 2011), pp. 996–999. DOI: 10.1126/science.1207239.

[282] T. Pellizzari. **Quantum Networking with Optical Fibres**. In: *Phys. Rev. Lett.* **79** (26 1997), pp. 5242–5245. DOI: 10.1103/PhysRevLett.79.5242.

[283] Y. Colombe, T. Steinmetz, G. Dubois, F. Linke, D. Hunger, and J. Reichel. **Strong atom–field coupling for Bose–Einstein condensates in an optical cavity on a chip**. In: *Nature* **450** (7167 2007), pp. 272–276. DOI: 10.1038/nature06331.

[284] P. Verlot, A. Tavernarakis, T. Briant, P.-F. Cohadon, and A. Heidmann. **Backaction Amplification and Quantum Limits in Optomechanical Measurements**. In: *Phys. Rev. Lett.* **104**.13 (Mar. 2010). DOI: 10.1103/physrevlett.104.133602.

[285] J. L. Hall and T. W. Hänsch. **External dye-laser frequency stabilizer**. In: *Opt. Lett.* **9**.11 (Nov. 1984), p. 502. DOI: 10.1364/ol.9.000502.

[286] R. Kohlhaas, T. Vanderbruggen, S. Bernon, A. Bertoldi, A. Landragin, and P. Bouyer. **Robust laser frequency stabilization by serrodyne modulation**. In: *Opt. Lett.* **37**.6 (2012), p. 1005. DOI: 10.1364/ol.37.001005.

[287] L. Botti, R. Buffa, A. Bertoldi, D. Bassi, and L. Ricci. **Noninvasive system for the simultaneous stabilization and control of magnetic field strength and gradient**. In: *Rev. Sci. Instrum.* **77**.3 (2006), p. 035103. DOI: 10.1063/1.2173846.

[288] A. Vilardi, D. Tabarelli, L. Botti, A. Bertoldi, and L. Ricci. **Measurement and modelling of enhanced absorption Hanle effect resonances in ^{85}Rb**. In: *J. Phys. B* **42**.5 (2009), p. 055003. DOI: 10.1088/0953-4075/42/5/055003.

[289] C. Chin, R. Grimm, P. Julienne, and E. Tiesinga. **Feshbach resonances in ultracold gases**. In: *Rev. Mod. Phys.* **82**.2 (Apr. 2010), pp. 1225–1286. DOI: 10.1103/revmodphys.82.1225.

[290] A. Bertoldi, L. Botti, D. Covi, R. Buffa, D. Bassi, and L. Ricci. **Noise and response characterization of an anisotropic magnetoresistive sensor working in a high-frequency flipping regime**. In: *Eur. Phys. J. Appl. Phys.* **33**.1 (2005), pp. 51–57. DOI: 10.1051/epjap:2005088.

[291] A. Bertoldi, D. Bassi, L. Ricci, D. Covi, and S. Varas. **Magnetoresistive magnetometer with improved bandwidth and response characteristics**. In: *Rev. Sci. Instrum.* **76**.6 (2005), p. 065106. DOI: 10.1063/1.1922787.

[292] L. Ricci, L. M. Martini, M. Franchi, and A. Bertoldi. **A current-carrying coil design with improved liquid cooling arrangement**. In: *Rev. Sci. Instrum.* **84**.6 (2013), p. 065115. DOI: 10.1063/1.4811666.

[293] D. E. Pritchard. **Cooling Neutral Atoms in a Magnetic Trap for Precision Spectroscopy**. In: *Phys. Rev. Lett.* **51**.15 (Oct. 1983), pp. 1336–1339. DOI: 10.1103/physrevlett.51.1336.

[294] L. Ricci, A. Bertoldi, and D. Bassi. **Winding shape optimization for asymmetric confinement magnets**. In: *Rev. Sci. Instrum.* **73**.9 (2002), pp. 3181–3186. DOI: 10.1063/1.1499209.

[295] F. Kéfélian, O. Lopez, H. Jiang, C. Chardonnet, A. Amy-Klein, and G. Santarelli. **High-resolution optical frequency dissemination on a telecommunications network with data traffic**. In: *Opt. Lett.* **34**.10 (2009), p. 1573. DOI: 10.1364/OL.34.001573.

[296] *Optical Frequency Transfer – a European Network (OFTEN)*. http://www.ptb.de/emrp/often_home.html.

[297] C. Lisdat et al. **A clock network for geodesy and fundamental science**. In: *Nat. Commun.* **7** (2016), p. 12443. DOI: 10.1038/ncomms12443.

[298] T. Steinmetz, T. Wilken, C. Araujo-Hauck, R. Holzwarth, T. W. Hänsch, L. Pasquini, A. Manescau, S. D'Odorico, M. T. Murphy, T. Kentischer, W. Schmidt, and T. Udem. **Laser Frequency Combs for Astronomical Observations**. In: *Science* **321** (2008), p. 1335. DOI: 10.1126/science.1161030.

[299] S. Schiller et al. **Einstein gravity explorer-a medium-class fundamental physics mission**. In: *Exp. Astron.* **23** (2008), p. 573. DOI: 10.1038/ncomms12443.

[300] *Réseau fibré métrologique à vocation européenne (REFIMEVE+)*. http://www.refimeve.fr/.